DISSERTATIONES SCHOLAE DOCTORALIS AD SANITATEM INVESTIGANDAM
UNIVERSITATIS HELSINKIENSIS

80/2015

MARI SAVOLAINEN

The Effects of Prolyl Oligopeptidase Inhibition in α-Synuclein Based Mouse Models of Parkinson's Disease

DIVISION OF PHARMACOLOGY AND PHARMACOTHERAPY
FACULTY OF PHARMACY
DOCTORAL PROGRAMME IN DRUG RESEARCH
UNIVERSITY OF HELSINKI

The Effects of Prolyl Oligopeptidase Inhibition in α-Synuclein Based Mouse Models of Parkinson's Disease

Mari Savolainen

Division of Pharmacology and Pharmacotherapy
Faculty of Pharmacy
University of Helsinki

Doctoral School in Health Sciences
Doctoral Programme in Drug Research

ACADEMIC DISSERTATION

To be presented, with the permission of the Faculty of Pharmacy,
University of Helsinki, for public examination at
Viikki Biocenter 2, auditorium 1041 on 30.10.2015 at 12 noon.

Supervisor

Docent Timo T. Myöhänen, PhD
Division of Pharmacology and Pharmacotherapy
Faculty of Pharmacy
University of Helsinki
Finland

Professor emeritus Pekka T. Männistö, MD, PhD
Division of Pharmacology and Pharmacotherapy
Faculty of Pharmacy
University of Helsinki
Finland

Reviewers

Professor Anne-Marie Lambeir, PhD
Laboratory of Medical Biochemistry
University of Antwerp
Belgium

Professor Markus Forsberg, PhD
School of Pharmacy
University of Eastern Finland
Finland

Opponent

Professor Heikki Tanila, PhD
A.I. Virtanen Institute
University of Eastern Finland
Finland

Layout: Tinde Päivärinta/PSWFOlders Oy

ISBN 978-951-51-1542-3 (Paperback)
ISBN 978-951-51-1543-0 (PDF)
ISSN 2342-3161 (Paperback)
ISSN 2342-317X (PDF)

Hansaprint - Helsinki, Finland 2015

“Above all, don’t fear difficult moments.
The best comes from them.”

-Rita Levi-Montalcini

CONTENTS

ABSTRACT

Parkinson's disease (PD) is, after Alzheimer's disease, the second most common neurodegenerative disorder. It is characterized by a slow and gradual loss of neurons in specific brain regions and subsequent loss of neurotransmitter dopamine in the movement-related brain tracts. This causes symptoms of PD, which are resting tremor, rigidity and slowness of movement. Genetic and environmental factors are linked to PD, but its etiology is still largely unknown. Current drug therapies can only relieve the symptoms of PD but treatment to stop or delay the disease progression does not exist at the moment.

The main findings in neuropathological characterization of the brain regions that are influenced in PD, are abnormal intraneuronal protein inclusions, called Lewy bodies. Insoluble, aggregated α-synuclein (aSyn) protein is the most abundant component of Lewy bodies. Pathological aggregation and accumulation of aSyn is associated with neuronal death in PD and some other brain diseases, named α-synucleinopathies. Therefore, approaches to target aSyn as a potential disease-modifying treatment for PD have been under investigation.

The aim of this study was to examine the role of prolyl oligopeptidase (PREP) and pharmacological inhibition of its enzymatic activity by KYP-2047 in aSyn aggregation. In the first part, direct protein-protein interaction between PREP and aSyn and its effect on aSyn aggregation was studied using purified proteins and cell culture models. We showed that PREP interacts with aSyn, thus enhancing its aggregation. PREP inhibition reduced the PREP-mediated aSyn aggregation in cell culture.

The second and third parts concentrated on studying the effects of PREP inhibition on aSyn aggregation *in vivo*. The purpose was to first characterize a genetic mouse model, carrying mouse A30P mutated aSyn, which is linked to early-onset PD in humans, in order to find out if the mutated mouse aSyn is more prone to aggregate; and to cause PD-like phenotype or to sensitize the mice for toxicity of 6-hydroxydopamine. Thereafter, the effects of KYP-2047 treatments were assessed in the model. The main findings were that the A30P mutation in mouse aSyn protein caused minor hyperactive behaviour in mice but did not change the brain dopamine levels, and A30P aSyn accumulated in the brain more than wildtype (WT) aSyn by age. KYP-2047 treatment reduced the amount of A30P aSyn in immunohistochemical and Western blot analysis. Western blot analysis revealed that the reduction was more specific for high-molecular weight aSyn oligomers. Furthermore, we observed elevated dopamine levels in the striatum and increased autophagy markers in brain tissue. Therefore, PREP inhibition was further studied in cell culture, where it was shown to enhance macroautophagic protein clearance pathway, which is an important pathway in the degradation of high-molecular weight aSyn forms.

In the fourth study, the effects of KYP-2047 were examined in a mouse model of PD that was based on lactacystin-induced inhibition of ubiquitin-proteasome protein degradation pathway. Proteasome inhibition was shown to induce rapid PD-like neurodegeneration recapitulating the cardinal features of PD. KYP-2047 treatment partially protected dopaminergic neurons in the brain and had beneficial effect on motor behaviour, but did not have an effect on aSyn amount in immunohistochemical analysis.

Taken together, the findings of this study have provided new insights into the role of PREP in aSyn aggregation and suggest that PREP inhibition has beneficial effects on reducing the aggregation process via two different mechanisms. PREP inhibition could be promising and further assessed in the treatment of PD, other α-synucleinopathies and possibly other protein accumulation diseases.

LIST OF ORIGINAL PUBLICATIONS

This thesis is based on the following publications:

I **Savolainen M***, Yan X*, Myöhänen T, Huttunen H: Prolyl oligopeptidase enhances α-synuclein dimerization via direct protein-protein interaction. J. Biol. Chem. 290, 5117-26, 2015 *equal contribution

II Piltonen M*, **Savolainen M***, Patrikainen S, Baekelandt V, Myöhänen TT & Männistö PT: Comparison of motor performance, brain biochemistry and histology of two A30P α-synuclein transgenic mouse stains. Neuroscience 231, 157-168, 2013 *equal contribution

III **Savolainen M**, Richie C, Harvey BK, Männistö PT, Maguire-Zeiss KA, Myöhänen TT: The beneficial effect of a prolyl oligopeptidase inhibitor, KYP-2047, on alpha-synuclein clearance and autophagy in A30P transgenic mouse. Neurobiol. Dis. 68, 1-15, 2014

IV **Savolainen M**, Albert K, Airavaara M, Myöhänen T: Prolyl oligopeptidase inhibition attenuates the toxicity of a proteasomal inhibitor, lactacystin, in the cell culture and mouse model of Parkinson's disease (manuscript)

The publications are referred to in the text by their roman numerals. Supplementary results to study IV are also presented. Reprints were made with the permissions of copyright holders.

ABBREVIATIONS

3-MA	3-methyladenine
5-HT	5-hydroxytryptamine
5-HIAA	5-hydroxyindole acetic acid
6-OHDA	5-hydroxydopamine
AAV	Adeno-associated virus
Aβ	Amyloid beta
AD	Alzheimer's disease
AADC	Aromatic amino acid decarboxylase
aSyn	α-Synuclein
ALP	Autophagy-lysosome pathway
Atg5	Autophagy-related protein 5
Baf	Bafilomycin A1
CaMKII	Calsium-Calmodulin kinase II
CBA	Chicken β-actin
CMA	Chaperone-mediated autophagy
CMV	Cytomegalovirus
DA	Dopamine
DAT	Dopamine transporter
DOPAC	3,4- dihydroxyphenylacetic acid
EM	Electron microscopy
ER	Endoplasmic reticulum
GAD	Glutamic acid decarboxylase
GFAP	Glial fibrillary acidic protein
GFP	Green fluorescent protein
GLuc	Gaussia princeps luciferace
HEK	Human embryonic kidney cells
HVA	Homovanillic acid
Hc	Hippocampus
HMW	High-molecular weight
HPLC	High-performance liquid cromatography
Hsp	Heat shock protein
Iba1	Ionized calcium binding adaptor molecule 1
IHC	Immunohistochemistry
KO	Knock-out
LAMP-2A	Lysosome-associated membrane protein type 2A
LB	Lewy body
LC	Lactacystin
LC3B	Microtubule associated protein light chain 3B
L-DOPA	Dihydroxyphenylalanine
LN	Lewy neurite
LV	Lentivirus
MFB	Medial forebrain bundle
MSA	Multiple system atrophy

MST	Micro-scale thermophoresis
mTOR	Mammalian target of rapamycin
NAC	Non-Amyloid-β component
NO	Nitric oxide
OB	Olfactory bulb
OD	Optical density
p62	SQSTM1/p62
PAGE	Polyacrylamide gel-electrophoresis
PB	Phosphate buffer
PBS	Phosphate-buffered saline
PCA	Protein-fragement complementation assay
PD	Parkinson's disease
PDGFβ	Platelet-derived growth factor-β
Pff	Pre-formed fibril
PK	Proteinase K
PREP	Prolyl oligopeptidase
ROS	Reactive oxygen species
TH	Tyrosine hydroxylase
SNARE	Soluble N-ethylmaleimide-sensitive-factor attachment protein receptor
STR	Striatum
SN	Substantia nigra
SNc	Substantia nigra pars compacta
SNr	Substantia nigra pars reticulata
SNCA	human aSyn coding gene
Snca	mouse aSyn coding gene
Tau	Microtubule-associated protein tau
TG	Transgenic
Tm	$Snca^{tmA30P}$ mouse
UPS	Ubiquitin-proteasome system
VMAT2	Vesicular monoamine transporter-2
VTA	Ventral tegmental area
WB	Western blot
WPRE	Woodchuck hepatitis virus posttranscriptional regulatory element
WT	Wildtype

1 INTRODUCTION

Parkinson's disease (PD) was originally described by James Parkinson (Parkinson, 1817) in *an Essay on the Shaking Palsy*. The defining symptoms of the patients he observed were muscle weakness, resting tremor, bent trunk and abnormal shortened gait. He also noticed that the intellectual and sensory abilities of these patients remained unaltered. PD is the most common neurodegenerative movement disorder, and is a slowly progressive disease (Fahn, 2003). It also encompasses a variety of other, non-motor, symptoms; mood disorders, sleep disturbances, hyposmia and autonomic nervous system dysfunctions (Simuni and Sethi, 2008). Lack of the neurotransmitter dopamine (DA) in the striatum (STR) is cause for the symptoms of PD as a result of selective and gradual destruction of DAergic neurons in the substantia nigra (SN) (Fearnley and Lees, 1991). The symptoms will manifest when approximately 30 % of the neurons in the SN pars compacta (SNc) are lost. Surviving neurons in the SN usually contain intracytoplasmic proteinaceous inclusions called Lewy bodies (LB), which are important neuropathological findings of PD.

Genetic mutations and exposure to environmental toxins, such as pesticides and herbicides, have been linked to PD etiology (Wirdefeldt *et al.*, 2011). At the cellular level, mitochondrial dysfunction, oxidative stress, protein aggregation, dysfunctional protein degradation and inflammation are thought to be the key mechanisms in PD pathology, but their relations remain largely to be elucidated (Fahn, 2003). The characterizing feature of PD pathology is the presence of LBs that contain a variety of proteins, of which fibrillar α-synuclein (aSyn) is the most abundant (Spillantini *et al.*, 1998). In recent years, the involvement and the role of aSyn in PD pathology has been extensively studied. Point mutations, like A30P and A53T, in aSyn coding gene (SNCA), and SNCA duplications and triplications are associated with PD (Polymeropoulos *et al.*, 1997, Krüger *et al.*, 1998, Singleton *et al.*, 2003, Chartier-Harlin *et al.*, 2004). aSyn aggregation is a process where its native soluble monomeric form changes into oligomeric and fibrillary species and finally into aggregates. In addition, the neurotoxicity of oligomeric species of aSyn has been proven and many factors affecting the aggregation of aSyn have been identified. Currently, LBs themselves are not considered to be the toxic aSyn species to the cells but rather represent an end stage of the aSyn pathology. Furthermore, cellular protein clearance systems, which participate in degradation of aSyn, are thought to have a potential role both in toxic accumulation and beneficial clearance of aSyn.

A serine protease, prolyl oligopeptidase (PREP), has also been associated with aSyn aggregation (Brandt *et al.*, 2008). PREP is expressed in various tissues, it takes part in neuropeptide cleavage and potentially has a role in cognition and mood, but its physiological role has remained partly unknown. The size of aSyn is too large for it to be digested by PREP, which cleaves small peptides on the C-terminal side of proline residue (Gass and Khosla, 2007). However, PREP has been shown to enhance *in vitro* aggregation of aSyn (Brandt *et al.*, 2008) and inhibition of PREP enzyme activity reduced the aggregation in cell culture and *in vitro* models.

This literature review focuses on the role of aSyn in PD pathophysiology, factors affecting the aggregation and deposition of aSyn as well as possible treatment strategies against the formation of toxic aSyn species and their accumulation. In order to study this, both good PD cell culture

and *in vivo* models are required, and mouse models that are based on aSyn will be overviewed here. The experimental part of this thesis concentrates on elucidating the role and mechanisms of PREP inhibition in aSyn cellular aggregation *in vitro* and in the clearance of aSyn *in vivo*. Furthermore, a transgenic aSyn mouse line and a proteasome inhibition-based lesion model will be characterized as PD mouse models.

2 REVIEW OF THE LITERATURE

2.1 α-synuclein

aSyn, together with β- and γ-synucleins belongs to the family of synuclein proteins (Surguchov, 2008). aSyn was first purified from cholinergic vesicles of *Torpedo californica* and thereafter from rat neuronal tissue in the late 1980s (Maroteaux *et al.*, 1988). aSyn proteins from different species were shown to have highly homologous sequences and localization in the presynaptic nerve terminal. In birds, a homologous protein, named synelfin, shares high sequence similarity (George *et al.*, 1995). In the early 1990s a precursor protein for non-amyloid-β component (NAC) of Alzheimer's disease (AD) amyloid was identified in human brain (Ueda, 1993), which was sequenced and verified to be aSyn (Jakes *et al.*, 1994). The initial finding of NAC-fragment of aSyn in AD pointed to a possible role of aSyn in AD pathophysiology and led the study towards its involvement in neurodegenerative diseases.

2.1.1 Physiological functions of α-synuclein

In immunohistochemical (IHC) and electron microscopy (EM) studies, aSyn has been found to be highly expressed in cortex, entorhinal cortex, STR and hippocampus (Hc), and it localizes in vesicles in presynaptic nerve terminal areas (Jakes *et al.*, 1994, Iwai *et al.*, 1995). In songbirds, synelfin mRNA and protein expression are shown to increase during critical periods of song learning, where *in situ* hybridization and immunofluorescence stainings point to a role for aSyn in neuronal plasticity (George *et al.*, 1995, Jin and Clayton, 1997). Moreover, songbird's synelfin localizes in nerve terminals. The finding of highly conserved sequence similarity between species and prominent neuronal tissue localization highlights the physiological role for aSyn in synaptic functions.

aSyn inhibits phospholipase D2 function (Jenco *et al.*, 1998) which has a role in membrane organization, vesicle trafficking and secretion (Colley *et al.*, 1997). It also interacts with acidic phospholipid vesicles, which induces aSyn's alpha-helixity (Davidson *et al.*, 1998, Perrin *et al.*, 2000, Jo *et al.*, 2000), suggesting a role in cellular processes involving lipid binding, such as regulation of synaptic vesicles. aSyn associates with synaptic vesicles (Jensen *et al.*, 1998) and regulates the presynaptic vesicular pool in hippocampal neuronal culture (Murphy *et al.*, 2000), where knocking down aSyn expression reduced the size of the vesicular pool. Study with aSyn knock-out (KO) mice supports the role for aSyn in synaptic maintenance (Abeliovich, 2000). aSyn KO mice have normal expression of tyrosine hydroxylase (TH) and vesicular release-associated proteins; synaptophysin and ras-related protein Rab3a as well as normal morphology of neurotransmitter vesicles, suggesting that aSyn is not required for normal neurogenesis of DAergic neurons. α-, β-, and γ-synuclein triple-KO mice develop age-associated neurological deficits which highlight the protecting and maintaining function of synuclein family in synaptic homeostasis (Burré *et al.*, 2010).

In cell culture experiments aSyn associates with microtubules, it binds to tubulin and overexpression of aSyn inhibits microtubule formation suggesting that aSyn also regulates the microtubular network (Zhou *et al.*, 2010). Although the results of another study by Chen et al. (Chen *et al.*, 2007) do not support the direct interaction between aSyn and tubulin, their results

are otherwise similar indicating that aSyn oligomers can disturb tubulin polymerization into microtubules.

In the light of current evidence, aSyn seems to be a regulator of neuronal activity and synaptic homeostasis but in general the physiological role of aSyn is not yet very well understood.

2.1.2 α-synuclein and dopaminergic neurotransmission

DA homeaostasis in the synapse is regulated by enzymes, transporters and other proteins that participate in DA synthesis, metabolism, release and vesicular packing (Nestler *et al.*, 2009). aSyn is the main component of LBs, aggregates found in the areas of a PD patient's brain where DAergic cell loss occur (Spillantini, 1997, Spillantini *et al.*, 1998). The role of aSyn in DAergic neurotransmission has therefore been studied extensively.

Studies with aSyn KO mice have shown that the striatal DA content as well as response to amphetamine-induced locomotion were reduced, while the study showed enhanced recovery of DA release after multiple stimuli (Abeliovich, 2000). In another study, where DA release was stimulated and burst firing was measured by voltammetry, aSyn KO mice showed enhanced DA release and enhanced facilitation of DA release between repeated stimuli compared to WT mice (Yavich *et al.*, 2004). This data indicates a regulatory role for aSyn in synaptic DAergic balance.

Dopamine transporter (DAT) is the main regulator of synaptic DA content in the STR, and it terminates the DA action by reuptaking it from the synapse back to the presynaptic terminals (Reith *et al.*, 1997). Several studies indicate a role for aSyn in DAT activity and trafficking, which may be disturbed due to mutated aSyn or its aggregated forms. aSyn interacts with DAT and inhibits DAT activity on the cell surface causing a decrease of the magnitude and rate of DAT-substrates uptake in neuronal cell cultures (Wersinger and Sidhu, 2005, Swant *et al.*, 2011). The mutant form A53T aSyn is unable to alter DAT-function (Wersinger and Sidhu, 2005). Higher extracellular DA levels in aSyn KO mice have been associated with reduced amount of DAT expression and consequently reduced re-uptake of DA (Chadchankar *et al.*, 2011). Aggregation of aSyn is associated with increased DAT expression and it causes DAT-redistribution away from the plasma membrane in a mouse model expressing truncated aSyn(120) (Bellucci *et al.*, 2011). The modulatory effects of aSyn on DAT are at least partially mediated by microtubules which are important mediators of cellular trafficking (Wersinger and Sidhu, 2005). Microtubular network may be regulated by aSyn and disrupted by its oligomerization (Chen *et al.*, 2007, Zhou *et al.*, 2010).

Soluble N-ethylmaleimide-sensitive-factor attachment protein receptor (SNARE) proteins are the major regulators of vesicle endocytosis and intracellular membrane fusion (Südhof, 1995). Complexes formed by these proteins are crucial for rapid release of the reserve vesicle pool and subsequent fast neurotransmission. SNARE complex assembly is regulated by several proteins, one of which is aSyn (Chandra *et al.*, 2005). In cell culture and transgenic (TG) mouse studies, aSyn promotes SNARE complex assembly by interaction with synaptobrevin-2/vesicle-associated membrane protein 2 and simulatenously binding to phospholipids (Burré *et al.*, 2010). In aSyn overexpressing rat neuronal cell culture, exocytosis of synaptic vesicles is reduced as a consequence of a reduced readily releasable vesicle pool size (Nemani *et al.*, 2010).

These observations are made with WT aSyn and A53T and E46K mutants, whereas A30P aSyn did not inhibit neurotransmitter release. Yet, reduced DA release, suggested to be related to reduced amount of dopamine vesicles, has been identified in a TG mouse line expressing A30P aSyn (Yavich *et al.*, 2005).

aSyn also has a regulatory role in DA biosynthesis, which is mainly rate-limited by TH enzyme, that is responsible for converting tyrosine into dihydroxyphenylalanine (L-DOPA). aSyn interacts with TH in brain and aSyn overexpression inhibits its activity via increased protein phosphatase 2A-dependent dephosphorylation and subsequently reduces DA in MN9D cell culture (Perez *et al.*, 2002, Peng *et al.*, 2005). In the BE2-M17 neuronal cell line, microarray and quantitative reverse transcription-PCR study have revealed that overexpression of aSyn modulates the expression of many genes related to DA synthesis (Baptista *et al.*, 2003). This could be linked to downregulation of Nurr1 (Baptista *et al.*, 2003), an important transcription factor in the maintenance of DAergic homeostasis (Jankovic *et al.*, 2005). In MN9D cells, aSyn overexpression decreased the activity and phosphorylation of aromatic amino acid decarboxylase (AADC), which converts L-DOPA to DA (Tehranian *et al.*, 2006).

These findings indicate that aSyn is not only an important regulator of normal DAergic neurotransmission but its overexpression or aggregation as well as mutated forms most likely result in dysregulation of DA homeostasis.

2.2 α-synuclein in pathophysiology of neurogenerative diseases

The discovery of the NAC-fragment of aSyn from AD plaques generated interest towards the role of aSyn in the pathogenesis of AD. Sequencing techniques and generation of specific antibodies against aSyn soon revealed that aSyn is the major component in LBs of PD. As the antibodies and detection methods evolved, the presence of NAC fragment of aSyn in the AD plaques has even been questioned. Evidence linking aSyn in PD pathophysiology will be reviewed in the next paragraphs.

2.2.1 α-synuclein in Lewy bodies of Parkinson's disease and other synucleinopathies

Neuropathological characterization of post-mortem PD brain samples has revealed that LBs are ubiquitinated intraneuronal filamentous inclusions (Goldman *et al.*, 1983, Kuzuhara *et al.*, 1988). Lewy neurites (LN) that are also associated with the pathology, are abnormal neurites containing filamentous aSyn, like LBs. Similar inclusions are also present in dementia with Lewy bodies (DLB) and multiple system athropy (MSA) (Galvin *et al.*, 2001). In DLB, LBs are found in the cortical and subcortical brain regions and the disease is characterized by late-onset memory impairment and is often associated with hallucinations or behavioural disturbances (Spillantini and Goedert, 2000, Galvin *et al.*, 2001), in the MSAs inclusions are present in the oligodendrocytes and they are termed glial cytoplasmic inclusions (Tu, 1998, Spillantini and Goedert, 2000). MSAs are clinically characterized by various symptoms from PD-like movement deficits to cognitive decline and cerebellar and autonomic problems.

In 1997, IHC stainining revealed that aSyn is the main component of the protein aggregates, LBs, in the SN of PD and cingulate cortex of DLB patients' post-mortem brain samples (Spillantini, 1997). In immune-EM, aSyn antibody labeled 9-12 nm-thick filaments of LBs in PD and DLB (Spillantini *et al.*, 1998, Arima, 1998). Then, aSyn was shown to exist as a full-length form but also in truncated and insoluble forms in the inclusions of PD and DLB (Baba *et al.*, 1998). In double label IHC, LBs were more intensively immunoreactive with aSyn antibodies than ubiquitin, which had earlier been the most sensitive detection for LB pathology (Spillantini *et al.*, 1998). aSyn positive inclusions were also shown to be specific for neurodegenerative diseases exhibiting LB formation, whereas in diseases where intracellular microtubule-associated protein tau (Tau) inclusions occur, aSyn did not co-localize with Tau in double label immunofluorecense staining (Takeda *et al.*, 1998). The possible role of aSyn in AD pathogenesis was also questioned when new specific NAC targeted antibodies failed to stain extracellular AD plaques and aSyn was shown only to be present in intracellular LB-like inclusion in mixed DLB/AD and PD cases (Culvenor *et al.*, 1999, Bayer, 1999).

During the year when aSyn was identified in IHC analysis of PD brain, the first genetic analysis was published, revealing a point mutation A53T in the aSyn coding gene connecting this mutation to the familial early-onset form of PD (Polymeropoulos *et al.*, 1997). Since then, other genetic missense mutations (A30P, E46K, H50Q and G51D) have been associated with familial Parkinsonism, and also duplications and triplications of the SNCA have been discovered from other families with PD (Krüger *et al.*, 1998, Singleton *et al.*, 2003, Chartier-Harlin *et al.*, 2004, Zarranz *et al.*, 2004, Proukakis *et al.*, 2013, Lesage *et al.*, 2013). The aggregation of aSyn has been thereafter extensively studied as a pathological mechanism of PD and other diseases displaying LB pathology.

2.3 Mechanisms of α-synuclein aggregation, accumulation and toxicity

Structurally aSyn is a natively unfolded protein (i.e. it is intrinsically disordered) (Weinreb *et al.*, 1996). It also has a hydrophobic core, which makes it unstable. Conformation of aSyn has minor secondary structure making the hydrophobic parts of the protein exposed and more prone to form protein-protein interactions, to misfold and self-aggregate. Three regions in aSyn contribute to the aggregation; 1) the N-terminal, amphipathic region, which contain the PD linked mutations, 2) the hydrophobic NAC-region in the central part, which is required for fibrillogenesis and 3) the acidic C-terminal region, which reduces the aggregation (El-Agnaf *et al.*, 1998b, Giasson *et al.*, 2001, Bisaglia *et al.*, 2009), (Figure 1). In solution, aSyn forms dimers and higher molecular weight conformers as shown with incubation of ^{125}I-labeled aSyn (Jensen *et al.*, 1997). Moreover, immunoblotting assay, atomic force microscopy and EM studies have shown that fibrils and aggregates form in both a concentration and time-dependent manner (Jensen *et al.*, 1997, Hashimoto *et al.*, 1998, El-Agnaf *et al.*, 1998b, Giasson *et al.*, 1999, Conway *et al.*, 2000a). Prolonged incubation of recombinant aSyn results in a formation of 8-10 nm width amyloid-like fibrils which stain positive in thioflavine-S staining, similarly to LBs taken from cortical brain areas (Hashimoto *et al.*, 1998). Similar to aggregation processes of other amyloid-like proteins, aSyn undergoes a conformational change from random coil structure to βl-sheet conformation during fibril formation (Serpell *et al.*, 2000). Fibril formation

is a nucleation-dependent process, where aSyn may seed its own fibrillogenesis (Wood, 1999), but self-oligomerization may occur also in the presence of amyloid beta (Aβ) fragement (25-35) (Paik *et al.*, 1998). The aggregation process, where soluble aSyn folds, dimerizes, further oligomerizes and forms fibrils and aggregates, is illustrated in Figure 2. Although aSyn self-oligomerizes in solution in time, there are multiple factors that are found to enhance the aggregate formation and accumulation of aSyn (Figure 2), which may lead to its toxicity (Figure 3), and they will be reviewed in more detail in the next paragraphs.

2.3.1 Genetic mutations and α-synuclein gene duplication and triplication

Point mutations, A30P, A53T, E46K, H50Q and G51D, which are associated with PD pathology, enhance the aggregation propensity or toxicity of human aSyn (Conway *et al.*, 1998, El-Agnaf *et al.*, 1998a, Conway *et al.*, 2000b, Li *et al.*, 2001, Choi *et al.*, 2004, Proukakis *et al.*, 2013, Lesage *et al.*, 2013). A30P, A53T and H50Q mutants enhance the fibril-formation of aSyn as shown in atomic force and EM, while A53T and E46K mutations accelerate the fibril formation more significantly than A30P (Conway *et al.*, 1998, El-Agnaf *et al.*, 1998a, Conway *et al.*,

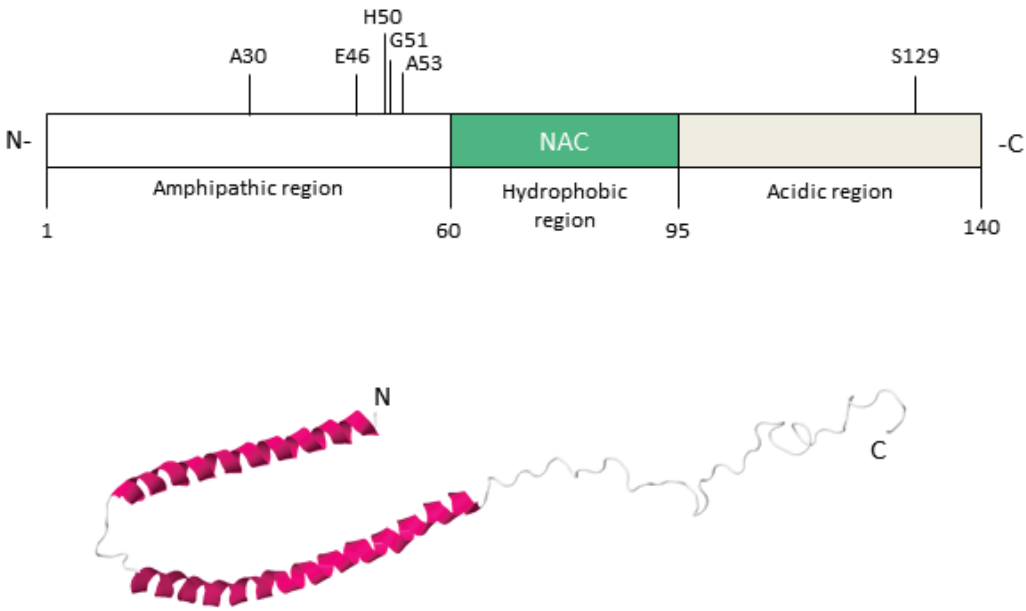

Figure 1: α-synuclein regions and structure. *α-synuclein consists of three regions; the N-terminal amphipathic region where aggregation accelerating mutations are located (amino acids that are known to have PD-associated mutations are marked), the non-amyloid-β component (NAC)-region is a hydrophobic part of aSyn and is required for fibrillation and aggregation, whereas the C-terminal acidic region protects from aggregation. Phosphorylation of serine at position 129 is a post-translational modification which is relevant for aSyn fibrillation and associated with PD pathology. The schematic representation of the biochemical structure of α-synuclein (bottom) shows α-helical N-terminal and NAC- region, whereas the C-terminal region is unstructured (structure of micelle-bound α-synuclein was determined by solution NMR spectroscopy ID: 1XQ8, was downloaded from RCSB Brotein Data Bank and rendered in JMol).*

2000a, Li *et al.*, 2001, Choi *et al.*, 2004, Rutherford *et al.*, 2014). Secondary structure analysis with fourier transform infrared spectroscopy of WT, A30P and A53T aSyn proteins has revealed that mutated aSyn exists in a more ordered β-sheet fold instead of an unfolded structure, which may increase their aggregation potency (Li *et al.*, 2001).

The E46K mutation enhances the phospholipid binding of aSyn, which could contribute to the fibril formation (Choi *et al.*, 2004). In contrast to other pathogenic mutations, the G51D mutation, which is linked to the early-onset rapidly progressing form of PD, does not enhance aSyn aggregation, but it has been shown to enhance aSyn toxicity under cellular stress *in vitro* (Lesage *et al.*, 2013, Rutherford *et al.*, 2014). Also C-terminally truncated aSyn (1-120), which is present in LBs of PD brain, accelerates the fibril formation (Crowther *et al.*, 1998, Baba *et al.*, 1998, Serpell *et al.*, 2000, Li *et al.*, 2005). Duplications (Chartier-Harlin *et al.*, 2004) and triplications (Singleton *et al.*, 2003) of the SNCA gene are associated with familial PD. In the cases of triplication, the onset of PD is early whereas duplications are more similar to sporadic PD, implicating a dose-dependent aSyn aggregation-tendency.

2.3.2 Post-translational modifications

Many posttranslational modifications that possibly affect aSyn aggregation and/or accumulation have been identified. In LBs aSyn is extensively phosphorylated at position Ser129 (pS129 aSyn), which also enhances the aSyn fibrillization *in vitro* (Okochi, 2000, Fujiwara *et al.*, 2002, Anderson *et al.*, 2006). aSyn and phosphorylated aSyn have been found to be ubiquitinated in LBs (Hasegawa *et al.*, 2002, Sampathu *et al.*, 2003). Therefore, aSyn ubiquitination may have a role in fibril-formation or is merely a sign of a defective degradation pathway because ubiquitination targets proteins for proteasomal clearance. However it has been suggested that ubiquitination is more likely to be an event occurring after fibril and aggregate formation and not to directly enhance the aggregation process (Sampathu *et al.*, 2003). It has also been proposed that aSyn phosphorylation has a role in its targeting for proteasomal degradation. Using mutant S129A aSyn, which does not undergo S129 phosphorylation, Tenreiro et al. (Tenreiro *et al.*, 2014) showed that cellular clearance of unphosphorylated mutant aSyn inclusions is reduced. S129A aSyn also failed to activate the autophagy pathway, which was activated upon WT aSyn accumulation. In contrast to aggregation enhancing posttranslational modifications, sumoylation of aSyn by small ubiquitin-like modifiers reduces aSyn aggregation by increasing aSyn solubility (Krumova *et al.*, 2011, Abeywardana and Pratt, 2015).

Cellular oxidative stress enhances the formation of reactive oxygen species (ROS) and consequent formation of reactive nitrogen species (Jenner, 2003, Ischiropoulos, 2009). Reactive oxygen and nitrogen species may, among other toxic cellular effects, cause posttranslational modifications that promote fibrillization of aSyn. Nitrated aSyn species are found in aSyn positive inclusions in synucleinopathies in IHC and Western blot (WB) experiments using antibodies against nitrated aSyn (Giasson, 2000). Nitration of tyrosine residues of aSyn has been shown to induce aSyn folding and secondary structure formation leading to enhanced oligomerization, stabilization of oligomeric form and inhibition of fibrillation (Duda *et al.*, 2000, Uversky *et al.*, 2005). Iron-catalyzed oxidation of aSyn induces aggregation, as shown with peroxide in the presence of ferric ion (Hashimoto *et al.*, 1998 and 1999a) or cytochrome c or hemin (Hashimoto *et al.*, 1999b). The phenomena can be blocked *in vitro* by iron chelators

or anti-oxidant N-acetyl-L-cysteine. Other metal ions are also linked to enhanced oxidative self-oligomerization of aSyn (Paik *et al.*, 1999, Rasia *et al.*, 2005). Copper(II)-mediated aggregation is dependent on the C-terminus of aSyn (Paik *et al.*, 1999) and is enhanced via acidic lipids, like phosphatidylinositol (Lee *et al.*, 2003). Binding of Fe(II). Cu(II) and Pb(II) metal ions to aSyn is also enhanced via aSyn phosphorylation (Lu *et al.*, 2011). Although methionine group oxidation has been reported to reduce fibrillation (Uversky *et al.*, 2002), this effect is hampered in the presence Zn(II) (Hokenson *et al.*, 2004) and may contribute to aSyn toxicity by inhibiting aSyn proteasomal degradation (Alvarez-Castelao *et al.*, 2014).

2.3.3 Interactions

DA causes conformational changes in aSyn secondary structure, which promotes its oligomeric state (Outeiro *et al.*, 2009). DA has also been shown to stabilize the protofibril conformer of aSyn and prevent the fibril formation, which prolongs the availability of neurotoxic aSyn conformer (Conway *et al.*, 2001). At physiological pH, DA may be oxidized into reactive intermediates which promotes the oxidative stress effect and aSyn aggregation (Pham *et al.*, 2009, Chan *et al.*, 2012).

Lipid- and protein-protein interactions between lipids or proteins and aSyn may enhance the aggregation of aSyn. Acidic lipids such as phosphatidic acid, phosphatidylinositol, phosphatidylserine, phosphatidylethanolamine, and arachidonic acid enhance the self-oligomerization of aSyn (Lee *et al.*, 2003). The lipid or protein binding partner may act as a nucleation point or facilitate aSyn folding. Vesicle and lipid rafts-associated protein, synphilin-1, interacts with aSyn and enhances its aggregation and toxicity in yeast model (Engelender, 1999, Büttner *et al.*, 2010). Therefore, synphilin-1 may facilitate the membrane toxicity of aSyn. FK506 binding proteins, which are peptidyl-prolyl isomerases, have also been shown to accelerate aSyn aggregation and their inhibition has been shown to reduce aSyn aggregation (Gerard *et al.*, 2010). Their influence on the aggregation enhancement is facilitated via C-terminal prolyl residues of aSyn. Tissue transglutaminase 2, an enzyme that catalyzes protein cross-linking, enhances the formation of aSyn aggregates *in vitro* and in cell culture (Junn *et al.*, 2003). Furthermore, PREP enhances aggregation of aSyn *in vitro* (Brandt *et al.*, 2008), suggesting that it acts as a seeding point for aggregation. A PREP inhibitor also reduces the aSyn aggregate formation in cell culture (Myöhänen *et al.*, 2012).

Heat shock proteins (Hsp) are chaperones that participate in protein quality control, have a role in protein folding and reduce protein-protein interactions, which makes them potential drug targets for protein aggregation diseases (Feder and Hofmann, 1999). Hsp104 have been shown to inhibit aSyn fibrillation and resolve formed aSyn fibrils *in vitro* and also to reduce A30P aSyn mediated neurodegeneration in an aSyn-lentivirus rat model (Lo Bianco *et al.*, 2008). Overexpression of Hsp70 together with human aSyn in a TG mouse was shown to have a beneficial effect on aSyn aggregation (Klucken *et al.*, 2004), but overexpression of Hsp70 together with A53T-aSyn in double TG mice failed to protect neurons from aSyn accumulation or death (Shimshek *et al.*, 2010). Similarly, inhibition of Hsp90 causes subsequent induction of Hsp70, which in other studies failed to protect against aSyn positive inclusion formation and DAergic cell loss in rat aSyn adeno-associated virus (AAV) model (McFarland *et al.*, 2014). However, Hsps increased striatal DA content suggesting some positive modulatory effects (McFarland *et al.*, 2014). Of

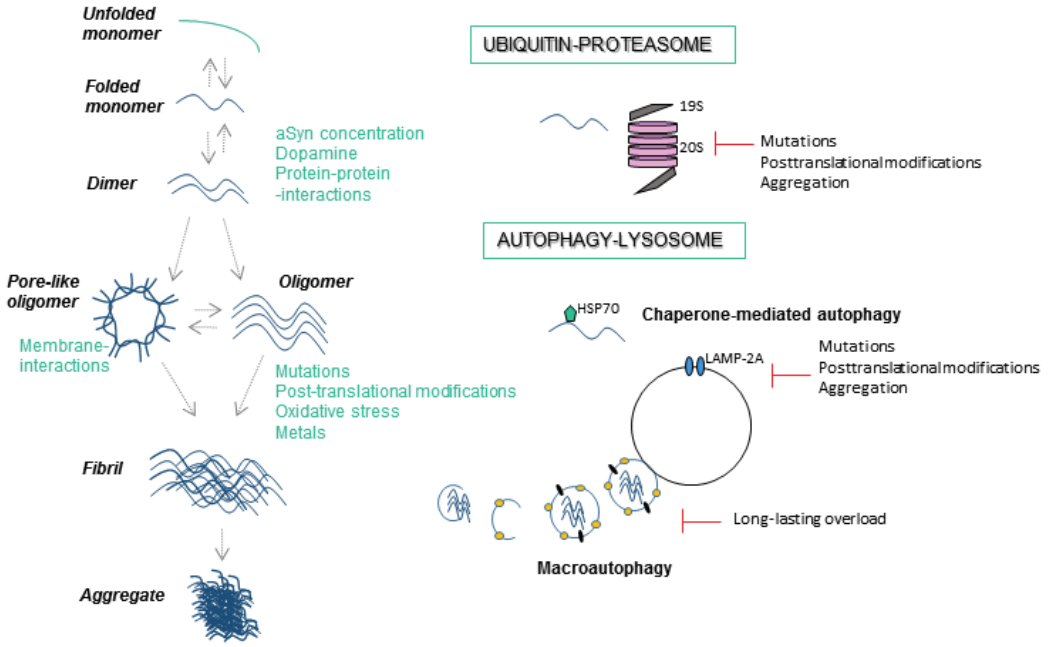

Figure 2: α-synuclein aggregation and clearance*. In its native form, α-synuclein (aSyn) exists in an unfolded monomeric state. Folded aSyn may undergo dimerization and subsequent oligomerization. Pore-like oligomers are formed upon membrane-interactions. Fibril-formation eventually leads to aggregation. Factors that enhance the aggregation process are written in green. Two protein clearance pathways, ubiquitin-proteasome and autophagy-lysosome, participate in α-synuclein degradation. α-synuclein-mediated factors that may compromise its own clearance pathway are marked with* ⊢*. HSP, heat shock protein; LAMP-2A, lysosome-associated membrane protein 2A*

other factors affecting aSyn aggregation, its close relative, β-synuclein inhibits aSyn aggregation and toxicity in a double TG mouse line and in double-transfected cell lines, suggesting that β-synuclein is an endogenous negative regulator of aSyn aggregation (Hashimoto *et al.*, 2001).

2.3.4 Factors affecting α-synuclein accumulation

Because the missense mutations in the SNCA gene comprise only a small part of PD cases, other cellular events over the genetic component most likely lie behind the disease pathology. If aSyn is transcribed more than the protein degradation systems are able to handle, it is likely that it starts to accumulate. aSyn genetic duplications and triplications are known to cause hereditary PD, which suggests that overexpression of aSyn leads to its dose-dependent accumulation (Singleton *et al.*, 2003, Chartier-Harlin *et al.*, 2004). In mouse and rat models, it has also been shown that TG overexpression of human aSyn together with endogenous murine aSyn gene (Snca) or using viral vector-mediated aSyn overexpression causes accumulation of aSyn (Chesselet *et al.*, 2012, Decressac *et al.*, 2012b, Oliveras-Salva *et al.*, 2013), but as stated already, genetic overexpression of aSyn can explain only a minority of PD cases. Multiple protein-clearance pathways in the cell degrade aSyn. Once aSyn starts to aggregate as a result of one or many of the above mentioned factors, the cellular protein clearance pathways may be

compromised. Decline in the activity of protein clearance systems could also contribute to the cellular deposition of aSyn and further promote the aggregation. Therefore, the relevance of protein degradation systems in aSyn accumulation will be reviewed next. Relevant pathways in aSyn degradation are illustrated in Figure 2.

Ubiquitin-proteasome system

UPS consists of the 26S proteasome, which degrades proteins that are targeted for degradation via poly-ubiquitination (Pickart, 2000). Ubiquitinylation of UPS substrates is carried out in cycles and is initiated by ubiquitin-activating enzyme E1, followed by ubiquitin-conjugating enzyme E2 and finalized by ubiquitin-ligase E3 (Haas and Siepmann, 1997). Poly-ubiquitinated proteins should have at least four ubiquitins linked to them in order to be targeted to the 26S proteasome. The 26S proteasome is formed of two parts, the 19S subunit, which recognizes, unfolds and deubiquitinates its substrates, and the 20S core part, which has proteolytic activity. Proteins may also undergo proteasomal degradation ubiquitin-independently by the 20S or 26S subunit (Jariel-Encontre *et al.*, 2008).

Several studies have shown that aSyn is degraded via UPS. In SH-SY5Y cell culture, UPS degrades aSyn after transient transfection and this was blocked with proteasome inhibitor β-lactone (Bennett *et al.*, 1999). A53T aSyn was shown to have slower degradation kinetics of clearance, suggesting an explanation for its enhanced toxicity and aggregation propensity. *In vitro,* aSyn interacts with the α7 subunit of the 20S proteasome, and aSyn and pS129 aSyn undergo UPS degradation ubiquitination-independently in aSyn overexpressing or pS129aSyn transfected SH-SY5Y cell lines, respectively (Tofaris *et al.*, 2001, Machiya *et al.*, 2010). Whereas, high-molecular weight (HMW) forms of aSyn, which represent oligomeric or larger aSyn species, are not degraded via UPS (Alvarez-Castelao *et al.*, 2014). In rat ventral mecencephalic neuronal culture, proteasome inhibition using lactacystin (LC) and subsequent immunocytochemistry analysis revealed aSyn positive inclusion bodies (McNaught *et al.*, 2002). There are some controversial results about the role of UPS in aSyn clearance. Proteasome inhibition in PC12 cell line failed to increase aSyn levels in WB analysis although ubiquitin and aSyn positive inclusions were formed when analysed using immunocytochemistry (Rideout *et al.*, 2001). Accumulation of aSyn in transfected PC12 cells after LC treatment was suggested to be dependent of LC-induced transcriptional activation, which enhances aSyn expression (Biasini *et al.*, 2004). It is also suggested that aSyn is not degraded by the proteasome in HEK293 cells or TSM1 neurons; Ancolio et al. (Ancolio *et al.*, 2000) showed that the amount of soluble monomeric aSyn is not affected by proteasome inhibitors, and it does not undergo ubiquitinylation in those cell cultures. Controversial results of different studies may be explained by the fact that aSyn is not degraded solely by one protein clearance pathway (Ebrahimi-Fakhari *et al.*, 2011) and other clearance pathways may be upregulated when one is inhibited. Furthermore, the contribution of different protein degradation pathways for cellular protein turnover seems to be cell type specific (Klionsky *et al.*, 2008).

Other lines of evidence supporting the role of UPS in aSyn accumulation and PD is from post-mortem SN samples of sporadic PD patients where proteasomal activity is shown to be decreased (McNaught and Jenner, 2001, McNaught *et al.*, 2003, Tofaris *et al.*, 2003) and of IHC and WB experiments, showing the loss of proteasomal 20S α-subunit in the same area (McNaught *et al.*, 2002 and 2003). When the effect of aSyn overexpression was studied in cell

cultures, aSyn overexpression reduced the activity of UPS in BE-M17 neuroblastoma cells (Snyder *et al.*, 2003). Moreover, monomeric (Snyder *et al.*, 2003) or aggregated (Snyder *et al.*, 2003, Alvarez-Castelao *et al.*, 2014) forms of aSyn were shown to inhibit 20S proteasomal activity. Aggregated aSyn also inhibited ubiquitin-independent and -dependent 26S proteasome pathways. Monomeric and aggregated aSyn forms bind to the 19S region of the proteasome. In cell culture studies, overexpression of A30P (Tanaka *et al.*, 2001) and A53T (Smith *et al.*, 2005) aSyn inhibits proteasomal activity and A30P aSyn enhances LC-mediated apoptotic cell death (Tanaka *et al.*, 2001).

UPS function seems to experience an age-dependent decline in its capacity, since aged aSyn TG mice accumulate more aSyn under proteasome inhibition (Ebrahimi-Fakhari *et al.*, 2011). Most LBs in human brain usually immunostain positively with ubiquitin (Spillantini *et al.*, 1998, Sampathu *et al.*, 2003), which suggests that defects in proteasome function could contribute to PD. But ubiquitinated aSyn is found only in the brain tissue fractions, which contain insoluble aSyn, and in a normal situation aSyn undergoes ubiquitin-independent UPS degradation suggesting that the ubiquitin-dependent aSyn degradation pathway may be important in disease states (Tofaris *et al.*, 2003). Sampathu's (2003) characterization of ubiquitination patterns of aSyn in human brain LBs and *in vitro* suggested that aSyn is aggregated in inclusions before ubiquitination. Furthermore, not all aSyn positive inclusions immunostain with ubiquitin in the brain areas exhibiting PD and DLB pathology. It is also shown that phosphorylated aSyn in LBs (Sampathu *et al.*, 2003, Tofaris *et al.*, 2003) and glycosylated aSyn in normal brain (Shimura *et al.*, 2001) are ubiquitinated, suggesting that only some disease-associated posttranslationally modified forms of aSyn undergo ubiquitin-dependent degradation.

In summary, this data indicate that ubiquitin-independent proteasomal degradation is important for the clearance of monomeric aSyn whereas HMW aSyn does not undergo UPS degradation. Overexpression and aggregation of aSyn as well as mutations in aSyn may inhibit UPS, and thus contribute to cellular protein accumulation. Furthermore, decline of UPS activity and reduced amount of proteasome subunits in the brain is associated with PD, but the relationship of aSyn accumulation and UPS dysfunction in the pathogenesis of PD is not yet fully understood.

Autophagy-lysosome pathway

Autophagy-lysosome pathway (ALP) consists of multiple pathways, which degrade proteins in the lysosomal compartment of the cell. Two of them are especially relevant for aSyn cellular clearance: chaperone-mediated autophagy (CMA) and macroautophagy (hereafter, autophagy). CMA substrates are targeted for lysosomal degradation by KFERQ-like peptide sequences (reviewed in Dice, 2007, Cuervo and Wong, 2014). Hsp70 is a chaperone protein, which takes part in substrate recognition by consensus motif and translocation across lysosomal membrane. In order to cross lysosomal membrane, substrate-Hsp70 complex interacts with lysosome-associated membrane protein (LAMP-2A) receptor, which is localized on the membrane of the lysosome. The CMA-substrates need to be unfolded before they are sequestered into lysosomes.

Ammonium chloride specifically inhibits lysosomal protein clearance irrespectively of the pathway targeting substrates to ALP. Ammonium chloride treatment in cell culture significantly increases aSyn half-life indicating that lysosomal clearance is important for its degradation

(Paxinou *et al.*, 2001, Cuervo *et al.*, 2004). There is a specific peptide sequence in the aSyn gene which targets it for CMA-mediated lysosomal clearance. WT aSyn carrying mutated consensus motif or lacking the consensus sequence for CMA targeting exhibits slower cellular turnover than WT aSyn in the PC12 cell line (Cuervo *et al.*, 2004, Vogiatzi *et al.*, 2008), the SH-SY5Y cell line and in primary cortical neurons (Vogiatzi *et al.*, 2008). A53T aSyn was shown to impair CMA-dependent lysosomal clearance in SH-SY5Y and rat-derived PC-12 cell lines (Xilouri *et al.*, 2009), which was followed by compensatory induction of autophagy. In differentiated SH-SY5Y cells, it produced more generalized ALP impairment and enhanced cell death, which could be blocked using autophagy inhibition with 3-methyladenine (3-MA) or silencing of autophagy-related gene 5 (Atg5), which is required for autophagosome formation.

Moreover, silencing of LAMP-2A expression induces aSyn deposition into cells (Vogiatzi *et al.*, 2008), implicating an important role of CMA degradation of aSyn. A30P and A53T mutations and DA-modified aSyn have been shown to have higher affinity towards LAMP-2A receptor but they have reduced translocation into the lysosome thus having reduced CMA degradation (Cuervo *et al.*, 2004, Martinez-Vicente *et al.*, 2008). Furthermore, they enhance the accumulation of other cellular CMA substrates, which means that they block overall CMA function. S129E aSyn, mimicking pS129 aSyn, also has reduced lysosomal translocation capacity as does nitrated, oligomeric aSyn (Martinez-Vicente *et al.*, 2008). This could implicate that aSyn mutations and posttranslational modifications play a role in causing defects in the cellular clearance.

In aSyn TG mice, CMA is induced under elevated aSyn burden as shown with LAMP-2A upregulation (Mak, 2010). LAMP-2A overexpressing cells have higher CMA activity and enhanced aSyn turnover in a stably overexpressing SH-SY5Y cell line (Xilouri *et al.*, 2013). LAMP-2A overexpression protects cells against AAV-aSyn-mediated toxicity in SH-SY5Y and rat cortical neuronal cultures. To support the compensatory roles of different protein clearance pathways this study shows reduced macroautophagy activity in the presence of CMA induction. In the rat SN, AAV-LAMP-2A protects nigral cells against AAV-aSyn-mediated neurotoxicity.

Autophagy is a conserved pathway in eukaryotes. It usually has low bulk degradation activity in basal conditions but it can be highly induced by various stimulations, such as nutrient starvation or cellular stress. Autophagy is regulated by different, complex pathways depending on starvation conditions of the cell (Yorimitsu and Klionsky, 2005). In autophagy, cellular compartments are sequestered into double membrane vesicles, called autophagosomes, which are then fused into the lysosome to form the autolysosome for degradation. Mammalian target of rapamycin (mTOR)-dependent and independent pathways are important players in autophagy induction; inhibition of mTOR induces autophagy (Laplante and Sabatini, 2009) whereas Atg7 is an important factor in induction of autophagosome formation (Komatsu *et al.*, 2005).

Pharmacological inhibition of autophagy by Bafilomycin A1 or 3-MA increases aSyn accumulation only minorly whereas autophagy induction with rapamycin markedly increases its clearance in inducible WT, A30P or A53T aSyn expressing PC12 cell lines (Webb *et al.*, 2003). These results suggested that in normal cellular conditions autophagy does not have major contribution to clearance of aSyn, but when autophagy is induced, it markedly reduces cellular aSyn levels (Webb *et al.*, 2003). In other studies 3-MA has been shown to significantly decrease aSyn clearance (Vogiatzi *et al.*, 2008) or not to have an effect on it (Lee *et al.*, 2004).

In analysis of DLB cortical neuronal samples (and in aSyn TG mice), increased mTOR and decreased Atg7 levels together with abnormal appearance of autophagosomes and lysosomes indicate that autophagy seems to be impaired in the affected brain areas (Crews *et al.*, 2010). Overexpression of WT, but not mutant aSyn, has been shown to impair autophagosome formation in the SKNSH cell line and in aSyn TG mouse brain (Winslow *et al.*, 2010).

In mouse brain, UPS and ALP both have a role in aSyn degradation and there seems to be some level of crosstalk between the systems (Ebrahimi-Fakhari *et al.*, 2011). There is also evidence that UPS acts as the main degradation pathway in normal as well as with increased aSyn burden but autophagy seems to be recruited only under increased aSyn load, as shown with WT and aSyn TG mice. The role of lysosomal clearance of oligomeric aSyn intermediates has also been studied in COS-7 and SH-SY5Y cell cultures, where inhibiting lysosomal clearance with Bafilomycin A1 reduced the clearance of rotenone-induced aSyn oligomers, whereas proteasome inhibition did not alter their clearance (Lee *et al.*, 2004).

Autophagy was shown to be induced after introduction of pre-formed aSyn fibrils (Pff) in the HEK293 cell line, while rapamycin enhanced the clearance of these aSyn inclusions, indicating the role of macroautophagy in the clearance of fibrils/aggregates (Watanabe *et al.*, 2012). Using aSyn Pffs and pharmacological inhibition or induction of autophagy or proteasome in HEK293 stably expressing aSyn cell culture, Tanik et al. (Tanik *et al.*, 2013), showed that macroautophagy and proteasomes are not able to degrade insoluble aSyn aggregates that were seeded by exogenous aSyn Pff's. They also show that autophagy function is impaired in Pff treated cells while aggregated aSyn associates with autophagosome-like structures in cells together with impaired degradation of other autophagy substrates.

In summary, these studies indicate that autophagy has a role in aSyn clearance depending on the cellular conditions. It also seems that autophagy could contribute to the clearance of aSyn fibrils but not insoluble aggregates.

2.3.5 α-synuclein toxicity

Several pathways are involved in aSyn-associated toxicity, which most likely occurs due to aSyn conformational changes, accumulation of toxic aSyn species and finally degradation-resistant aggregates. Toxic conformations of aSyn disturb normal cellular functions and homeostasis. Mechanisms associated with aSyn toxicity are illustrated in Figure 3.

Membrane destabilizing pore-like oligomers

A number of studies have suggested that the prefibrillar or oligomeric form of aSyn is the toxic species of aSyn (Gosavi *et al.*, 2002, Schmidt *et al.*, 2012). To support this, A30P and A53T aSyn mutants are both shown to have enhanced oligomerization capacity whereas they differ in the later stages of the aggregation process; A53T is more prone to fibrillize whereas A30P aSyn aggregates more easily, suggesting that the oligomeric form of aSyn is toxic for the cell (Conway *et al.*, 2000b).

WT, A30P and A53T aSyn form ring-like protofibrils *in vitro*, which have been shown to bind cellular, vesicular and mitochondrial membranes more tightly than the monomeric form (Ding

et al., 2002). A30P and A53T aSyn were shown, by using EM, to promote formation of pore-like (A30P) and annular, tubular (A53T) protofibrils (Lashuel *et al.*, 2002). The membrane-bound aSyn has also been shown to adopt ring-like/annular structure, which resembles pore-forming conformation that has been observed in some bacterial toxins (Ding *et al.*, 2002). In molecular modeling, molecular dynamics simulations and biochemical and ultrastructural analysis of aSyn, it has been found to undergo a conformational change into a dimer form which may be "propagating" in nature, thus facilitating the formation of octameric pore-like protofibrils on the membrane surfaces (Tsigelny *et al.*, 2007 and 2012). aSyn protofibrils that have pore forming activity are shown to affect membrane conductance of the artificial lipid bilayer in ion channel measurement (Kim *et al.*, 2009). In cell culture, overexpression of WT and A53T aSyn increased cell permeability as measured with the calcein assay (Tsigelny *et al.*, 2012). The cells also had increased intracellular Ca(II) levels, and these results are consistent with computer models that suggest increased membrane permeability by aSyn. Taken together, these studies propose that annular membrane-bound aSyn has membrane permeabilizating properties that contribute to its toxicity.

ER stress, mitochondrial dysfunction and apoptosis

Endoplasmic reticulum (ER) stress is induced by incompletely synthetized proteins and buildup of misfolded proteins in the ER (Doyle *et al.*, 2011). It induces an activation of different pathways, collectively called unfolded protein response, which promote cell survival and quality

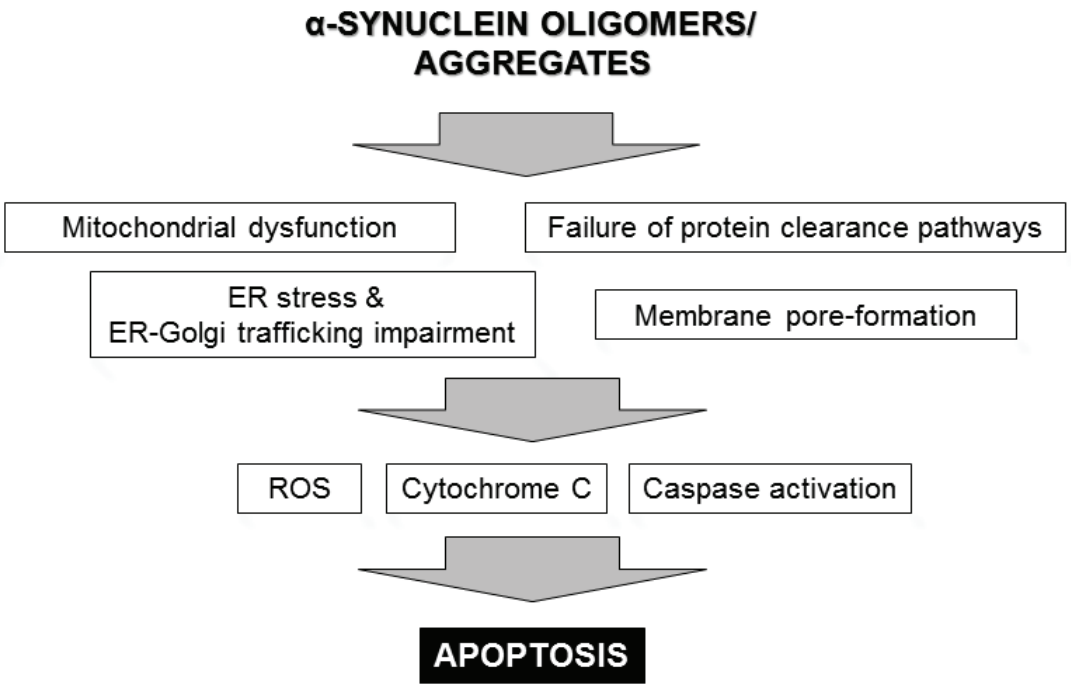

***Figure 3: Mechanisms of α-synuclein toxicity**. Oligomers and aggregates of α-synuclein may disturb normal cellular functions in various ways leading to induction of apoptosis-promoting cascades and finally cell death (modified from Lashuel et al., 2013, Gallegos et al., 2015). ER, endoplasmic reticulum; ROS, reactive oxygen species*

control; autophagy could be one example of an activated quality control pathway. If ER stress is prolonged and survival mechanisms fail this may induce apoptotic cell death pathways via cytochrome c and caspase-activation. Mitochondrial dysfunction and oxidative stress have been linked to PD and toxicity of aSyn (Abou-Sleiman *et al.*, 2006). Mitochondrial outer membrane permeabilization and cytochrome c and pro-caspase release into cytoplasm are markers of early apoptosis (Kroemer and Reed, 2000, Ott *et al.*, 2002).

In A53T aSyn TG mice, overexpression of mutated aSyn causes accumulation of toxic aSyn oligomers in the ER resulting in pathological ER stress, which is similar to what is observed in human PD cases (Colla *et al.*, 2012a and 2012b). In mice, the accumulation of oligomers in the ER was reported to precede the onset of the disease symptoms. In cell culture studies, overexpressed WT, A30P and A53T aSyn aggregates colocalize with mitochondria in immunocytochemistry and immune-EM (Parihar *et al.*, 2009). In addition, aSyn overexpression is associated with mitochondrial dysfunction, ER stress, increased levels of ROS, NO and Ca^{2+} and decreased UPS activity (Smith *et al.*, 2005, Parihar *et al.*, 2008 and 2009). Inducible A53T aSyn overexpression was shown to promote cell death via caspase 3 and 9- activation (Smith *et al.*, 2005).

aSyn interferes with protein secretion which is a sign of defect in ER-Golgi transport (Winslow *et al.*, 2010). aSyn overexpression (Winslow *et al.*, 2010) or oligomers (Gosavi *et al.*, 2002) have also caused Golgi fragmentation in cell culture, which led to subsequent cellular trafficking impairment as noted with reduced cell surface expression of DAT (Gosavi *et al.*, 2002). Impairment of cellular trafficking has also been reported to be associated with aSyn oligomer-mediated disturbances in the microtubular network (Wersinger and Sidhu, 2005, Chen *et al.*, 2007, Zhou *et al.*, 2010).

Dysfunction of protein degradation pathways

Different aggregation states of aSyn may also cause dysfunction of autophagy-lysosome and ubiquitin-proteasome protein clearance pathways, potentially leading to enhanced accumulation of aSyn itself as well as other substrates of these pathways (Betarbet *et al.*, 2005, Ebrahimi-Fakhari *et al.*, 2011, Lynch-Day *et al.*, 2012). Compromised degradation of misfolded and damaged proteins in the cell harms cellular functions and homeostasis (Vilchez *et al.*, 2014). aSyn degradation pathways were reviewed more thoroughly in the previous chapter.

2.4 Propagation of α-synuclein pathology

Neuropathological characterization of aSyn immunostained PD and DLB patients' brain and incidental LB cases, the latter representing non-symptomatic or early stage of PD, has revealed that the amount of LBs and LNs increases during disease progression (Del Tredici *et al.*, 2002, Braak *et al.*, 2003 and 2004, Jellinger, 2004). The LB pathology seems to proceed anatomically from the dorsal IX/X motor nucleus and intermediate reticular zone towards the lower brainstem and eventually reaching up to the cerebral cortex. Clinical PD symptoms usually fully manifest at Braak stages 5-6 (Figure 4) (Braak *et al.*, 2003 and 2004).

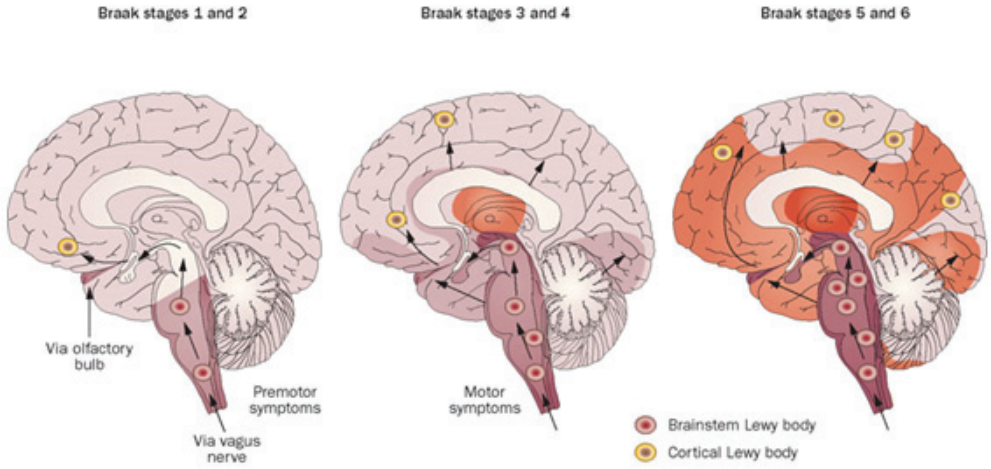

Figure 4. Progression of α-synuclein pathology in the human brain. *Braak stages 1-6 represent different phases of pathology, which starts from the lower parts of the brain and slowly progress towards cortical areas. The darkness of the color represents the amount of pathology observed in the areas at different time points (Adapted by permission from Macmillan Publishers Ltd: Nature Reviews Neurology, Doty, 2012).*

Although there is a substantial amount of evidence that aSyn LB formation and DAergic neuron loss correlate, there seems to be variation between the cases, especially in subjects with a LB-presenting condition other than PD. LB accumulation was shown to be more pronounced in the cortical areas of the patients with non-tremor dominant PD, suggesting a variation of LB spread and load between types of PD (van de Berg *et al.*, 2012). It has also been reported that DAergic neuron loss may occur before aSyn pathology in cases of incidental LBD (Dijkstra *et al.*, 2014). Although this was not the case with PD brains in the same study, where the authors confirmed the earlier findings that DAergic neuron loss occurs as the aSyn-containing inclusions appear in the SNc.

Transplantation of fetal nigral grafts into putamen to replace loss of DA of the PD patients proved to improve motor function in short term studies (Kordower *et al.*, 1995, Hauser *et al.*, 1999). The interest towards the progressive and propagating nature of aSyn pathology was initiated when aSyn and ubiquitin positive LBs and LNs were found in the 10 - 16-years old striatal neuronal grafts in post-mortem PD patients (Li *et al.*, 2008, Kordower *et al.*, 2008a and 2008b, Chu and Kordower, 2010). The accumulation of aSyn in the grafts also correlated with decreased DAT function and worsening of PD symptoms (Chu and Kordower, 2010).

In the studies exploring aSyn cell-to-cell transmission, it is shown to be released from aSyn overexpressing cells (Desplats *et al.*, 2009, Hansen *et al.*, 2011, Kisos *et al.*, 2012) and transferred into cocultured cells in cortical neuronal stem cell culture, in SH-SY5Y derived cells (Desplats *et al.*, 2009) and in HEK293 and SH-SY5Y cell lines (Hansen *et al.*, 2011), but also in the oligodendrocytic cell lines Oli-neu and OLN93 (Kisos *et al.*, 2012). Extracellularly introduced synthetic Pffs are taken up from culture medium into cortical neurons (Lee *et*

al., 2008), mouse cortical neuronal stem cells (Desplats *et al.*, 2009), primary neuronal cells (Volpicelli-Daley *et al.*, 2011) and in HEK-293 cells (Luk *et al.*, 2009), where they are able to form LB-like inclusions. The pathology also recapitulates posttranslational modifications observed in PD, aSyn phosphorylation and ubiquitination (Luk *et al.*, 2009). Oligodendocytic cell lines, Oli-neu and OLN93, primary oligodendrocyte cultures from rat brain (Kisos *et al.*, 2012) and astrocytes, microglial cells and BV2 microglial cells (Lee *et al.*, 2008) also take up extracellular aSyn (Kisos *et al.*, 2012).

In primary neuronal cell culture, Pffs recruit endogenous aSyn to form insoluble PD-like LB and LN inclusions. Fibrils derived from either mouse or human full-length aSyn or truncated aSyn forms 1-120, 58-140 or 61-95 (NAC domain) were all able to seed the pathology/ insoluble aggregate formation, which occurs time-dependently (Volpicelli-Daley *et al.*, 2011). aSyn cellular uptake seems to be endocytosis-dependent because it is blocked or reduced by inhibitors of clathrin-mediated endocytosis, dynasore and monodansylcadaverine, respectively (Hansen *et al.*, 2011). Clathring silencing, which also inhibits chlathrin-mediated endocytosis, reduces aSyn uptake (Kisos *et al.*, 2012). This data indicates that aSyn can be internalized into cells where it may act as a nucleation core to recruit endogenous aSyn for further aggregate formation. Moreover, cytochalacin D, an inhibitor of clathrin-independent endocytosis did not have an effect on aSyn internalization supporting the role of clathrin-mediated endocytosis in aSyn cellular translocation (Ahn *et al.*, 2006). However, there might also be other routes for aSyn translocation into cells, because endocytosis inhibition under reduced temperature did not reduce its cellular penetration.

Seeding of LB/LN pathology and aSyn spreading to connected brain areas is observed in mouse models. In human aSyn overexpressing mouse brain, human aSyn propagates into hippocampally (Desplats *et al.*, 2009) and striatally (Hansen *et al.*, 2011) grafted mouse neurons, which do not express human aSyn endogenously. Additionally, tissue homogenates derived from brainstem and spinal cord from symptomatic (aged over 12 months) human A53T aSyn overexpressing mice (line M83), which were stereotactically injected into the neocortex or STR of non-symptomatic mice, were able to induce bilateral LB/LN pathology 3 months after injection (Luk *et al.*, 2012b). The pathology spread distally from the injection sites in cortex, thalamus, brainstem and major whitematter tracts. Host aSyn expression is required for the pathology to occur because injection of Pffs into aSyn KO mice did not result in inclusion formation. In non-TG mice, striatally injected recombinant aSyn Pff spread into interconnected brain areas within 30 days post-injection and LB/LN pathology was visible at 90 to 190 days post-injection (Luk *et al.*, 2012a). Spreading of LB/LN-like pathology is also seen after injection of aSyn Pffs or homogenate from DLB brains into the SN of C57BL/6J mice (Masuda-Suzukake *et al.*, 2013). Recombinant pre-formed aSyn monomers, oligomers and fibrils are taken up by oligodendrocytes *in vitro* and *in vivo* after injection into mouse cortex (Reyes *et al.*, 2014). aSyn also transferred into grafted oligodendroglial cells in rat brains. This may have relevance in MSA pathology, which is associated with aSyn accumulation into oligodendrocytes.

Altogether, aSyn transmission from neuron to neuron and neuron to glia has been demonstrated *in vitro* and *in vivo*. Once introduced into cell culture or brain, exogenous PD-associated species of aSyn are able to recruit endogenous aSyn into pathological species. When triggered, aSyn pathology has been shown to propagate throughout the brain.

2.5 α-synuclein as a drug target

There is a considerable amount of evidence suggesting that the neurotoxic form of aSyn is the oligomer (Feng *et al.*, 2010, Winner *et al.*, 2011, Rockenstein *et al.*, 2014), which is able to propagate throughout the brain via prion-like mechanisms (Desplats *et al.*, 2009, Crews *et al.*, 2010, Danzer *et al.*, 2012). Although there is no evidence of over-production of aSyn in sporadic PD, aSyn overexpression caused by SNCA duplications and triplications (Singleton *et al.*, 2003, Chartier-Harlin *et al.*, 2004) enhances its accumulation in neurons. Another significant factor in aSyn buildup are defects in protein degradation systems (McNaught *et al.*, 2003, Crews *et al.*, 2010, Winslow *et al.*, 2010, Metcalf *et al.*, 2012, Tanik *et al.*, 2013). Furthermore, aSyn cellular deposition is thought to lead to secretion and pathological spreading of aSyn (Lee *et al.*, 2010b, Alvarez-Erviti *et al.*, 2011, Danzer *et al.*, 2012, Lee *et al.*, 2012, Luk *et al.*, 2012a). Therefore the disease-modifying treatment options targeting aSyn in synucleinopathies aim to reduce the amount and formation of oligomeric aSyn in the neurons and/or to prevent the extracellular cell-to-cell transmission of aSyn (Outeiro and Kazantsev, 2008, Masliah *et al.*, 2011, Lashuel *et al.*, 2013, Valera and Masliah, 2013). Possible treatment strategies targeting aSyn are illustrated in Figure 5.

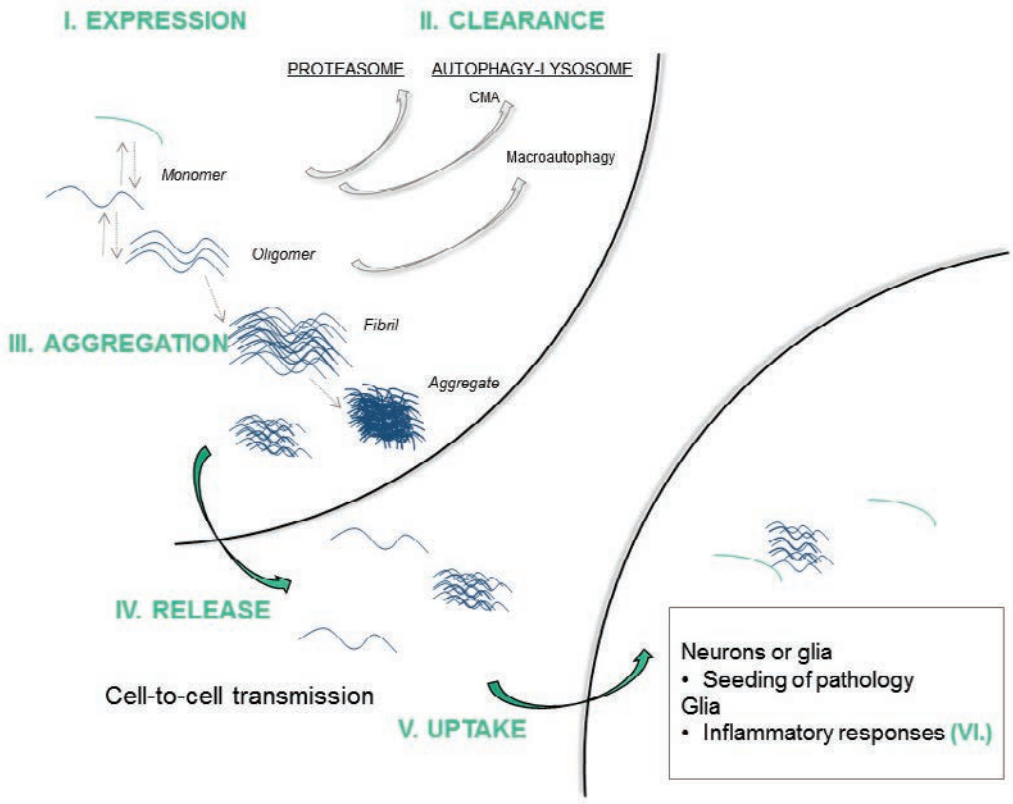

Figure 5: Drug targets against α-synuclein toxic oligomer formation, cellular accumulation and cell-to-cell propagation. *I) reduction of protein expression, II) enhancing the proteolytic clearance, III) reduction of oligomer and aggregate formation, IV) inhibiting aSyn secretion and pathological spreading, V) inhibition of aSyn uptake into neighboring cells, VI) modulation of aSyn-induced inflammatory responses. CMA, chaperone-mediated autophagy*

aSyn overexpression or expression when aSyn degradation is compromised could be suppressed by RNA interference, which is a tool to silence gene expression by preventing the protein synthesis. RNA interference promises to be a feasible way to reduce aSyn amount and consequently reduce its aggregation potential. Small interfering RNAs against aSyn have been tested in the monkey brain where they provided effective aSyn reduction and were proved to be safe (McCormack *et al.*, 2010). AAV-mediated aSyn silencing also proved to be effective in rat, but the silencing vector had some neurotoxic effects, questioning the safety of AAV-vector-mediated drug delivery (Khodr *et al.*, 2011 and 2014).

An approach to prevent oligomer formation and aggregation are molecular stabilizers of the native conformation, such as chaperones and small molecules. At least in theory, chaperones participate in protein unfolding, reduce aggregation and target proteins for degradation, and Hsps have been under investigation for the treatment of PD but the results of their efficacy in animal models have been controversial (Auluck *et al.*, 2002, Ono *et al.*, 2009, Shimshek *et al.*, 2010).

Approaches to promote the cellular proteolytic clearance of aSyn include 1) modulation of endogenous factors that have been shown to directly cleave aSyn, like neurosin (Iwata *et al.*, 2003) and matrix metalloproteinases (Sung *et al.*, 2005) 2) proteasome or autophagy activators, 3) enhancers of lysosomal storage-associated protein, glucocerebrosidase, activity (Schapira, 2015), and 4) active and passive immunization against aSyn (Masliah *et al.*, 2005 and 2011). Active immunization induces an immune reaction against aSyn and has been proposed as an option to reduce intracellular aSyn accumulation (Masliah *et al.*, 2005). Mice expressing human aSyn (Masliah, 2000) were vaccinated with human aSyn. They developed antibodies against human aSyn, and showed sequential reduction of neuronal aSyn accumulation. In passive immunization, antibodies targeted against a specific sequence of the protein are introduced into an organism. It is proposed that the antibodies could recognize the secreted form of aSyn or membrane-bound aSyn therefore reducing the toxic form of aSyn. Passive immunization was tested in the above mentioned mouse line, where it was proved to reduce neuronal aSyn accumulation and associated with improved performance in behavioural tests (Masliah *et al.*, 2011). Passive immunization was also shown to induce microglial aSyn clearance and reduce cell-to-cell transmission of aSyn (Bae *et al.*, 2012). PD vaccinations have further been developed commercially under a company, AFFiRiS, and their vaccination intended for active immunization against aSyn have been shown to reduce aSyn and have beneficial effects related to aSyn pathology in multiple aSyn overexpressing mouse models (Schneeberger *et al.*, 2012, Mandler *et al.*, 2014 and 2015).

2.6 α-synuclein-based mouse models in the modeling of Parkinson's disease

In the previous chapters I have reviewed aSyn pathology, fundamental findings in human PD and other α-synucleinopathies, and mechanisms of aSyn aggregation and propagation. To study these phenomena, it is essential to build disease models, which recapitulate the human condition as closely as possible including pathological hallmarks and measurable behavioural features (face validity of the model) (Beal, 2010, Chesselet and Richter, 2011)). A model should also be

based on a known cause of the disease, such as triplication of SNCA gene (construct validity) (Chesselet and Richter, 2011). Furthermore, predictive validity of the animal model would tell that it is responsive for a treatment that has been proven to also be effective in human – the model predicts symptomatic efficacy. Current therapeutic focus is also largely on neuroprotective effect of new drugs, but predictive validity of a model on neuroprotection cannot be established until the therapy is validated in clinic.

In the sense of cost-effective drug discovery, it would be important to generate a model with a short disease course (Beal, 2010). A suitable PD animal model should aim to produce progressive and selective DAergic neurodegeneration, with loss of striatal DA and SNc cell bodies. Accumulation of ubiquitin, aSyn and phosphorylated aSyn into LB-like fibrillar inclusions, at least in the brainstem and SN, should be the distinguishing feature of the model. Behavioural observations should include reduced grip strength, shortened gait, hypolocomotion, postural instability and tremor. Using pharmacological tools, altered responses to pharmacological challenging of DAergic system or reduction of the behavioural symptoms with levodopa could be observed. Other behavioural measures could monitor non-motor symptoms, like sleep-wake rhythm, hyposmia and constipation assuming that relevant brain or other areas are affected. Although many models have been established in order to mimic aSyn pathology and neurodegeneration in mice, the challenge has been to comprehensively recapitulate the above-mentioned characteristics. Next chapters will review PD mouse models that are based on transgenic or viral vector-mediated aSyn overexpression or toxin-induced aSyn accumulation.

2.6.1 α-synuclein transgenic mice

Since aSyn gene duplications, triplications and mutations have been linked to PD, it is reasonable to use TG overexpression of aSyn as a genetics-based approach to study the role of aSyn in PD pathogenesis. There are many fundamental differences in the used models which will affect the mouse phenotype; is the type of used aSyn mutated, truncated or WT, expression promoters and homozygous or heterozygous expression will all have their influence. Different TG aSyn mouse lines are collected into Table 1. The expression promoters guide the transgene expression to desired cell types that should be brain neurons in PD models. The expression pattern between different promoters varies markedly. Commonly used promoters are mouse brain neuron specific elements from Thy1.2 glycoprotein (Thy1), mouse prion promoter (PrP) and platelet-derived growth factor β (PDGFβ). In a study comparing Thy1 and PDGFβ promoters, Thy1-driven expression was higher and seen in Hc, neocortex, olfactory system, brainstem and SN, whereas PDGFβ-driven expression was observed to be highest in the Hc, neocortex and olfactory system but low in SN and brainstem (Rockenstein *et al.*, 2002). PDGFβ-driven aSyn expression was also observed in glial cells and therefore it could resemble some aspects of MSA pathology. PrP-driven expression was observed in spinal cord, brainstem, deep cerebellar nuclei, white matter and thalamic areas but not in SN (Lee *et al.*, 2002). aSyn expression using calcium/calmodulin-dependent protein kinase IIα (CaMKIIα) promotor resulted in an expression in olfactory bulb (OB), cortex, STR, Hc, thalamus, ventral tegmental area (VTA) and SN (Nuber *et al.*, 2008). In the same study, PrP promoter was compared, and it resulted in much weaker expression in those areas. Thus, it is not only the promoter which will affect the expression pattern and level, but also the method of how the TG mouse is produced. In order to target DAergic neurons more specifically, pituitary homeobox3 (PITX3), TH and DAT promotes have been used in TG mouse

models (Tofaris *et al.*, 2006, Bellucci *et al.*, 2011, Lin *et al.*, 2012, Chen *et al.*, 2015). They produce high to moderate expression in SN, VTA, STR and OB. In conclusion, distinct mouse strains exhibit differentiating expression patterns and levels of aSyn, which may be explained by the expression promotor and method of making the transgenic strain. This may influence the face validity of the model.

Usually human aSyn is overexpressed in the mouse background strain, which either has or does not have endogenous aSyn expression. The A30P mutation has also been inserted in the mouse Snca gene (Plaas *et al.*, 2008). Several mouse lines are made to express WT, A30P or A53T mutated aSyn, and also a double mutated mouse line has been developed. In some studies they have been compared, and A53T seems to produce more toxicity than WT or A30P (Lee *et al.*, 2002, Giasson *et al.*, 2002, Kurz *et al.*, 2010), while A30P accumulates at the same level as WT (Kahle *et al.*, 2001, Lee *et al.*, 2002). Mouse lines expressing C-terminally truncated aSyn, aSyn(120) (Tofaris *et al.*, 2006) and A53T aSyn(130) (Wakamatsu *et al.*, 2008), which has been shown to be part of the LBs in human, have also been generated. They both express truncated aSyn under TH promoter, and show aSyn accumulation in TH+ SNc neurons associated with SNc neuron loss. In addition, both models showed hypolocomotion in locomotor activity test. In the model of Tofaris et al (Tofaris *et al.*, 2006), there were aSyn and Thioflavin S-positive LB-like inclusions present in SN neurons, which were shown to be insoluble aggregates by urea extraction and aSyn WB.

The toxicity of aSyn seems to be dependent both on the expression level of aSyn which is guided by the promoter, as well as on gene dosage by homozygosity versus hemi/heterozygosity. Homozygous animals show more severe and earlier pathology (Neumann *et al.*, 2002). When aSyn was expressed at the normal level relative to endogenous mouse aSyn expression, no toxicity or abnormalities were observed in mice homozygous to human S129AaSyn or S129D aSyn (Escobar *et al.*, 2014).

In order to recapitulate human PD characteristics, the mouse line should show age-dependent accumulation of aSyn and LB pathology in the SN. Various mouse lines show high or moderate aSyn expression throughout the brain, and accumulation is seen in the SN (Tofaris *et al.*, 2006, Lim *et al.*, 2010, Chesselet *et al.*, 2012, Lin *et al.*, 2012), but quite often the expression seems to be minor or absent in the SN area (Masliah, 2000, van der Putten *et al.*, 2000, Giasson *et al.*, 2002, Neumann *et al.*, 2002, Rockenstein *et al.*, 2005). aSyn pathology is generally seen in cortical and hippocampal brain areas, which resembles DLB pathology. aSyn accumulation in the Hc results in minor to moderate memory and learning impairment (Nuber *et al.*, 2008) whereas accumulation in OB is connected with olfactory deficit (Farrell *et al.*, 2014). Some models also show gross spinal cord motor neuron aSyn pathology associated with motor neuron disease which leads to fast paralysis and death in a few weeks from the onset of the symptoms (van der Putten *et al.*, 2000, Martin *et al.*, 2006). This is not a phenotype associated with PD pathology in humans, which is slow-progressing and does not have an effect on motor neurons, although it provides information about aSyn toxicity.

The LB-like aSyn pathology, characterized by proteinase K (PK)-resistant aSyn inclusions observed in IHC or detergent-insoluble aSyn in WB, aSyn phosphorylation and possible ubiquitination seem to associate with neuronal loss in different brain areas (van der Putten *et*

al., 2000, Neumann *et al.*, 2002, Martin *et al.*, 2006, Freichel *et al.*, 2007, Ikeda *et al.*, 2009, Clark *et al.*, 2010, Lim *et al.*, 2011, Chesselet *et al.*, 2012, Farrell *et al.*, 2014). Some of the studies have shown findings of reduced TH staining in the SN and striatal DA content associated with aSyn pathology (Masliah, 2000, Tofaris *et al.*, 2006, Ikeda *et al.*, 2009, Ono *et al.*, 2009, Chesselet *et al.*, 2012), whereas some fail to show any effect or the effect is mild on nigral TH positive neurodegeneration, as may be expected if no major aSyn pathology exists in the area (Neumann *et al.*, 2002, Nuber *et al.*, 2008, Kurz *et al.*, 2010).

Studies comparing A53T aSyn to WT and/or A30P aSyn TG models did not generally find motor behavioural deficit in WT and A30P aSyn expressing mice whereas A53T has more pronounced pathology (Lee *et al.*, 2002, Giasson *et al.*, 2002, Lim *et al.*, 2011, Chen *et al.*, 2015). In some models hyperactive and anxiety-like behaviours were observed (Bellucci *et al.*, 2011, Lin *et al.*, 2012, Chesselet *et al.*, 2012, Farrell *et al.*, 2014), which indicates the imbalance of DAergic system of the brain and is suggested to be related to impaired DAT trafficking and dysregulation of DAergic signaling. In TG mice, typical findings of impaired motor performance are difficulties in challenging motor tests: rotarod, beam walk and pole test, and reduced activity in horizontal and vertical movement test (Tofaris *et al.*, 2006, Chesselet *et al.*, 2012). These usually develop in mice over 12 months old.

aSyn overexpression produces varying pathology depending on gene dosage, expression site in the brain and type of aSyn. Common challenges with the TG expression of aSyn seem to be to direct the expression in the SN, recapitulate the LB-like inclusion formation and progressive neurodegeneration in the SNc. Although the models overexpress moderate to high levels of aSyn, the disease phenotype progression in mice is not always comparable to human; phenotype of motor decline may not present itself as it does in human or it is not progressive, and in some cases it may present itself as a motor neuron degeneration. Moreover, the TG aSyn models usually overexpress either WT or mutated human aSyn, whereas most of the sporadic PD cases do not have pathophysiological overexpression of aSyn.

2.6.2 Viral vector-mediated α-synuclein gene-delivery

An approach to target the gene expression more locally in the brain is to use stereotactic injection to deliver the viral vectors containing the desired gene directly in the brain. Viral vector is utilized to transduce the gene of interest in the desired neurons without being toxic to neurons themselves. Lentiviruses (LV) and AAV are most commonly used as gene delivery systems. The overall difference appears to be that LVs have longer-lasting expression capacity than AAVs, but in AAV vectors the overexpression starts quicker. Nowadays, AAV is preferred over LV because it is considered to be a safer option. The transduction efficacy of viral vector preparations is defined, in addition to vector origin, by promoter elements, which have different strengths and may vary on the cell type specificity, and the titer of the purified vector. AAVs have a variety of serotypes, which are shown to have different transduction capacities in mice (Korecka, 2010). In mice, neutralizing antibodies against viral vectors have been detected, which could decrease the transduction and therefore prevent the expression of the gene (Rapti *et al.*, 2012).

Much greater number of TG mouse models than viral vector-based models exist. An explanation could be that the TG models are more common in mice whereas a lot of viral vector studies have

Table 1: *Transgenic aSyn-based mouse strains*

Mouse strain (Line) / Promotor / Background	Motor behaviour	Findings:				Ref.
		aSyn expression	Pathology	DAergic system	Other	
A30P aSyn (heterozyg 31 & 18) WT aSyn (14 & 23) / Thy1 C57BL/6	No behavioural deficit up to age 12 m	A30P: 2x accumulation into neurites and cell bodies: Purkinje cells, nucleus dentatus, SN, STR, Hc, neoctx, and brainstem	Both: cytosolic and neuritic accumulation, no LBs, but swollen neurites present, detergent-insol aSyn	ND	ND	Kahle, 2000 and 2001
A30P aSyn (homozyg 31H, heterozyg 31 & 18) / Thy1 / C57BL/6J	12 m: locomotor activity ↑ Rotarod from 70 weeks memory acquisition ↓ 9 m hom: Progressive symptoms from abnormal gait & tail posture to paralysis of the hind limbs	zona incerta, superior colliculus, deep mesencephalic reticular field, central gray, pontine and medullary reticular formation and cerebellar nuclei	PK-resistant & paSyn , ubiq+ (fibrils) in brainstem, midbrain and spinal cord Hom 9 m, het 24 m 12 m: somal & neuritic pathology in amygdala some in motor & somato-sensory ctx	DA normal at 24 m/het, and at 8 m/hom minor changes in 5-HT and 5-HIAA	Astrogliosis (GFAP IHC)	Neumann *et al.*, 2002, Freichel *et al.*, 2007
A30P aSyn / PrP / C57BL/6J	ND	Increased brain aSyn expression	12 m: no LB/LN, intra-cellular aSyn accumulation in ctx, Hc, SN	normal TH, DA storage capacity ↓		Jäkälä *et al.*, 2002, Yavich *et al.*, 2004

Table 1 cont.

Mouse strain (Line) / Promotor / Background	Motor behaviour	Findings:				Ref.
		aSyn expression	Pathology	DAergic system	Other	
aSyn (61) / Thy1 / C57Bl6	Young: cylinder, locomotor activity ↑ colon dysfunction, disrupted circardian rythm Beam walk, nest building ↓ 14 m:locomotor activity ↓	Neurons, presynaptic terminals, neuropil SNc (3.4x), Thalamus (6x), DG, Hc CA1-3, OB & olfactory nucleus, orbital/ association ctx, motor ctx, sensory ctx in SN TH+	Proteinase K-resistant inclusions pS129 aSyn ↑ in ventral mesencephalon/ SN, STR, ctx, frontal ctx, and Hc	6 m: STR extracellular DA & 3-methoxytyramine ↑ 14 m: STR DA 40% ↓ TH: WB, 23% ↓ IHC 17% ↓	ND	Rockenstein *et al.*, 2002, Fleming *et al.*, 2004 and 2008, Fleming and Chesselet, 2006, Wang *et al.*, 2008, Wu *et al.*, 2010, Lam *et al.*, 2011, Kudo *et al.*, 2011, Chesselet *et al.*, 2012
aSyn A30P+A53T/ Thy1 / BDF1 heterozygous	3-11 m: rotarod ↓ pole test ↓	1.3x brainstem, Hc, thalamus, cerebral ctx and cerebellum	Cytoplasmic inclusion in SN aSyn+, paSyn, nitrated aSyn+, ubiquitin + 8mo: EM: intracytoplasmic inclusions in brainstem	17 m: STR DA 20%↓ ACh ↓ Thalamus DA & 5-HT ↓ SN TH+ neurons 12 m: WB TH 30% ↓ STR DA 40%↓	16 m: Cerebellar astrocytosis	Ikeda *et al.*, 2009, Ono *et al.*, 2009
A53T aSyn (9831 & 9956) / Thy1 / C57BL/6	early-onset >3 weeks progressive motor decline, rotarod	Cellbodies & dendrites Telencephalon, brainstem, Hc CA1 & spinal cord	LB-like pathology in spinal cord motoneurons, ubiq.+ & p-tyrosine + no fibrillar aSyn	ND	Neuromuscular degeneration Astrogliosis (GFAP) in spinal cord motor neurons	van der Putten *et al.*, 2000
aSyn(120) truncated / TH / C57BL/6JOlaHsd	18 m: locomotor activity ↓ motor response to D-amph ↑	TH+ neurons; synaptic terminals soma & dendrites OB, SN, STR	12-14 m: pathological alterations in SN, neurites, perinuclear aggregates and inclusions	3-12 m: STR DA & HVA 30%↓ 12 m: STR & SN abnormal DAT distribution STR DAT 59% ↑	ND	Tofaris *et al.*, 2006, Bellucci *et al.*, 2011

Table 1 cont.

Mouse strain (Line) / Promotor / Background	Motor behaviour	Findings:				Ref.
		aSyn expression	Pathology	DAergic system	Other	
A53T aSyn(130) truncated (1702) h A53T aSyn / Rat TH / C57BL/6J	Locomotor activity ↓ Recovers with L-DOPA	1.5 x in soma, axons and nucleus. SNc , VTA and NAcc and STR terminals	ND	8 w human A53T aSyn (130) : SNc TH+ neurons 45% ↓, not progressive rt-PCR: TH, DAT & c-ret ↓ STR DA & HVA 50 % ↓	GAD1 and GFAP normal	Wakamatsu *et al.*, 2008
h aSyn (D) / PDGF-β / C57BL/6× DBA/2F	12 m: rotarod ↓	human aSyn expression in nerve terminals	2 m: IHC inclusions in neoctx, Hc CA3, OB some in SN TH+ neurons 11 m: EM intracellular inclusions amorphous, non-filamentous aggregates	12 m: STR: TH+ terminals (IHC), total TH (WB), TH activity ↓ STR: TH+ terminals 45% ↓ DAT+ terminals 43 % ↓	IHC: also in glial cells	Masliah, 2000, Rockenstein *et al.*, 2002, Clark *et al.*, 2010
aSyn-eGFP/ PDGF**β** / C57BL/6× DBA/2F	ND	high expression in neoctx & Hc, lower level in brainstem, thalamus, basal ganglia and cerebellum	Large cytoplasmic inclusions and granular aggregates	Presynaptic synaptophysin+ terminals 25 % ↓	Lysosomal pathology Co-localization of GFP/ aSyn & Cathepsin D	(Rockenstein *et al.*, 2005)
WT aSyn (3 & 9) A53T aSyn (9 & 12) Conditional KO/ CaMKIIα / C57Bl/C3H	ND Memory deficit (impaired contextual fear) correlates with aSyn pathology	WT: 2-3x A53T: 2-5x OB, ctx, STR, Hc, thalamus, VTA, SN	4 m: abnormal aSyn in IHC 20–22 m: ↑ in neoctx, Hc CA1, cingul & entorh ctx ThioS+ inclusions, aSyn in FA-insol. WB paSyn ↑ ubiq ↑	ND	14 days: NeuN+ cells in DG & Hc ↓ caspase-3 activation 21 days: Synaptic loss Progressive gliosis (GFAP)	Lim *et al.*, 2010 and 2011

Table 1 cont.

Mouse strain (Line) / Promotor / Background	Motor behaviour	Findings:				Ref.
		aSyn expression	Pathology	DAergic system	Other	
aSyn Conditional KO / CaMKIIα or PrP / C57BL/6 /	18 w: rotarod ↓ Motor learning ↓ Long-term memory deficit; Morris water maze ↓	OB, ctx and basal gaglia ↑ (WB) CaMKIIα driven expression ↑ than PrP	Colocalization of aSyn and TH in OB and SN	CaMKIIα aSyn 25 m: DA in OB ↓ normal in STR or midbrain	ND	Nuber *et al.*, 2008
A53T aSyn (M83 ja M91) WT aSyn (Lines M7, M12, M20) / PrP / C57Bl/C3H "model of aSynucleinopathy"	7 m homozygous A53T: disease start and proceed in 10-21 to mice being unable to feed themselves. No disease phenotype in WT mice	Similar expression pattern between mouse and human aSyn	A53T: inclusions in, spinal cord, brainstem, deep cerebellar nuclei & white matter, neurites in STR, motor ctx, 10-11 m: filamentous inclusions (IEM), in deep cerebellar nuclei & spinal cord	ND	Astrocytic gliosis, (GFAP IHC)	Giasson *et al.*, 2002, Betemps *et al.*, 2014
WT aSyn A53T (G2-3, H5 & N2-5) A30P (O-2)/ PrP / C57Bl6/J	A53T: Onset of symptoms at 10-15 m, fast-progressing symptoms including Locomotor activity ↓ bradykinesia, dystonia, progressive paralysis leading to death in 21 days WT & A30P: no abnormalities	4-15x A53T: Pathological accumulation in neuronal cell bodies and neurites in midbrain, brainstem and spinal cord motor neurons	Ubiquitin+ accumulation, Thio-S+ inclusions Symptomatic mice: insol. HMW aSyn in brainstem, dendritic aSyn inclusions with abnormal mitochondria A30P: high expressing line, accumulation in cell bodies, but no ubiquitin accumulation	ND	GFAP ↑ A53T (G2-3) 9-15 m: motor neurons 75% ↓ Brainstem & spinal motor neurons IHC cleaved caspase-3 ↑ spinal motor neurons p53 ↑ Symptomatic A53T: ER stress & caspase-12 activation	Lee *et al.*, 2002 used also in Martin *et al.*, 2006, Colla *et al.*, 2012a, and 2012b

Table 1 cont.

Mouse strain (Line) / Promotor / Background	Motor behaviour	Findings:				Ref.
		aSyn expression	Pathology	DAergic system	Other	
A53T aSyn (PrPmtA & B) H WT aSyn / PrP / FVB/N	Aged mice: Rearing, step length and grip strength ↓	human aSyn in neuropil, cell bodies & neurites A53T aSyn: abnormal distribution OB, cerebral ctx, STR, basal forebrain, Hc, midbrain, pons, medulla oblongata, cere-bellum, spinal cord	A53T aSyn accumulation in the TH+ cell bodies in SN at the age of 7 & 16 m, some insol. monomeric aSyn in SN no aSyn containing filamentous LBs at 13 m	Normal TH cell counts & TH WB Aged A53T: STR DA ↑ DA receptors D1 & D2 ↑ STR COMT ↓	no astrocytosis Aged A53T lack of LTD in corticostriatal neurons	Gispert *et al.*, 2003, Kurz *et al.*, 2010
A53T aSyn / PrP / B6; C3-Tg-Prnp/SNCA*A53T/83Vle/J	Locomotor activity ↑ anxiety-like phenotype 14-16 m: olfactory impairment	Not measured in other areas	HMW aSyn in adrenal gland, PK-resistant aSyn in myenteric plexus OB: LB-like aggregates; Thio S+ & paSyn+	TH activity & phosphorylation ↑ Protein phosphatase 2A activity ↓	ND	Farrell *et al.*, 2014
A53T aSyn, (DASYN53) Conditional KO/ DAT/ Tg(tetO-SNCA× A53T)E2Cai/J	No motor deficit	6 w: 5-8x expression compared to endogenous aSyn expression In 95% of midbrain DAergic neurons, hypothalamus, OB	Colocalization of COX1, SOD2 & aSyn in SNc; mitochondrial inclusions	DASYN53 SN DA 3 m: 21%↓ 6 m: 35% ↓ 12 m: DA, DOPAC & HVA ↓ normal NE, 5-HT & 5-HIAA TH terminals in dorsal STR 12 m: 39 % ↓	mitochondrial fragmentation Mitochondrial inclusions precede DA neuron pathology p62 & LC3B + inclusions ↑	Chen *et al.*, 2015
A53T aSYn Conditional KO / PITX3-IRES2- tTA/ tetO- / C57BL/6J	Horizontal and vertical movement ↓ stride length ↓ rotarod ↓	2-4x cytosol, nucleus & processes SN & VTA cerebral ctx, OB, STR cerebellum, brainstem, spinal cord, Hc, and	12 and 18 m: IHC: aSyn accumulation in midbrain DAergic neurons WB: HMW aSyn	STR: DA release ↓ DA ↓ 12 m: SN & VTA: DA neurons 40 % ↓	SN: GFAP and Iba1 ↑ Golgi fragment. P62, LC3B & LAMP2 ↑ LC3BII --	Lin *et al.*, 2012

Table 1 cont.

Mouse strain (Line) / Promotor / Background	Motor behaviour	Findings:				Ref.
		aSyn expression	Pathology	DAergic system	Other	
SNCA S129A *SNCA* S129D / PAC / FVB/N×129S6	normal colon motility	6-8 w: 0.7x vs. endogenous mouse aSyn (rt-PCR, WB) No inclusions at 9-12 m	No	ND	Normal synapses, synaptic vesicles, development and breeding	Escobar *et al.*, 2014
mouse A30P aSyn / C57BL/6	Beam walk ↓ Stride length ↓ Response to amph.+ reserpine ↓	ND	ND	STR DA & DOPAC ↓	ND	Plaas *et al.*, 2008

Abbreviations: 5-HIAA, 5-hydroxyindole acetic acid; 5-HT, serotonine; ACh, acetylcholine; aSyn, a-synuclein; COMT, catechol-o-methyl transferase; COX1, cyclooxygenase, ctx, cortex; DA, dopamine; DAT, dopamine transporter; DG, dentate gyrus; DOPAC, 3,4-dihydroxyphenylacetic acid; EM, electron microscopy; ER, endoplasmic reticulum; GAD, glutamic acid decarboxylase; GFAP, glial fibrillar acid; h, human; Hc, hippocampus; HMW, high-molecular weight; HVA, homovanillic acid; Iba1, Ionized calcium binding adaptor molecule 1; IHC, immunohistochemistry; KO, knock out; LB, Lewy body; LC3B, microtubule associated protein light chain 3B; LAMP2, lysosome-associated membrane protein; LTD, long-term depression; m, month; NAcc, nucleus accumbens; ND, not determined; NE, noradrenaline; OB, olfactory bulb; p62, SQSTM1/p62; paSyn, phosphorylated aSyn; PCR, polymerase chain reaction; PK, proteinase K; SN, substantia nigra; SOD2, superoxide dismutase; STR, striatum; TH, tyrosine hydroxylase; ThioS, thioflavin S; Ubiq, ubiquitin; VTA, ventral tegmental area w, week; WB, Western blot; WT, wildtype

been done in rat. Published aSyn viral vector based mouse models are combined in Table 2. The fact that the virus will be injected via microinjection which can be made unilaterally, leaving the other side of the brain as a control makes it easier to analyse and compare the pathology than with TG expression. Moreover, by using viral vectors, the overexpression of the protein can be started at any age, whereas TG expression starts when the gene-expression starts, unless the model has been designed as a conditional expression system. Usually studies are controlled by the use of a green fluorescent protein (GFP) viral vector, which makes it convenient to also analyse the transduction and spreading of the expressed gene.

In the LV-based model, the expression is seen moderately fast, in weeks to months, but the aSyn pathology takes some months to occur (Lauwers *et al.*, 2003, Gerard *et al.*, 2010). aSyn-containing inclusions were formed in the model of Lauwers et al. (Lauwers *et al.*, 2003) in STR and SN, where the injections were directed. But they could not find any Thioflavin S or Congo red positive inclusions, which describe the fibril formation. Although mild neurodegeneration was observed in the model by silver staining, the effect on the DAergic system was mild at one year post-injection and the mouse motor behaviour was not analysed in the study.

In all the AAV studies the vector was injected into the SN and it produced faster-onset, within weeks, aSyn accumulation in the injection area than LV. In these studies, AAV2 serotype was the most frequently used and in all vectors, the woodchuck hepatitis virus posttranscriptional regulatory element (WPRE) enhancer element was present. The promoters that have been used vary from cytomegalovirus (CMV), chicken β-actin (CBA), and Synapsin-1 to PDGFβ.

In only one of the studies, LB-like inclusion formation, striatonigral DAergic system and motor behaviour of the mice were studied, in the model of Olivera-Salva (Oliveras-Salva *et al.*, 2013). AAV2/7 human aSyn and human A53T aSyn both induced fast accumulation and localization of LB-like, paSyn positive and urea insoluble, inclusions in TH+ SN neurons, which degenerated as was shown with the loss of TH+ cells in the SN and STR terminals by 8 weeks post-injection. Mice developed later-onset motor deficit in cylinder, locomotor activity and rotarod tests at week 12 post-injection. Furthermore, this was the only model where viral vectors were shown to cause motor impairment. Motor behaviour was measured by Decressac et al (Decressac *et al.*, 2012b), but AAV human aSyn did not cause toxicity and therefore no turning behaviour was observed in the amphetamine-induced rotation test. In most of the models, the viral vector-delivered aSyn is shown to be expressed in the DAergic neurons in the SN or nigral area within two months post-injection, but it does not induce any toxicity, the effect is very mild or the effect on the SN neurons was not quantified (Dong *et al.*, 2002, Lauwers *et al.*, 2003, St Martin *et al.*, 2007, Theodore *et al.*, 2008, Cao *et al.*, 2010, Decressac *et al.*, 2012b).

Viral vector-mediated gene delivery has a good potential to offer a time- and cost-efficient alternative to conventional TG mice. In most of the studies, the vectors are shown to guide the expression of aSyn locally, in the SN. But the data about their efficacy of producing PD-like phenotype, LB-like inclusions, DAergic cell loss and motor impairment is still partially unclear and not sufficient to draw a conclusion about their real usefulness in modeling PD.

Table 2: *Viral vector-mediated aSyn gene delivery*

aSyn/ Virus	Promoter Enhancer	Titer Injection site	Behaviour	Findings: aSyn	Findings: DAergic system	Findings: Other	Ref.
h aSyn h A30P aSyn LV	hCMV WPRE	"high"/ 2 µl, STR, SN (A30P only) or amygdala unilaterally	ND	2-10 m: neuronal soma & neurites in the injected areas, no difference btw WT & A30P aSyn STR inj. 6m: inclusions in STR, 60 % ubiq+ 12 m: larger inclusions but no fibrillar aSyn (ThioS/ Congo red -)	SN inj. 10-12 m: TH 10-25 % ↓	Degeneration of neurons detected by silver-staining in STR	Lauwers *et al.*, 2003, Gerard *et al.*, 2010
h aSyn rAAV	CMVie-CBA WPRE	$8.9x10^{10}$ (VG/ml) 3 µl, SNc unilaterally	ND	Colocalization of h aSyn in TH+ neurons, also other cell types affected	4 w: No TH+ cell loss 6 m: TH+ cells 25% ↓	ND	St Martin *et al.*, 2007
h aSYn rAAV2	CBA WPRE	3.5×10^{12} (VG/ml) 2 µl SN unilaterally	ND	Cytoplasmic expression in SNc and STR processes	ND	Immune activation by aSyn over-expression: CD68+ microglial activation, CD3+ & IgG+ cells in SNc/ SNr, peak at 4 w	Theodore *et al.*, 2008
h aSyn AAV2	not stated	$6.0x10^{10}$ (VG/ml) 2 µl SNc unilaterally	ND	Expression in SNc, not quantified	SNc TH-neurons 27% ↓	4 w: activation of nuclear factor-κB p65, microglia activation	Cao *et al.*, 2010
h aSyn AAV6	synapsin-1 WPRE	$2,5 \times 10^{13}$ (GC/ml) 2.0×10^{7} gc/3µl	6 w: no change in amph-induced rotation	ND	SN: TH 91 ± 4% of control side	Nurr1 cKO mice: 8 w: SN & STR TH 56% ↓ SN: VMAT2 65% ↓ amph-induced ipsilateral turning	Decressac *et al.*, 2012a
h A53T aSyn rAAV	PDGFβ WPRE	"high"	ND	7 w: Colocalization of h aSyn in TH+ neurons	No TH+ cell loss in SN or TH+fibre loss in STR	aSyn overexpression did not enhance MPTP toxicity	Dong *et al.*, 2002

Table 2 cont.

aSyn/ Virus	Promoter Enhancer	Titer Injection site	Behaviour	Findings:			Ref.
				aSyn	DAergic system	Other	
h aSyn h A53T aSyn rAAV2/7	CMVie- synapsin-1 WPRE	$8{,}0x10^{11}$ $2{,}7x10^{12}$ (GC/ml) 2µl SNc unilaterally	8 w: No motor deficit >12 w, WT aSyn: Cylinder ↓ Open field↓ Rotarod ↓	Colocalization of aSyn in TH+ SN neurons SN: 4 & 8 w: inclusions & urea-sol aSyn↑ paSyn in SN ↑, dose & time dependently up to 8 w	Progressive AV-dose-dependent TH+ cell loss, **SN:** A53T: 4 w 51% 8 w 9% ↓ WT: 4 w 45% 8 w 50% ↓ **STR**: A53T: 4w 57% 8w 91% ↓ WT: 4w 56% 8w 86% ↓	ND	Oliveras-Salva *et al.*, 2013

Abbreviations: AAV, adeno-associated virus; aSyn, a-synuclein; CBA, Chicken β-actin ; CMV, cytomegalovirus; DA, dopamine; GC, genome copy; h, human; KO, knock out ; LV, lentivirus; m, month; MPTP, 1-methyl-4-phenyl-1,2,3,6-tetrahydropyridine; ND, not determined; paSyn, phosphorylated aSyn; PDGFβ, Platelet-derived growth factor-β; SN, substantia nigra ; STR, striatum ; TH, tyrosine hydroxylase; ThioS, thioflavin S; Ubiq, ubiquitin; VG, vector genome; VMAT2, vesicular monoamine transporter 2; w, week; WPRE, Woodchuck hepatitis virus posttranscriptional regulatory element; WT, wildtype

2.6.3 Other mouse models showing α-synuclein accumulation

In this chapter, I will review non-TG mouse models of PD, where aSyn accumulation is induced by toxins or by inoculating the brain with exogenous aSyn fibrils. The models are collected to Table 3. In the past few years, models using recombinant aSyn Pffs or brain homogenate of TG mouse or human PD cases showing aSyn pathology and clinical symptoms have been established. These models were set up after evidence of aSyn cell-to-cell transmission in grafted neurons (Li *et al.*, 2008, Kordower *et al.*, 2008a and 2008b, Chu and Kordower, 2010). They are based on an intracerebral stereotactic injection of Pffs (Luk *et al.*, 2012a and 2012b, Masuda-Suzukake *et al.*, 2013, Osterberg *et al.*, 2015) or human (Masuda-Suzukake *et al.*, 2013, Recasens *et al.*, 2014) or mouse (Luk *et al.*, 2012b) pathological brain tissue homogenates. The common feature of all the published models seems to be sonication of the preparation before stereotaxic brain injection, suggesting that certain forms of aSyn are pathogenic and able to spread in the brain. In all models, injected aSyn seems to be recruiting endogenous mouse aSyn into progressive time-dependent LB-like inclusion formation and interestingly, injected human aSyn fibrils were visible 24h after the brain injection but had disappeared at the later time points (Recasens *et al.*, 2014). This suggests that exogenous pathogenic aSyn species could convert endogenous aSyn into a pathogenic conformation. Inclusions typically contain paSyn and colocalize with ubiquitin (Luk *et al.*, 2012a and 2012b, Masuda-Suzukake *et al.*, 2013, Recasens *et al.*, 2014, Osterberg *et al.*, 2015) and Thioflavin S (Luk *et al.*, 2012b, Osterberg *et al.*, 2015). Inclusions are spreading to the adjacent brain areas and to the contralateral side. Endogenous mouse aSyn expression is required for the pathology because the effect is not seen in aSyn KO mice (Luk *et al.*, 2012a and 2012b). Furthermore, monomeric aSyn injection did not cause the pathology.

Although the mice were followed up to 15 months post-injection, the DAergic SNc neuronal loss was moderate (Luk *et al.*, 2012a, Recasens *et al.*, 2014), was not seen in the studies

(Masuda-Suzukake *et al.*, 2013) or was not measured (Luk *et al.*, 2012b, Osterberg *et al.*, 2015). Mouse line M83, which was initially characterized by Giasson et al. (2002), has been shown to develop symptoms leading to paralysis and death within 21 days after onset. Luk et al (2012b) showed that injection of both aSyn fibrils and brain homogenate from symptomatic mice into non-symptomatic, young mice advanced the development of these symptoms and earlier death. Recasens (2014) and Luk (2012a) observed approximately 35 % cell loss in the SN at 17 and 6 months after inoculation, respectively. They both showed reduced motor coordination in mice at 4 and 6 months post-injection, respectively, but in Recasens' study, the impairment vanished at later time points. Considering that this loss of neurons is mild, it is not surprising that mice may learn to cope with it over time.

Taken together, administration of exogenous aSyn species directly into the brain has provided new evidence about spreading of aSyn, but most of these models fail to recapitulate the core features of PD-related pathology. This supports the idea that multiple mechanisms act together in PD, of which the abnormal, toxic form of aSyn is one contributing factor, but aSyn overload itself does not necessarily lead to PD.

Three different toxin models have been shown to induce aSyn accumulation in the SN. LC is a proteasome inhibitor, which could induce aSyn accumulation by blocking its degradation. It

Table 3: *Other mouse models showing aSyn accumulation*

Method/ Delivery	Strain	Time for pathology	Findings				Ref.
			Behaviour	aSyn pathology	DAergic system	Other	
aSyn fibrils/ brain homogenates							
Sonicated brain-stem & spinal cord homogenate from symptomatic mice (>12 m) OR recombinant h aSyn fibrils (truncated h aSyn120 OR full length protein) / Unilateral micro-injection, Neoctx OR STR	2-5 months h A53T aSyn PrP mice (Line M83), at healthy status	30-90 days	Reduced survival (Age 204 vs. 3016 days)	Progressive, bilateral spread of LB/LN pathology in ctx, thalamus, hypothalamus, brainstem nuclei, and major whitematter tracts Colocalization of aSyn with Ubiq. & ThioS SDS & FA-sol. aSyn forms No pathology in aSyn KO mice	ND	ND	Luk *et al.*, 2012b
Sonicated SNc homogenate from h PD brain / Intracerebral injection, above SNc	C57Bl/6	4 to 17 months	4 m: pole test, but no motor impairment at 17 m	h aSyn visible 24 hours post-injection but not at later time points from 4 to 7 m, 4 m: PK-resistant aSyn, paSyn in injected SN, co-localization with TH, but not at 17 m	Progressive pathology, SNc neurons 37%↓	Astrogliosis	Recasens *et al.*, 2014
Injection of sonicated recombinant aSyn fibrils / Unilateral micro-injection, dorsal STR	C57BL6/C3H F1	30, 90 & 180 days	Rrotarod ↓ Wire hang ↓	LB/LN pathology in interconnected brain areas visible at 30 days, progressive paSyn colocalization with Ubiq. & Hsp90 No pathology in aSyn KO mice	At 180 days: SNc: TH+ cells at 180 d 35 % ↓ STR: TH & DAT OD ↓ ThioS staining in AADC+ cells	ND	Luk *et al.*, 2012a)

Table 3 cont.

Method/ Delivery	Strain	Time for pathology	Findings				Ref.
			Behaviour	aSyn pathology	DAergic system	Other	
Sonicated recombinant h aSyn fibrils OR sonicated insol. fraction of DLB brain / unilateral microinjection, SN	female C57BL/6 J mice 4-6 months	15 months	No motor behavioural deficit	Bilateral LN-like pathology in SN, Hc, hypothalamus, somatosensory area, visual ctx, cingulate ctx, corpus callosum, amygdala & stria terminalis IHC: pSyn colocalization with ubiq. & p62 WB: endogenous mouse aSyn in insol. fraction	No DAergic degeneration	No astrogliosis / inflammation Loss of enkefalin in amygdala, globus pallidus	Masuda-Suzukake *et al.*, 2013
Sonicated recombinant m aSyn fibrils / unilateral microinjection, Sensory ctx	aSyn-GFP PDGFb mice (Rockenstein, 2005) 2-3 months	2.5-13 months	ND	Progressive LB-like inclusion formation around ctx injection site, bilat. spreading paSyn, colocali-zation with ThioS & Ubiq.	ND	ND	Osterberg *et al.*, 2015

Table 3 cont.

Method/ Delivery	Strain	Time for pathology	Findings				Ref.
			Behaviour	aSyn pathology	DAergic system	Other	
Lactacystin							
Lactacystin 1.25 µg unilateral microinjection MFB	C57Bl/6	7, 21, 28 days 2 months	28d Locomotor activity ↓ Rotarod ↓	ND	Progressive loss: SN DA neurons 7 d 22.5%↓ 28 d 65%↓ *2 m: 51 %* ↓ STR DA, DOPAC & HVA 28 d: 66, 63 & 47% ↓, *2 m: 52, 46 & 51 %* ↓	Microglia & astroglia activation Ubiq+ (IHC) aggregates in 5.2% of SN neurons & HMW Ubiq in insol. midbrain fraction	Zhang *et al.*, 2005, Zhu *et al.*, 2007, Pan *et al.*, 2008
Lactacystin, 1.25 µg, bilateral MFB microinjection,	C57Bl/6 10-12 weeks	28 days	Locomotor activity ↓ Rotarod ↓	ND	STR DA, DOPAC & HVA ↓	Microglia & astroglia activation	Li *et al.*, 2010
Lactacystin, 3 µg, unilateral SNc microinjection	C57Bl/6J 12-14 weeks	1 6 3 weeks	Rotarod ↓ Cylinder ↓ Adhesive removal ↓ Activity ↑	50 % increase in aSyn 150% increase in paSyn, in SNc & SNr (IHC)	SNc TH+ cells ↓ STR DA 40% ↓	ND	Bentea *et al.*, 2015
Rotenone							
Rotenone, 2.5-4.0 mg/kg s.c. 30-45 days	C57Bl/6 Age 2.5, 5 & 12 months	30-45 days	Activity ↓ catalepsy ↑ rotarod ↓ abnormal gait	ND	Normal SN TH cell count, STR TH ↑	ND	Richter *et al.*, 2007
Rotenone, 30mg/kg p.o. gavage 28 days	C57Bl/6J	28 days	Rotarod ↓	ND	SN TH cells & STR terminals↓	ND	Takeuchi *et al.*, 2009
Rotenone, 30 mg/kg p.o. (100 mg/kg 85% †, not included in the table)	C57Bl/6N	56 days	Rotarod ↓	Time-dependent aSyn increase in SNc TH+ neurons	TH IHC: SN neurons ↓	No activated astroglia, microglia or pTau	Inden *et al.*, 2011
Rotenone, 5 mg/kg p.o. gavage 45 or 90 days	C57Bl/6J 12 months (local effect in the bovel)	45 & 90 days	90 days: Rotarod ↓	Spinal cord and brainstem and SNc accumulation	TH IHC: SNc neurons 15.4 % ↓ STR normal	aSyn inclusion-pathology in ENS: paSyn, ThioS+, gliosis (GFAP)	Pan-Montojo *et al.*, 2010

Table 3 cont.

Method/ Delivery	Strain	Time for pathology	Findings				Ref.
			Behaviour	aSyn pathology	DAergic system	Other	
Paraquat							
Paraquat i.p.10 mg/kg once a week	h aSyn Thy1 (Line 61, Rockenstein 2002)	3 weeks	No change Beam walk Pole test	PK resistant inclusions in SNc	STR TH ↓ SNc neurons ↓	Normal microglia	Fernagut *et al.*, 2007
Paraquat i.p. 10 mg/kg twice a week	C57Bl/6m x129S	6 weeks	ND	STR aSyn ↑ STR & midbrain aSyn colocolization with pTau	ND	Protesomal (26S) activity ↓ mTor↓ Beclin 1 ↑ pTau	Wills *et al.*, 2012
Paraquat i.p.	C57BL6 ctrl and C57BL/6 with mouse aSyn over-expression (Chandra 2005), 10 weeks	3 days	ND	at 3 d, lysosomal accumulation of aSyn in midbrain	ND	LAMP-2A ↑ Hsc70/ aSyn interaction In tg mice w/out paraquat, LAMP2A ↑ together with aSyn mRNA ↑ Hsc70 IHC ↑	Mak *et al.*, 2010, Manning-Bog *et al.*, 2003
Paraquat i.p. 5 mg/kg twice a week	h A30P aSyn PrP, Dox KO (Nuber, 2011)	6 weeks	Locomotor activity ↓	OB, aSyn ↑ truncated, HMW & insol. aSyn ↑	OB, STR & SN TH neurons ↓	OB: Astrogliosis ATG12, LC3BII & LAMP-2A ↑	Nuber *et al.*, 2014
Paraquat 10mg/kg i.p. once a week	C57Bl/6, 8 weeks, h aSyn & A53T aSyn-TH TG & WT controls	1-3 3 weeks	ND	2 d after inject-tion: aSyn, WB↑, 3 w: SN aSyn ↑ Colocalization of aSyn &ThioS, not in TH+ cells	ND controls: SNc TH+ & Nissl neurons ↓	ND In controls Silver staining ↑	Manning-Bog *et al.*, 2002 and 2003

Abbreviations: AADC, Aromatic amino acid decarboxylase; aSyn, a-synuclein; ctx, cortex; DA, dopamine; DAT, dopamine transporter; DLB, Lewy body dementia; DOPAC, 3,4- dihydroxyphenylacetic acid; ENS, enteric nervous system; FA, formic acid; GFAP, glial fibrillar acid; h, human; Hc, hippocampus HMW, high-molecular weight; HVA, homovanillic acid; IHC, immunohistochemistry; KO, knock out; LAMP2A, lysosome-associated membrane protein; LB, Lewy body; LC3B, microtubule associated protein light chain 3B; LN, Lewy neurite; m, month; ND, not determined; paSyn, phosphorylated aSyn; PK, proteinase K; SDS, sodium dodecyl sulfate; SN, substantia nigra; STR, striatum; TH, tyrosine hydroxylase; ThioS, thioflavin S; Ubiq, ubiquitin; w, week; WB, Western blot; WT, wildtype

has been administered stereotactically into the medial forebrain bundle (MFB) (Zhang *et al.*, 2005, Zhu *et al.*, 2007, Pan *et al.*, 2008) or SN (Bentea *et al.*, 2015). Accumulation of aSyn was not measured in the studies using MFB lesion, but they show mild accumulation of ubiquitin positive aggregates into the SN, microglial activation and moderate (50- 60 %) neuron loss in the SN and depletion of DA and its metabolites in the STR. In the studies where LC was injected above the SN, it induced marked accumulation of aSyn, together with TH positive cell loss in the SN, STR DA loss and motor behavioural deficits (Bentea *et al.*, 2015). Furthermore, LC produces rather quick and robust pathology in the SN in just 7 to 56 days.

Epidemiological studies have linked the use of pesticides and herbicides to an increased risk of PD (Uversky, 2004). Therefore, mouse models that are based on an exposure to possible neurotoxic agents may offer good means of studying the environmental factors and mechanisms affecting PD pathogenesis. Rotenone and paraquat have both been connected to PD, and they have also been shown *in vitro* to accelerate aSyn fibril formation (Uversky *et al.*, 2001b). The pesticide rotenone is an inhibitor of mitochondrial complex 1, which in PD research has mainly been administered as daily subcutaneous injection or gavage to mice. In 30-90 days rotenone produces motor decline in all studies (Richter *et al.*, 2007, Takeuchi *et al.*, 2009, Pan-Montojo *et al.*, 2010, Inden *et al.*, 2011). The administration of rotenone was associated with mild to moderate decrease in the SNc cell bodies and STR terminals (Takeuchi *et al.*, 2009, Pan-Montojo *et al.*, 2010, Inden *et al.*, 2011) and in one study, it was associated with increased STR TH and did not alter SNc TH (Richter *et al.*, 2007).Two of the studies have analysed aSyn in the brain and it was shown to be increased after rotenone exposure (Pan-Montojo *et al.*, 2010, Inden *et al.*, 2011). Interestingly Pan-Montojo et al. (2010) used rotenone as a form which did not absorb from the gut and studied the effects of rotenone toxicity for the enteric and central nervous systems. They observed LB-like aSyn pathology in the enteric nervous system and subsequent increase of aSyn in the spinal cord, midbrain and SNc, which they suggested to have spread from the enteric nervous system.

Paraquat is a herbicide of which the mechanism of toxicity is not fully understood but it is connected to oxidative stress, mitochondrial dysfunction (Franco *et al.*, 2010) and reduced proteasomal activity and autophagy alterations (Mak *et al.*, 2010, Wills *et al.*, 2012). In mouse models, administration of 5-10 mg/kg once or twice a week for 3-6 weeks have been used (Manning-Bog *et al.*, 2002, Fernagut *et al.*, 2007, Mak *et al.*, 2010, Wills *et al.*, 2012, Nuber *et al.*, 2014). In all studies, paraquat exposure was associated with aSyn accumulation in the midbrain (Mak *et al.*, 2010, Wills *et al.*, 2012), SN (Manning-Bog *et al.*, 2002, Fernagut *et al.*, 2007) or OB (Nuber *et al.*, 2014). If TH-positive neurons were analysed, they were shown to be reduced in the SN, STR and OB (Manning-Bog *et al.*, 2002, Fernagut *et al.*, 2007, Nuber *et al.*, 2014) but DA content was not measured. In most of the studies, the motor phenotype of the mice was not assessed, but Nuber (Nuber *et al.*, 2014) showed reduced locomotor activity of the mice whereas in the study of Fernagut et al. (2007), no motor decline was seen. Furthermore, Manning-Bog et al (2002) did not observe pathological alterations in aSyn TG mice whereas paraquat-induced neurodegeneration was observed in WT littermates, suggesting a neuroprotective effect of aSyn overexpression against paraquat toxicity. Paraquat may be useful to study the influence of environmental stressors on PD pathogenesis. Limitations of studies using paraquat, however, seem to be that in most of them all of the PD characteristics have not been quantified, especially

DA content in the brain and motor behaviour, therefore it is difficult to estimate the usefulness of paraquat as a PD model.

2.7 Prolyl oligopeptidase in neurodegeneration and α-synuclein pathology

PREP (also known as POP, PEP, PO, EC 3.4.21.26) belongs to a family of serine proteases, which cleaves small peptides (less than 30 amino acids) at the C-terminal side of proline residues (Gass and Khosla, 2007). It was first discovered in the 70s as a uteral, oxytocin cleaving enzyme, and has shown thereafter to cleave angiotensin, substance P, neurotensin and vasopressin (Cunningham and O'Connor, 1997). PREP has been identified in bacterial and eukaryotic cells at approximately 75 kDA in size and consisting of two domains: catalytic and β-propeller (Gass and Khosla, 2007). The catalytic domain has α/β-hydrolase fold and the catalytic triad of the peptidase is formed of three residues: S554, D641 and H680. The β-propeller domain (amino acids 73-427) consists of a seven-fold repeat of four-stranded antiparallel β-sheets, which are arranged radially around a central pore. The active site is located in the cavity at the interface of these two domains (Fülop *et al.*, 1998).

PREP is expressed throughout the body, while the expression is the highest in the brain, liver, lung and spleen (Myöhänen *et al.*, 2007, 2008 and 2009). Relatively high PREP activity in the brain and the *in vitro* results of PREP being able to cleave neuropeptides raised the interest towards the possible physiological and pathological functions of PREP related to the central nervous system. PREP enzyme activity has been correlated to various neurological disorders such as AD, depression, schizophrenia and eating disorders (Mantle *et al.*, 1996, Myöhänen *et al.*, 2009). PREP inhibitors have been utilized in the study of the role of PREP in the disease, and the inhibitors have been shown to have a positive effect on learning and memory, which is thought to occur via regulation of neuropeptide levels (Shishido *et al.*, 1998). However, there are some studies that have shown controversial data about the correlation between PREP inhibition and neuropeptide levels *in vivo*. (Toide *et al.*, 1997, Miyazaki *et al.*, 1998, Morain *et al.*, 2002, Jalkanen *et al.*, 2007 and 2011b). At the subcellular level, PREP localizes mainly in the cytosol, but membrane-bound and nuclear localizations have been identified. It has been associated with neurotransmitter systems (Peltonen *et al.*, 2011) and inositol-1,4,5-triphosphate receptors (Myöhänen *et al.*, 2008) suggesting a potential role in the regulation of their signalling. Furthermore, association of PREP with tubulin (Schulz *et al.*, 2005) points to a possible role in protein secretion or trafficking.

To link PREP in brain disorders characterized by protein aggregate deposition, PREP has been shown to colocalize in human post-mortem brain samples with marker proteins of neurodegenerative diseases: Aβ, tau, aSyn and astroglia (Hannula *et al.*, 2013). PREP inhibitors have been shown to inhibit the formation and accumulation of Aβ in mouse *in vivo* and in cell culture studies (Shinoda *et al.*, 1997, Kato *et al.*, 1997). And it had been demonstrated in vitro that PREP enhances the aggregation of aSyn, which can be blocked with PREP inhibitors (Brandt *et al.*, 2008). PREP is not able to directly cleave Aβ nor aSyn (Petit *et al.*, 2000, Brandt *et al.*, 2008) suggesting a possible indirect or non-enzyme activity-related effects of PREP in protein aggregation.

These interesting findings about PREP and the relevance of aSyn aggregation and deposition in the pathophysiology of PD that have been revised in this literature review form the basis for the work that is described in this thesis.

3 AIMS OF THE STUDY

Aggregation and cellular deposition of aSyn are strongly linked to pathogenesis of PD. The findings that 1) PREP could accelerate the aggregation process of aSyn *in vitro* and that 2) PREP inhibitors were able to block this effect, generated an interest for further studies of PREP inhibitors as a potential new treatment strategy for PD. The aim of this study was to examine the role of PREP inhibition in the aSyn aggregation process and the effects of PREP inhibition in mouse models, which were also characterized as PD models.

The role of a PREP inhibitor, KYP-2047, in aSyn aggregation and clearance has now been studied using *in vitro*, cell culture and mouse *in vivo* models. The specific aims of the study were:

I. To study if PREP and aSyn form direct protein-protein interaction in cell culture and *in vitro* models. And to find out effects of the protein-protein interaction and KYP-2047 on aSyn aggregation.

II. To characterize a mouse strain carrying the A30P point mutation in the mouse aSyn coding gene ($Snca^{tm(A30P)}$ strain) as a mouse model of PD by assessing mouse behaviour, brain aSyn load and DAergic system and 6-hydroxydopamine neurotoxin sensitivity

III. To clarify what is the mechanism of increased aSyn clearance after administration of KYP-2047 in $Snca^{tm(A30P)}$ mouse strain and in cell culture.

IV. To characterize lactacystin-induced proteasome inhibition as a novel PD mouse model and to study the neuroprotective effect of KYP-2047 in this model.

4 MATERIALS AND MAIN METHODS

4.1 Animals

For study II and III homozygous TG mice carrying the A30P knock-in point mutation in their own Snca gene ($Snca^{tm(A30P)}$) and WT littermates were obtained from the University of Tartu, Estonia. Generation of the mouse strain is originally described in (Plaas *et al.*, 2008). The difference of this mouse line to others was that it carried only mutated mouse Snca gene and did not have aSyn overexpression. Mice were 6–17 months old when used for the experiments in study II. $Snca^{tm(A30P)}$ mice were also used for study III at the age of 12-16 months. For the study IV, 8-9 weeks old male C57Bl/6RccHsd mice were obtained from Harlan (Horst, Netherlands) while aged (12-14 months old) male C57Bl/6RccHsd mice were from University of Helsinki laboratory animal facilities. All the animals were maintained at 20-22 °C room temperature with 12:12 hours light:dark cycle and had access to food and water *ad libitum*. The experiments were carried out under licences ESLH-2009-02210/Ym-23, ESAVI-553/041003/, ESLH-2007-06679/Ym-23, 2011ESAVI-2010-07863/Ym-23 and ESAVI/198/04.10.07/2014 according to the European Community guidelines for the use of experimental animals and approved by the Finnish National board of animal experiments.

4.2 Drugs and treatments

Chemicals were purchased from Sigma-Aldrich (St- Louis, MO, USA) unless otherwise stated. 6-hydroxydopamine (6-OHDA) was diluted in saline with 0.02% ascorbic acid (Study II). Desipramine (25 mg/ kg i.p.) was dissolved in sterile water and administered approximately half an hour before 6-OHDA injection to protect noradrenergic neurons. Lactacystin (#L-1147, A.G. Scientific; San Diego, CA, USA) was diluted in PBS (2mg/ml) (Study IV). PREP inhibitor, KYP-2047 (4-phenylbutanoyl-L-prolyl-2(S)-cyanopyrrolidine), was synthetized in Univeristy of Eastern Finland, as described in Jarho (Jarho *et al.*, 2004). KYP-2047 is a specific inhibitor of PREP with no significant inhibition on related peptidases (Jalkanen *et al.*, 2011a). KYP-2047 was dissolved in 0.5 % DMSO in 0.9 % saline for i.p. injections (10 mg/ kg/ day; Studies III and IV) and in 50 % DMSO in 0.9 % saline for i.p. osmotic pump administration (Study III). 0.5 % or 50 % DMSO in 0.9 % saline was used as a control in the studies. KYP-2047 was injected twice a day for 5 days or if an osmotic pump was used, the duration of the treatment was four weeks. For cell culture work, 100 mM KYP-2047 stock was dissolved in DMSO (studies III and IV). D-amphetamine sulphate (Faculty of Pharmacy, University of Helsinki, Finland) was dissolved in 0.9 % saline and injected i.p. (2.5 mg/kg, calculated as free base). Lidocaine (Orion Pharma, Espoo, Finland) was used as a local anesthetic during all the surgical operations. Subcutaneous injection of buprenorphine (0.1 mg/kg; Temgesic, Reckit Benckiser Healthcare Ltd, Slough, UK) was used for post-operative pain relief in studies II, III and IV. Lethal dose of sodium pentobarbital (100 mg/kg; Orion Pharma) was used for terminal anaesthesia before perfusions.

4.3 Cell Culture, transfection and treatment

Mouse Neuro-2A (N2A) neuroblastoma cells (Study I) were cultured in full DMEM with additional 10% (v/v) FBS (Gibco, Life Technologies, Paisley, UK), 1% (v/v) L-Glutamine-Penicillin-Streptomycin solution (Lonza, Basel, Switzerland). Cells were maintained at 37°C, 5% CO_2/water saturated air. Transfection of N2A was done using JetPei (Polyplus, New York, USA) according to manufacturer's instructions. Human embryonic kidney (HEK) -293 cells (Study III) were cultured in Dulbecco's modified Eagle's medium (DMEM; Product #10-013, Cellgro/Mediatech, Manassas, VA, USA) containing 10% fetal bovine serum (FBS, Product #F2442).

4.3.1 PREP inhibition and macroautophagy in cell culture

24h after plating, autophagy inhibitors, 3-methyladenine (3-MA; 1 or 5 mM; Product #M9281) or bafilomycin A1 (10 nM or 50 nM; Product #B1793) in the presence of KYP-2047 (1 μM) or vehicle (0.001% DMSO) were added on the cell culture. The cells were incubated for an additional 24 h. Following treatment, cells were homogenized and used for WB analysis.

4.3.2 Beclin 1 mRNA

HEK-293 cells were homogenized, and the total RNA was extracted with an Aurum Total RNA Mini Kit (Bio-Rad, Hercules, CA, USA), including DNase treatment. Reverse transcriptase reaction was done on 10 ng of RNA in standard conditions using an iScript™ cDNA Synthesis kit (Bio-Rad). PCRwas performed with primers designed to amplify a fragment of beclin 1 cDNA (Miracco *et al.*, 2007) (forward, 5′ CAA GAT CCT GGA CCG TGT CA 3′; reverse, 5′ TGG CAC TTT CTG TGG ACA TCA 3′) or GAPDH cDNA (forward, 5′ TGC ACC ACC AAC TGC TTA 3′; reverse, 5′- GAG GGC ATG GAC TGT GGT CAT-3′), using iQ™SYBR® Green Supermix (Bio-Rad). Determination was done in triplicate. The fold change of expression of beclin 1, with respect to GAPDH, is reported as $-2\Delta\Delta C(t)$.

4.4 Surgical procedures

The mice were deeply anaesthetized (Univentor anaesthesia unit, Zejtun, Malta) with 2-4 % isofluran (Baxter, Deerfield, IL, USA) and placed on a stereotactic frame (Stoelting, Wood Dale, IL, USA) for stereotactic injections. A unilateral, intrastriatal injection containing 0.33, 1.0 or 3.0 μg of 6-OHDA (in 2 μl) was delivered with a 10 μl microsyringe (Hamilton, Bonaduz, Swizerland) connected to an injector (Quintessential stereotactic injector, Stoelting) at 0.5 μl/min to the following coordinates in relation to the bregma: A/P +0.7; M/L +1.8; D/V -2.7, and the needle was slowly retracted 2 min after the cessation of the injection (Study II). LC (2 μg in 1 μl) or PBS as a control were injected above the SNc using 10 μl microsyringe (World Precision Instruments, Hertfordshire, UK) at 0.2 μl/min to the following coordinates: A/P -3.2; M/L -1.2 ; D/V -4.3 (Study IV). The needle was left in place for 5 min after injection until it was slowly withdrawn.

Alzet osmotic pumps (Durect, Cupertino, CA, USA) for continuous KYP-2047 delivery were surgically inserted into mice intraperitoneum under isoflurane anesthesia (Study III). Mice were single-housed after the surgical procedures until they were sacrificed.

4.5 Behavioural tests

4.5.1 Horizontal and Vertical activity

In order to quantify locomotor activity of freely moving mice, the animals were put in a transparent plexiglass cages (dimensions: 25 cm x 25 cm x 15 cm) and the activity monitor measured infrared beam interruptions (MED Associates, St. Albans, GA, USA). Moving distance and vertical activity were measured in 15-min intervals. 24-h locomotor activity tests were done to compare phenotypes of genotypes (Study II). Mice were given water and food pellets during the 24-h test. 3-h measurement was done to study the responses to D-amphetamine challenge between mouse genotypes (Study II) and 2-h measurement to mice after LC and KYP-2047/ vehicle treatment (Study IV).

4.5.2 Cylinder test

Unilateral toxin administration induces a one-sided lesion of the nigrostriatal pathway, which may result in a disability of contralateral paw use and increased use of ipsilateral paw. In study IV, paw use preference was measured using a cylinder test after lactacystin injection. Mice were put in a plexiglass cylinder and camera was attached below the cylinder to record each mouse for 5 min. Videos were analysed afterwards in slow motion to count paw touches on the wall or floor upon mouse rearing and landing, respectively. Paw use percentages were calculated based on the numbers of left, right and both paw use.

4.5.3 Rotational behaviour

Drug-induced rotational bias can be observed after one-sided lesion of nigrostriatal pathway. In study II, rotational behaviour was measured 2 and 4 weeks after unilateral 6-OHDA lesioning of WT and $Snca^{tm(A30P)}$ mice. To induce rotations, 2.5 mg/kg of D-amphetamine was injected i.p. Mice were then fastened to the apparatus (MED Associates) with collars made from cable ties. Rotational behaviour was automatically detected and measured for 120 min in 5-min intervals. Net ipsilateral rotations (ipsilateral-contralateral) were used for data analysis.

4.6 Analysis of brain neurotransmitters and metabolites

4.6.1 Tissue samples

For brain dissection mice were deeply anesthetized with sodium pentobarbital (150 mg/kg) and transcardially perfused with ice-cold phosphate-buffered saline (PBS) to remove blood. The brains were quickly removed and placed in a cooled brain matrix to obtain striatal 2 mm slices from which the tissue samples were punched (radius 2 mm) (Study II and IV). Alternatively, the brain was separated in two hemispheres and the other one was quickly frozen on dry ice. Striatal samples from the brain halves were punched later (Study III). All samples were quickly frozen on dry ice and stored at -84°C until analysis. The samples were prepared in 0.5 ml of homogenization buffer consisting of six parts of 0.2 M $HClO_4$ and one part of antioxidant solution (oxalic acid, acetic acid and L-cysteine) and sonicated. The homogenates were centrifuged for 35 min at 20,800g at 4°C. Supernatant was removed to 0.5 ml Vivaspin 500 filter

concentrators (Molecular weight cut-off 10,000; polyethersulfone membrane; Sartorius Stedim Biotech GmbH, Goettingen, Germany) and centrifuged for 35 min at 8,600g at 4°C.

4.6.2 High-pressure liquid chromatography analysis

The concentrations of DA and its two main metabolites 3,4-dihydroxyphenylacetic acid (DOPAC) and homovanillic acid (HVA), and 5-hydroxytryptamine (5-HT) and its metabolite 5-hydroxyindoleacetic acid (5-HIAA) were analysed using high-pressure liquid chromatography (HPLC) equipped with an electrochemical detector (ESA CoulArray, Chelmsford, MA, USA) as earlier described (Airavaara *et al.*, 2006). The chromatograms were analysed and concentrations were calculated using CoulArray for windows software.

4.7 Immunohistochemistry

4.7.1 Sample preparation

To prepare the tissue for IHC the remaining caudal parts of the brain (cerebellum removed) (Study II) or the left hemisphere of the brain (Study III) were immersed in 4% paraformaldehyde (PFA) overnight. In study IV, mice were transcardially perfused with PBS to remove blood and then with 4 % paraformaldehyde (in PBS) to fix the tissue. Brains were removed and immersed in 4 % paraformaldehyde overnight to post-fix the tissue at room temperature. The brains were then immersed in 10 % sucrose solution (in PB) at +4°C overnight and thereafter in 30 % sucrose solution, kept at +4°C until they sank, after which the samples were quickly frozen with isopentane on dry ice and stored at -80 °C until sectioning. Brains were sectioned at 30 µm thickness. Floating sections were stored at -20 °C.

4.7.2 Immunohistochemistry

IHC was used for detection of aSyn (Studies II, III and IV), TH (Studies II, III and IV), DAT (study II), glutamic acid decarboxylase (GAD), ionized calcium binding adaptor molecule 1 (Iba1) and glial fibrillary acidic protein (GFAP) (Study IV). Briefly, sections were quenched in 10% methanol and 3% H_2O_2 in PBS (pH 7.4) for 10 min to block endogenous peroxidase activity, and non-specific binding was blocked with 10% normal serum in PBS containing 0,5 % Triton-X-100. The sections were incubated overnight at room temperature with sheep anti-aSyn (1:500, #ab6162, Abcam, Cambridge, UK), rabbit anti-TH (1:2000, #ab152, Millipore, Darmstadt, Germany), rat anti-DAT (1:1000, MAB369, Millipore), rabbit anti-GAD65/67 (1:2000, #G5163, Sigma), rabbit anti-GFAP (1:2000 ab7260, Abcam) or rabbit anti-Iba1 (1:1000, #019-19741, Wako Chemicals, Ltd., Richmond, VA, USA), antibodies. The sections were then incubated with appropriate HRP conjugated secondary antibodies for 2 h; donkey anti-sheep (aSyn) (1:500, #ab6900, Abcam), goat anti-rabbit (GAD) (1:500, #31460, Thermo Scientific, Rockford, USA) or rabbit anti-rat (DAT) (1:750, BA4000, Vector Laboratories, Burlingame, CA, USA). For TH, GFAP and Iba1 goat anti-rabbit biotinylated secondary antibody (1:200, BA1000, Vector Laboratories) was used and the signal was enhanced with the avidin-biotin complex –method (Vectastain® ABC kit standard, Vector Laboratories). The antigen-antibody complexes were visualized with 0.05% 3,3'-diaminobenzidine and 0.03% hydrogen peroxide solution. Finally, the sections were moved to objective glass, dehydrated in ethanol series (Altia, Finland) and mounted with Depex (BDH, Poole, UK).

4.7.3 Optical density analysis

For optical density (OD) analysis sections were imaged using pictures taken with a Nikon stereomicroscope combined with a DS-Fi1 camera head and DS-L2 camera control unit (Nikon, Japan) (Study II and III) or with 3DHISTEC slide scanner (3DHISTEC Ltd., Budabest, Hungary) (Study IV). Analysis was done in Image Pro Plus program (v. 3.0.1., Media Cybernetics, Bethesda, MD, USA) (Study II and III) or using ImageJ (NIH, Bethesda, MD, USA) (Study IV). Images were converted into grayscale 8 and inverted before analysis. Brain area to be analysed was selected using freehand selection tool. For each brain section background staining values were subtracted from raw data values.

4.8 Immunoblotting and native polyacrylamide gel-electrophoresis

More detailed description of the sample preparation protocols for WB can be found in respective original publications. In brief, samples were mechanically homogenized in modified RIPA- (50 mM Tris-HCl, 150 mM sodium chloride, 0.25 % sodium deoxycholate, 1 % NP-40, protease inhibitors; pH 7.4) (Studies II, III and IV) or TBS-buffer (Study IV). Supernatants were collected after centrifugation (14,000g at 4 °C). For aSyn and Ubiquitin detection, pelleted samples were further fractionated in SDS soluble and/or Triton-X soluble samples. Protein amounts were measured from soluble fractions using bicinchoninic acid (BCA) assay (Thermo Scientific). Samples were prepared in denaturing sample buffer, boiled for 5 min and centrifuged for 1 min. Lysates (10-50 µg) were loaded onto a polyacrylamide–SDS-gel (4-20 % or 8-16 %, Bio-Rad). Standard transfer and blocking techniques were used. Primary antibodies were diluted in 5% skim milk containing 0.05% Tween20: anti-mouse aSyn (1:1000; #ab1903, AbCam), mouse anti-ubiquitin (1:1000; #3936S, Cell Signaling Technology, Danvers, MA, USA) , mouse anti-SQSTM1/p62 (p62, 1:5000; #ab56416, AbCam), rabbit anti-microtubule associated protein light chain 3B I-II (LC3BI-II, 1:1000; #L7843), rabbit anti-beclin 1 (1:2000; #ab16998, AbCam), rabbit anti-parkin (1:1000; #ab15954), rabbit anti-β-actin (loading control, 1:2000; #4967S, Cell Signaling Technology) and glyceraldehyde 3-phosphate dehydrogenase (GAPDH, loading control, Millipore). After an overnight incubation at +4°C, membranes were incubated with appropriate HRP-conjugated secondary antibodies for 2 h at room temperature: for aSyn and SQSTM1/p62, goat anti-mouse HRP (dilution 1:2000 in 5% milk, #31430; Thermo Fischer Scientific); for ubiquitin, LC3BI-II, beclin 1, parkin and β-actin, goat anti-rabbit (dilution 1:2000; Product #31463, Thermo Fisher Scientific). β-actin and SQSTM1/p62 (p62) goat anti-mouse (tissues; dilution 1:5000; Product #7076, Cell Signaling Technology/ cells; dilution 1:2000; Product# AP130P, Millipore),

The images were captured using GeneGnome (Syngene, Cambridge, UK) or C-Digit imaging system (Licor, Lincoln, NE, USA). Three independent WB experiments were performed. ImageJ program was used for analyzing bands, and the OD value was calculated by comparing the OD value to the corresponding loading control OD value.

For native polyacrylamide-gel- electrophoresis, 6µg of recombinant protein samples were diluted in 1:1 native sample buffer (Bio-Rad) and loaded onto a 10 % native gel containing a

stacking gel. Gel, sample buffer and Tris-glycine running buffer did not contain SDS. Coomassie staining was performed after electrophoresis. Gel was fixed for 30 min in destaining buffer, (45% methanol, 10% acetic acid), stained with 0.1% Coomassie Brilliant Blue R-250 (Thermo Scientific) for 2 h and destained 3-4 times for 30 min with destaining buffer.

4.9 PREP and proteasomal activity measurement

The brain tissue or cell culture samples were homogenized in PREP assay buffer (0.1 M Na–K-phosphate buffer, pH 7.0) and centrifuged at 16,000 g at 4 °C for 20 min. Supernatants were collected and stored at -80 until PREP or proteasome activity measurement. Protein amount was measured using bicinchoninic acid method (BCA Protein Assay Kit, Thermo-Scientific)

Both activity assays are based on formation of fluorescent 7- amino-4-methylcoumarin (AMC) upon specific substrate cleavage. In PREP activity assay, post-proline-cleavage activity is measured. The protocol is described in Myöhänen et al (2008), samples were pre-incubated with assay buffer for 30 min at 30°C, then the substrate (4 mM Suc-Gly-Pro-AMC) was added and reaction was incubated for 1 h at 30°C. 1 M sodium acetate buffer (pH 4.2) was used to stop the reaction. In order to measure the chymotrypsin-like activity of the 20S proteasome, the protocol described in Ebrahimi-Fakhari (Ebrahimi-Fakhari *et al.*, 2011) was used. Homogenates were incubated with substrate (Suc-Leu-Leu-Val-Tyr-AMC) (Product #I-1395, Bachem, Bubendorf, Switzerland) at 37 °C for 60 min. Assay buffer for 20S activity contained 250 mM HEPES, pH 7.5, 5 mM EDTA and 0.01% SDS. The specificity of the proteasomal assay was ascertained by the ability of additional lactacystin (50 μM) to inhibit the fluorescence change. The formation of AMC was measured using The Wallac 1420 Victor fluorescence plate reader (PerkinElmer, Waltham, MA, USA). The excitation and emission wavelengths were 360 and 460 nm, respectively. PREP and proteasomal activities were expressed as the nanomolar amount of free AMC/min ∗ mg protein.

4.10 Microscale thermophoresis

Microscale thermophoresis (MST) measures interactions of biomolecules by detecting movement of fluorescently labeled molecules along temperature gradient upon changes in their hydration cell, charge or size). MST was used for a protein-protein and a ligand-protein interaction study (Study I). Purified recombinant porcine PREP and PREP(S554A) proteins were labeled with red fluorescent dye NT-647 NHS (amine-reactive) using Monolith NT.115 labeling kit (NanoTemper Technologies, München, Germany) according to the manufacturer's instructions. Labeled proteins were eluted in PBS with 0.05% Tween-20. Interaction studies were performed with a Monolith NT.115 MST device using standard capillaries from NanoTemper Technologies. During measurements, fluorescence signal was kept above 200 units by diluting labeled protein with assay buffer (0.05% Tween-20, 0.5 mg/ml BSA and 2.5 mM DTT in PBS). Constant amount of labeled protein (concentration 1-100 nmol) was titrated by purified recombinant human aSyn (#S7820, Sigma) in 1:1 series dilution starting from 35 μM, or with KYP-2047 in 10:1 and 1:1 series dilution starting from 10 μM. Curve fitting was done by NTanalysis software (NanoTemper Technologies) in the Thermophoresis + T-jump mode. Assimilated curves were analysed and K_d values were calculated in GraphPad Prism using non-

linear regression and one-site specific binding with the Hill slope according to the following equation: $K_d = B_{max}*X / Y - X$. Where B_{max} = is the maximum binding, X= concentration of aSyn and Y= normalized fluorescence change. Curves were generated from 3 replicate interaction assays.

4.11 α-synuclein and PREP plasmid construction

Plasmids were cloned for expression of luciferace-tagged aSyn and PREP in protein-fragment complementation assay (PCA). The split Gaussia princeps luciferace (GLuc) expression plasmids were previously described in (Nykänen *et al.*, 2012). The human aSyn cDNA to clone aSyn-GLuc1/HA and asyn-GLuc2/HA was obtained from ORFeome library (version 3.1, Genome Biology Unit, Institute of Biotechnology, University of Helsinki, accession number: BC013293), and was PCR-cloned in the Gluc-vector with HA-tag using the KpnI-XhoI restriction site. The open reading frame for human PREP (hPREP) was amplified from pCMV XL5 plasmid (Origene, Rockville, MD, USA) using polymerase chain reaction with oligonucleotide primers containing linkers for ligation-independent cloning. These inserts were recombined into the BamHI and EcoRV sites of pAAV-EF1a-backbone vector (pOTTC374) using an In-Fusion HD cloning kit (Clontech, Mountain View, USA). To create expression plasmid for hPREP (S554A), pAAV EF1α hPREP plasmid was used as a source for mutatation. Two separate PCR amplicons were constructed to contain the desired S554A mutation and linkers for the ligation-independent cloning. Amplicons were inserted into backbone vector using In-Fusion (Clontech) to create pAAV EF1α hPREP (S554A). An insert containing clones of newly generated plasmid were sequence verified. The PREP and PREP(S554A) plasmids were then used for cloning the PREP-GLuc2 and PREP(S554A)-GLuc2 constructs. All GLuc constructs used in this study have the GLuc-reporter fragment placed at the N-terminus separated by a (GGGGS)2SG linker.

4.12 Protein-fragment complementation assay

PCA is based on a luminescence, which occurs when proteins tagged with a complementary GLuc-fragments are close enough proximity to form a functional reporter protein. This was used to study aSyn-PREP protein-protein interaction and aSyn dimerization. PCA was performed as described in (Nykänen *et al.*, 2012). N2A cells were plated on 96-well plates (Perkin Elmer, white wall) (10,000 cells/ well). 24 h post-plating, reporter plasmids were transfected (125 ng of total plasmid DNA/ well). PCA signal was read 24 h post-transfection. GLuc PCA signal was detected by injecting 25 µl of native coelenterazine (Nanolight Technology, Pinetop, AZ, USA) per well (final concentration of 20 µM), and the emitted luminescence was read by Varioskan Flash multiplate reader (Thermo Scientific). For each experimental condition, 4 replicate wells were used, and 3-4 replicates of independent experiments were performed. A 100 mM stock solution of KYP-2047 was prepared in DMSO, further diluted to PBS and added at various concentrations (1 µM-10 µM) 4 h before the measurement. The corresponding amount of DMSO was used as vehicle control. 4 wells per experiment and 3-4 independent replicates were performed.

4.13 Statistical analysis

Statistical analyses were conducted with SPSS 18 (Study II) or Graph Pad Prism (studies I, III and IV) softwares. Student's t-test, 1-way analysis of variance (ANOVA) with Bonferroni or Newman Keuls post hoc test, 2-way ANOVA with Bonferroni post hoc test or repeated measeures ANOVA were used as statistical tests for the data analysis. Data is presented as Mean ± SEM.

5 RESULTS

5.1 PREP forms protein-protein interaction with α-synuclein and enhances its dimerization (I)

The protein-protein interaction between PREP and aSyn was studied in two models. In MST, a method to screen and study protein-protein interactions of purified, recombinant proteins, and in PCA, which allows investigation of protein interactions in cell culture. Catalytically inactive mutant, PREP(S554A) was used to study the involvement of PREP enzyme activity on the interaction. The effects of PREP and inhibition of PREP on aSyn self-association were also studied in PCA.

The findings of the experiments are summarized in Figure 6. In MST, both PREP and inactive PREP(S554A) interact with aSyn in μM affinity, K_d for PREP-aSyn was 2.96 μM and PREP(S554A)-aSyn 1.41 μM (Fig. 6 A-B). aSyn and PREP or PREP(S554A) were tagged with complement luciferace fragments and expressed in N2A cells. Bioluminescence signal, which occurs upon protein-fragment complementation, was significantly increased indicating a protein-protein interaction of aSyn with PREP and aSyn with PREP(S554A) (Fig. 6 C). The effect of PREP on aSyn dimerization was also studied in the same system by making two luciferace-fragment-tagged versions of aSyn. Bioluminescence signal, which is generated upon aSyn dimerization, represents the first step in the aSyn aggregation process. Indeed, we saw increased aSyn dimerization when PREP or PREP(S554A) were co-expressed with tagged aSyn constructs (Fig. 6 D). Once aSyn was expressed with PREP and incubated with KYP-2047, aSyn dimerization signal decreased significantly. KYP-2047 did not have an effect on PREP(S554A)-induced aSyn dimerization (Fig. 6 E).

To study the conformational forms of purified recombinant PREP and PREP(S554A) proteins, the proteins were incubated with KYP-2047 and applied on a native polyacrylamide gel electrophoresis (PAGE). Native PAGE revealed that PREP exists in three conformations: compact monomer, which is most likely the closed form; open monomer and slowly migrating oligomeric form. KYP-2047 incubation shifted open PREP conformation into a closed monomer but had no effect on PREP(S554A) (Fig. 6 F). KYP-2047 was shown to bind to both of the PREP proteins in our MST experiment (Kd at 0.1 nM range; data not shown).

5.2 Characterization of A30P α-synuclein transgenic mouse strain as a model of Parkinson's disease (II and III)

5.2.1 Horizontal and vertical activity (II)

In order to characterize possible effects of A30P aSyn on mouse locomotor activity, horizontal and vertical activities of 6-month (young) and 16-month old (aged) $Snca^{tm(A30P)}$ (Tm) and WT mice were compared. A30P aSyn appeared not to cause very prominent effects on locomotion because overall total activities did not differ between the genotypes. However, young Tm mice were significantly more active than their WT littermates during first hours of measurement; 0–4 hours significantly more horizontal activity ($F_{1,19}$=6.209, P=0.022, repeated measures ANOVA)

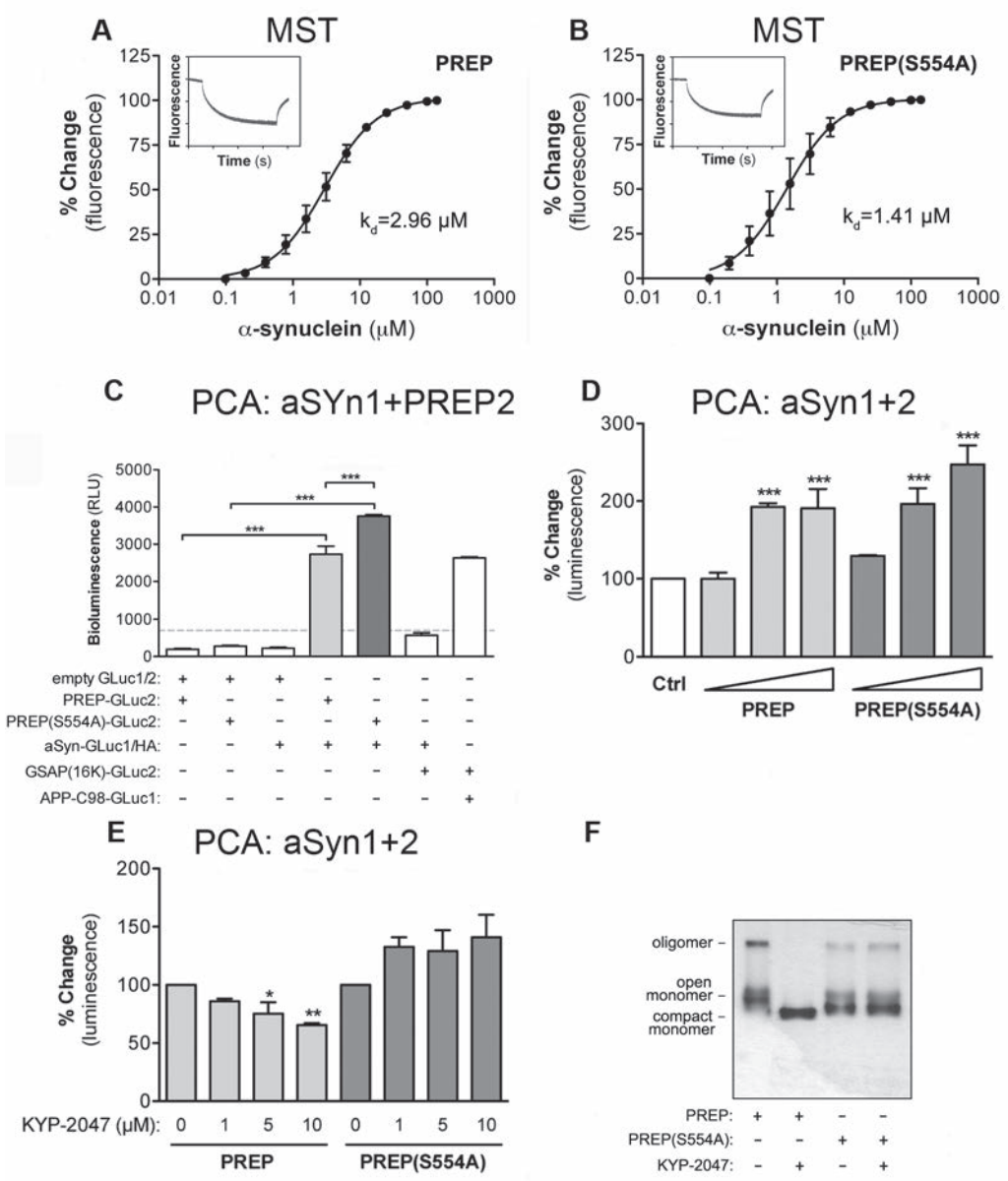

Figure 6: *Prolyl oligopeptidase (PREP) and catalytically inactive PREP(S554A) form protein-protein interaction with α-synuclein (aSyn) in microscale thermophoresis (MST) (A and B). In protein complementation assay (PCA) (C), PREP interacts with aSyn as transfection of PREP and aSyn tagged with complementary luciferace (GLuc) fragments (1 and 2) significantly enhances PCA signal in N2A cells. PREP and PREP(S554A) enhance aSyn dimerization in PCA (D), where aSyn tagged with complemetary GLuc fragments (1 and 2) was kept constant and PREP or PREP(S554A) were transfected at increasing levels. PREP-induced aSyn dimerization is reduced by PREP-inhibitor KYP-2047 whereas KYP-2047 does not have an effect on PREP(S554A)-induced aSyn dimerization (E). KYP-2047 induces conformational change of purified recombinant PREP into compact monomeric form but does not have an effect on PREP(S554A) in native polyacrylamide gel electrophoresis and Coomassie blue staining. Purified recombinant PREP or PREP(S554A) were incubated with 150 μM KYP-2047 30 minutes before gel electrophoresis (F). n=3-4. * P<0.05; ** P<0.01; ***P<0.001, Bonferroni post hoc test, 1-way ANOVA.*

and during 0–2 hours significantly more rearing ($F_{1,20}$=9.173, P=0.007, repeated measures ANOVA) (Fig. 7 A-B) was observed. Similarly, aged Tm mice moved significantly more during 0-2 hours compared to WT mice (P = 0.012, $F_{1,38}$=6.994, repeated measures ANOVA) (Fig. 7 E). Aged mice of each genotype appeared to be significantly more active than young mice when total distance travelled and vertical counts were compared but no effect was seen in the post hoc test (Total distance: age effect, P = 0.0484, $F_{1,56}$=4.073, Total vertical activity: age effect, P = 0.0263, $F_{1,56}$=5.207, 2-way ANOVA).

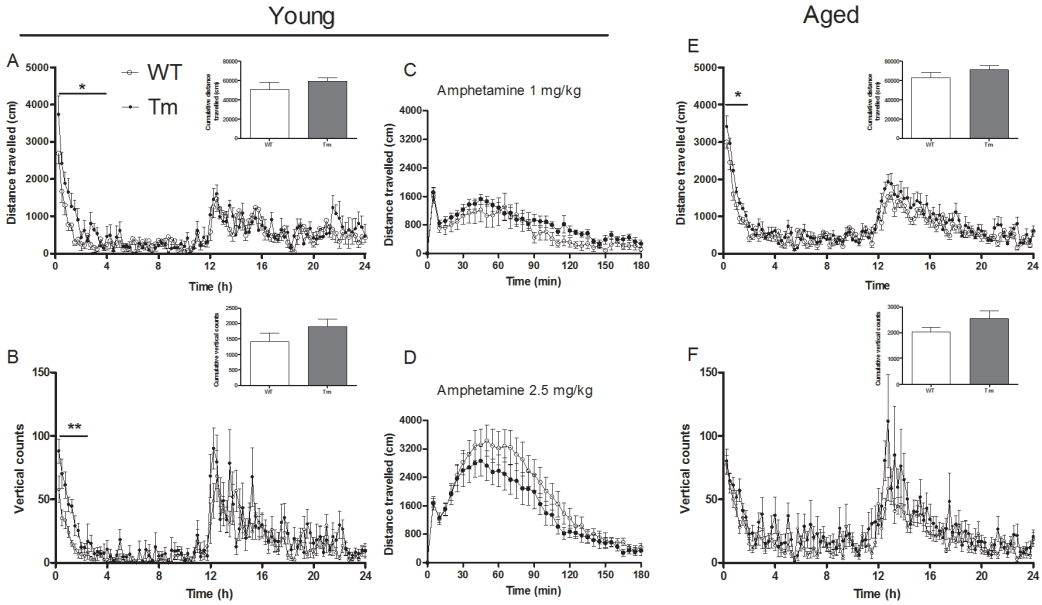

Figure 7: *Overall total (inserts) horizontal and vertical activities of young (A,B) and aged (E,F) wildtype (WT) and Snca$^{tm(A30P)}$(Tm) mice did not differ between the genotypes in 24 hours activity measurement. On closer inspection, Tm mice were significantly more active at the beginning of the measurement. In young mice, increased horizontal activity during first four hours (A) and vertical activity during first two hours (B), whereas in aged mice increased horizontal activity during first two hours were observed. No significant genotype differences were observed when mice were challenged with D-amphetamine 1 mg/kg (C) or 2.5 mg/kg (D) and horizontal activity was measured for 3 hours. n=8-20. Lights off at 12-24h. * P<0.05; ** P<0.01 repeated measures ANOVA.*

Young mice were also challenged with D-amphetamine and horizontal activity was measured for 3 hours. No significant alterations in the response for D-amphetamine were observed between genotypes (Fig. 7 C-D).

5.2.2 Sensitivity to 6-OHDA – D-amphetamine-induced rotational behaviour and HPLC analysis of striatal dopamine, 5-HT and their metabolites (II)

Young Tm and WT mice were randomly divided into groups that received 0.33 μg or 1.0 μg unilateral, striatal 6-OHDA microinjection. To assess progression and severity of the lesion of the nigrostriatal tract, amphetamine-induced (2.5 mg/kg) rotational behaviour was measured 2 and 4 weeks post-lesion (Fig. 8 A-B). Interestingly, at both time points lower dose of 6-OHDA caused a slight contralateral turning. The dose of 1.0 ug did not cause clear rotational behaviour at 2 weeks post-lesion but caused some ipsilateral turning in WT mice at 4 weeks although not significantly. Tm mice that received 1.0 ug of 6-OHDA did not show clear turning bias at any time point. This data indicates that the 6-OHDA did not cause an extensive enough lesion to the nigrostriatal trackt for mice to rotate after D-amphetamine challenge.

Measurement of striatal dopamine content supports our observations in the rotational experiment. In HPLC DA measurement, the genotypes had opposite responses on small dose of 6-OHDA (Fig. 8 C) ($P = 0.0382$; $F_{1,54}=4.512$, 2-way ANOVA); 0.33 ug induced 20 % DA loss in WT but 18 % increase in Tm mice. WT mice had more DA loss in the STR at 4 weeks post-lesioning (Treatment effect $P = 0.0161$; $F_{2,54}=4.459$, $P < 0.05$, WT intact side vs 1.0 ug 6-OHDA, Bonferroni post hoc test, 2-way ANOVA), which could explain the observed mild ipsilateral turning after D-amphetamine. DOPAC content decreased dose-dependently but the effect did not reach significance in post hoc tests (Treatment effect $P = 0.0355$, $F_{2,54}=3.553$) (Fig. 8 D), and HVA was reduced only mildly (ns, $P = 0.0842$, $F_{2,54}=2.592$) (Fig. 8 E). There were some alterations in the DA metabolite and DA ratios between the genotypes but it did not reach significance in post hoc tests (DOPAC/DA $P = 0.0285$, $F_{1,54}=5.068$, HVA/DA $P = 0.0329$ $F_{1,54}=4.795$, 2-way ANOVA) (Fig. 8 F-G). 6-OHDA did not cause alterations in 5-HT and 5-HIAA concentrations (data not shown). HPLC analysis from the intact hemisphere revealed that genotypes had the basal levels of striatal DA, DOPAC, HVA, 5-HT and 5-HIAA.

5.2.3 Effect of age, genotype and PREP inhibition on brain α-synuclein amount in Snca$^{tm(A30P)}$ mice (II and III)

aSyn OD was analysed from 6 and 12-16 months old mice to compare amount of WT and A30P aSyn and influence of ageing on the accumulation. aSyn OD increased age-dependently in the STR of both genotypes ($P = 0.0001$, $F_{3,30}=15.57$, 2-way ANOVA; $P < 0.01$ STR: WT and Tm young vs aged, Bonferroni post hoc test) and in the M1 motor cortex in Tm mice ($P < 0.05$ M1 cortex: Tm young vs aged, Bonferroni post hoc test). Cortical aSyn OD was also significantly higher in aged Tm mice compared to aged WT mice ($P < 0.05$, Bonferroni post hoc test) (Fig. 9).

Myöhänen et al. (2012) showed that PREP inhibition significantly reduced aSyn amount in the brain of aSyn overexpressing mice. Therefore the effect of PREP inhibition on aSyn amount and oligomerization was further studied in Snca$^{tm(A30P)}$ mouse line. Aged mice received 5-day (16 months old mice) or 28-day (12 months old mice) treatments with PREP inhibitor KYP-2047 or vehicle. aSyn OD was analysed from the STR, SN and motor cortex after immunostaining. KYP-2047 treatments significantly reduced aSyn immunoreactivity in the studied brain areas of Tm mice (5-day: $P = 0.002$, $F_{1,18} = 10.46$ and 28-day: $P = 0.0028$, $F_{1,10} = 6.95$, 2-way ANOVA) (Fig. 10 G-H). Most reduction of aSyn OD was observed in the SN (5-day: $P < 0.01$ and 28-day: $P < 0.05$, Bonferroni post hoc test).

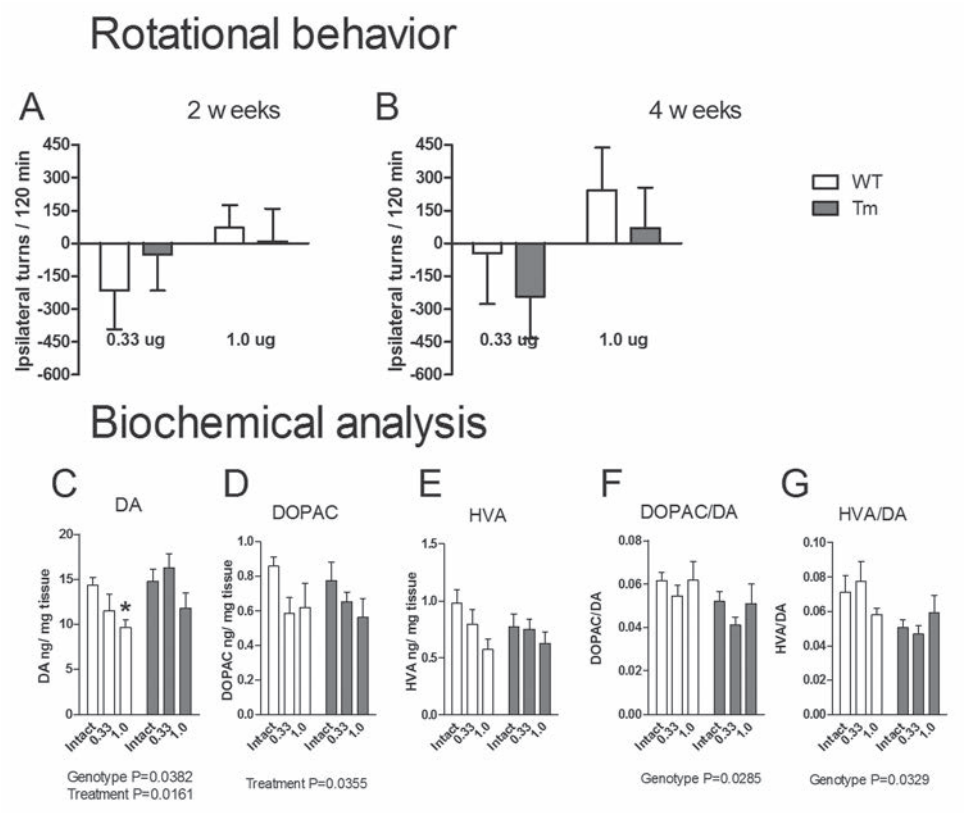

Figure 8: *Sensitivity of wildtype (WT) and Snca$^{tm(A30P)}$ (Tm) mice for 6-hydroxydopamine (6-OHDA). D-amphetamine-induced rotations were measured 2 and 4 weeks after unilateral, striatal 0.33 (A) or 1.0 μg (B) 6-OHDA injection, where no significant rotational bias was observed at any time point or group. Analysis of striatal dopamine (DA) (C) and its metabolites 3,4- dihydroxyphenylacetic acid (DOPAC) (D) and homovanillic acid (HVA) (E) and ratios of DOPAC/DA (F) and HVA/DA (G) 4 weeks after 6-OHDA injection revealed that only 1.0 μg dose of 6-OHDA significantly reduced striatal DA in WT mice. n=6-10. * P<0.05 Intact vs 1.0 μg, Bonferroni post hoc test, 2-way ANOVA.*

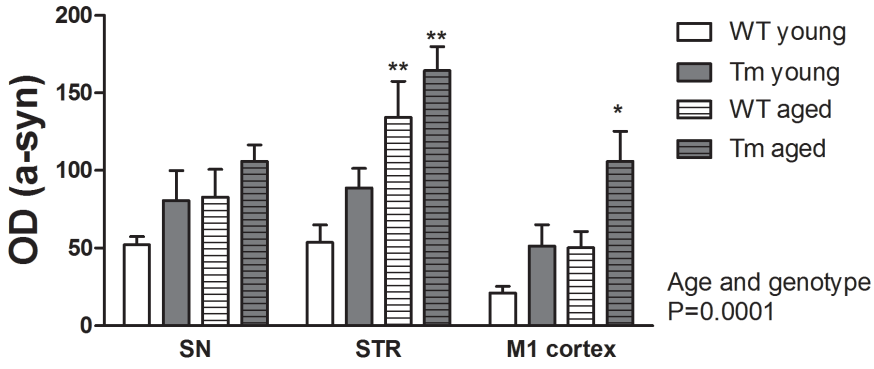

Figure 9: *Optical density (OD) analysis of α-synuclein immunoreactivity in the substantia nigra (SN), striatum (STR) and motor cortex (M1 cortex) of young and aged WT and Snca$^{tm(A30P)}$ (Tm) mice. n=3-4. * P<0.05; ** P<0.01 vs. young of same genotype, Bonferroni post hoc test, 2-way ANOVA.*

Soluble and insoluble forms of aSyn were separated by fractionation and analysed using WB. HMW (over 100 kDa) oligomeric forms of aSyn were increased in Snca$^{tm(A30P)}$ mice compared to WT littermates and also A30P aSyn dimers seemed to have increased, although this did not reach significance. 28-day KYP-2047 treatment significantly reduced the amount of A30P aSyn HMW oligomers ($P = 0.019$, $F_{1,12} = 7.217$, 2-way ANOVA, $P < 0.05$ Snca$^{tm(A30P)}$, Bonferroni post hoc test) and had a tendency to decrease A30P aSyn dimers (Fig. 10 J and M). Levels of soluble and insoluble monomeric aSyn forms remained unchanged after treatments and between genotypes (Fig. 10 K-L and N-O).

5.2.4 Effects of PREP inhibition on brain dopaminergic system in Snca$^{tm(A30P)}$ mice (III)

In the previous paper from Plaas et al (2008), striatal DA content of Snca$^{tm(A30P)}$ mice was decreased in comparison to WT mice. In our HPLC analysis, there was no baseline difference in the STR DA content between genotypes at 16 or 12 months of age. Because we observed reduced aSyn amount in the brains of Tm mice, which could potentially have an impact on the brain dopaminergic system, the DAergic system after the KYP-2047 treatment was characterized. Subchronic 5-day treatment with KYP-2047 increased DOPAC and HVA levels but DA concentration was unchanged in both groups (Treatment effect: DOPAC: $P = 0.0444$, $F_{1,34}=4.356$, HVA: $P = 0.027$, $F_{1,34}=5,329$, 2-way ANOVA; Fig. 11 A-B). Chronic 28-day KYP-treatment had opposite effects between the genotypes on DA and metabolite levels.

The STR DA content significantly increased in the Tm mice (Interaction: $P = 0.01$, $F_{1,17} = 15.72$; genotype effect: $P = 0.02$, $F_{1,17} = 6.647$; Bonferroni post hoc test: Tm vehicle vs. KYP-2047 $P < 0.01$, 2-way ANOVA; Fig. 11 C). DOPAC and HVA amounts seemed to increase in Tm and slightly reduce in WT mice after KYP-2047 (HVA: interaction: $F_{1,17}= 5.428$; $P = 0.032$, 2-way ANOVA; $P < 0.01$, Tm veh vs Tm KYP-2047, Bonferroni post hoc test) and DOPAC (Interaction: $P = 0.008$, $F_{1,17}= 8.909$ 2-way ANOVA) (Fig. 11 D). To analyse the DAergic markers in the STR, IHC staining and OD analysis of DAT and TH were performed. 5-day KYP-2047 did not have an effect on DAT immunostaining but 28-day treatment significantly decreased DAT OD in both genotypes (Treatment effect: $P = 0.02$, $F_{1,12} = 7.37$; 2-way ANOVA) (Fig. 11 E). TH was not changed due to aSyn genotype or KYP-2047 treatment (data not shown).

28-day KYP-2047 treatment was delivered using i.p. micro-osmotic pumps. Their functionality was confirmed by measuring PREP activity from the brain, which was reduced by 50 % compared to vehicle treated controls (Fig. 11 F).

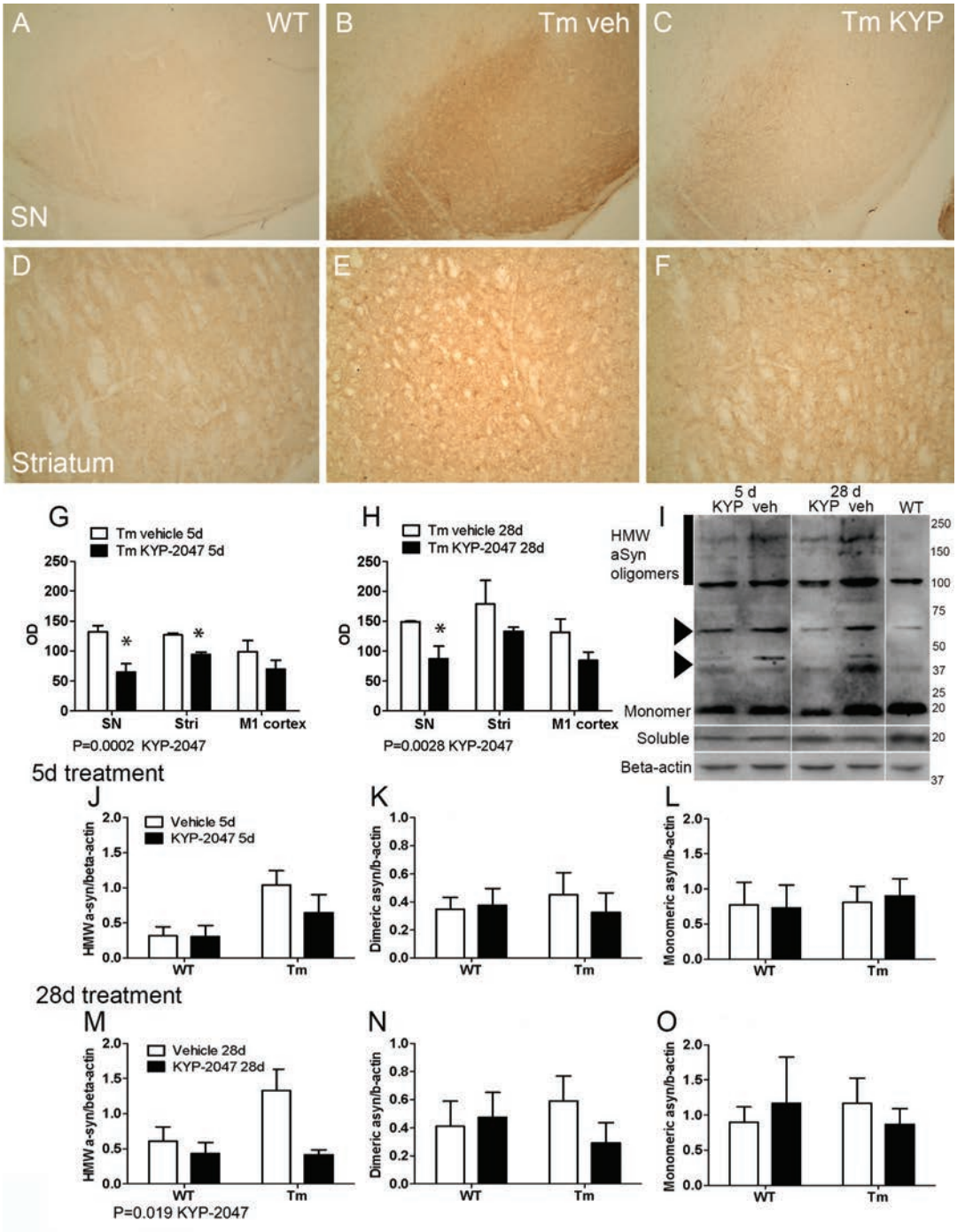

Figure 10: *Brain α-synuclein (aSyn) analysis of KYP-2047(a prolyl oligopeptidase inhibitor, KYP) or vehicle (veh) treated wildtype (WT) and Snca$^{tm(A30P)}$ (Tm) mice. Representing images of aSyn immunohistochemistry of WT (A,D), Tm vehicle (B,E) and Tm KYP-2047 (C,F) samples. Substantia nigra (SN) top row and striatum (Stri) bottom row. 5-day (G) and 28-day (H) KYP-2047 treatment reduced aSyn optical density (OD). Representing image of aSyn Western blot (I). High-molecular weight (HMW) (J,K), dimers (K,N) and monomers (L,K) of aSyn after 5 and 28-day KYP-2047 treatments. n=3-4. * P<0.05 Bonferroni post hoc test, 2-way ANOVA.*

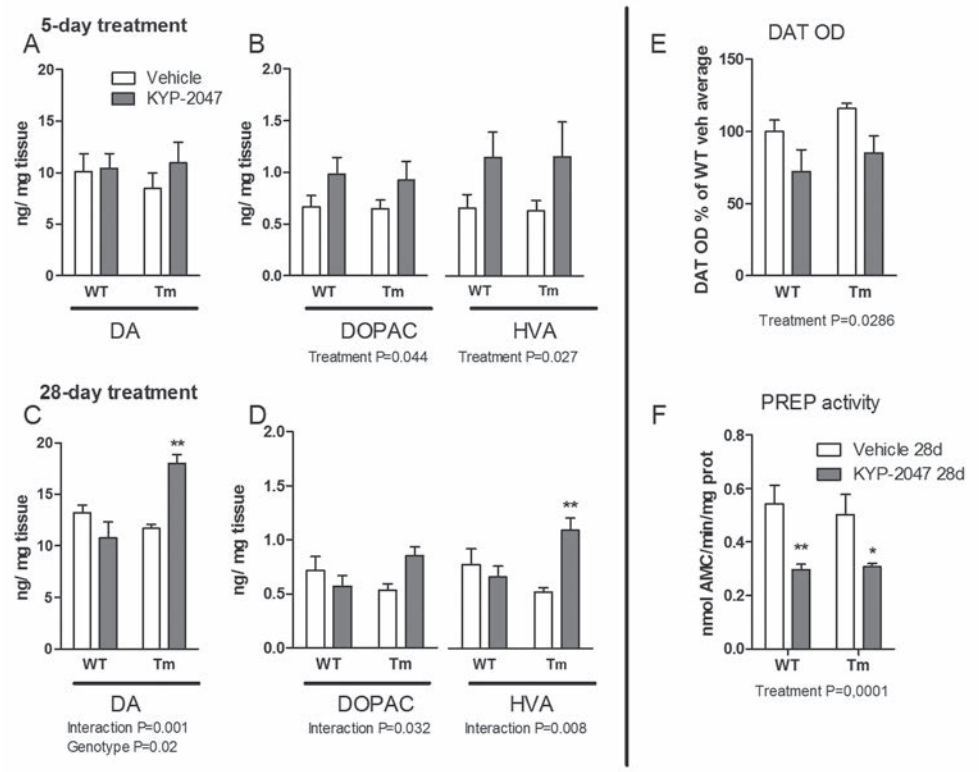

Figure 11: *Analysis of striatal dopamine (DA) (A, C) and its metabolites 3,4- dihydroxyphenylacetic acid (DOPAC) and homovanillic acid (HVA) (B, D) of wildtype (WT) and and Snca$^{tm(A30P)}$ (Tm) mice after 5 and 28-day KYP-2047, a prolyl oligopeptidase (PREP) inhibitor, treatment. Immunohistochemical staining and optical density (OD) analysis of striatal dopamine transporter (DAT) after 28-day KYP-207 treatment (E). PREP activity measurement from the brain after 28-day KYP-2047 administraion with intraperitoneal micro-osmotic pumps (F). n=3-10. * P<0.05; ** P<0.001; Bonferroni post hoc test, 2-way ANOVA.*

5.3 PREP inhibition induces macroautophagy in Snca$^{tm(A30P)}$ mice and in HEK-293 cell culture (III)

To clarify the mechanism of KYP-2047-induced aSyn clearance, we decided to investigate the markers of UPS and autophagy pathways, which both take part in aSyn degradation and are interesting candidates for aSyn-modulating drug therapy. 20S proteasome activity seemed to be reduced in Tm animals, whereas 28-day but not 5-day KYP-2047 treatment increased the activity in Tm mice (Interaction: P = 0.066, $F_{1,32}$ = 3.598, 2-way ANOVA; Fig. 12 A-B).

In addition, macroautophagy could be altered due to A30P-mutated aSyn or KYP-2047 treatment. Therefore, we used WB to investigate autophagosome marker, LC3BII, levels, which is known to accumulate in the cells when more autophagosomes are formed or if their lysosomal degradation is compromised. In Tm mice, increased LC3BII levels were observed indicating higher basal activity of macroautophagy (Genotype effect: P = 0.02, $F_{1,8}$ = 8.427, 2-way ANOVA). A 5-day KYP-2047 treatment significantly increased LC3BII levels in both

genotypes, especially in the Tm mice (Treatment effect: P = 0.017, $F_{1,8}$ = 8.980; 2-way ANOVA, P < 0.05 KYP-2047 vs. vehicle in Snca$^{tm(A30P)}$, Bonferroni post hoc test; Fig. 12 C). Yet, the same effect was not seen after 28-day treatment (Fig. 12 D).

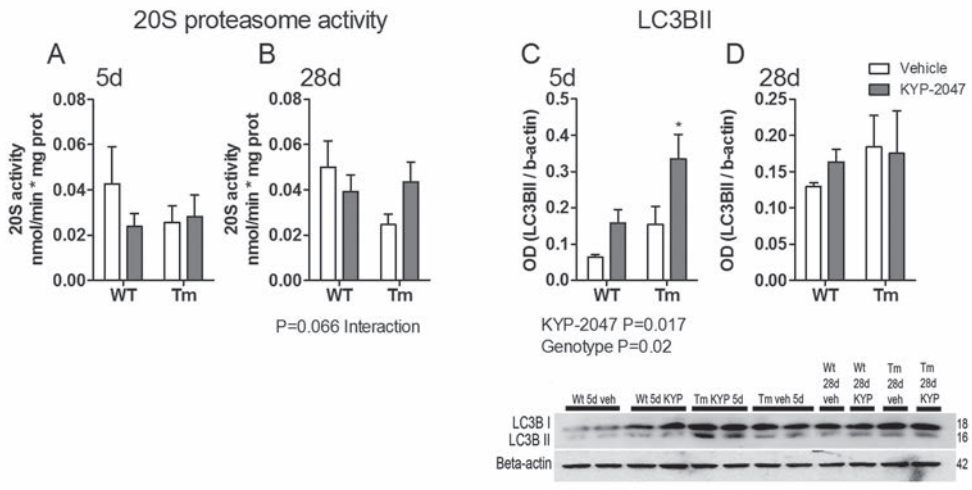

Figure 12: *In vivo brain 20S proteasome activity of KYP-2047 (a prolyl oligopeptidase inhibitor) or vehicle treated wildtype (WT) and Snca$^{tm(A30P)}$ (Tm) mice; 5-day (A) and 28-day (B) treatments. Brain autophagosome marker, LC3BII, levels after 5-day (C) and 28-day (D) treatments. n=3-10. * P<0.05 KYP-2047 vs. vehicle, Bonferroni post hoc test, 2-way ANOVA.*

We utilized pharmacological inhibition of autophagy with 3-MA, an inhibitor of autophagosome formation, and Baf, an inhibitor of lysosomal autophagosome degradation, together with PREP inhibition. WB analysis showed that inhibition of autophagosome formation by 3-MA significantly increased accumulation marker, p62, levels ($F_{2,12}$ = 4.042; P = 0.045; 3-MA vs. control, 2-way ANOVA), and KYP-2047 returned p62 levels to the normal in the 5 mM 3-MA group (P < 0.05, KYP-2047 vs. vehicle, Bonferroni post hoc test; Fig. 13 A). Baf caused minor increase in the accumulation of p62.

3-MA decreased the amount of the autophagosome marker, LC3BII, pointing to impaired autophagy, and KYP-2047 (1 μM), significantly increased LC3BII levels in all groups (Fig. 13 B; $F_{1,12}$ = 19.28; P = 0.0009 KYP-2047 effect;: P < 0.01 KYP-2047 vs. vehicle in 5 mM 3-MA, Bonferroni post hoc test, 2-way ANOVA). To study that the observed increase in autophagosome amount was due to autophagy induction via KYP-2047 and not blocked lysosomal degradation, the degradation of autophagosomes was inhibited by 10 or 50 nM Baf. The levels of LC3BII were increased by 2–3-fold compared to control (Fig 13 B; $F_{2,22}$ = 15.73; P = 0.0001 Baf effect, 2-way ANOVA), and KYP-2047 further increased the LC3BII levels, pointing to autophagosome formation enhancing effect ($F_{1,22}$ = 5.762; P = 0.025 KYP-2047 effect; P < 0.05 KYP-2047 vs. vehicle in Baf 50 nM group, Bonferroni post hoc test, 2-way ANOVA).

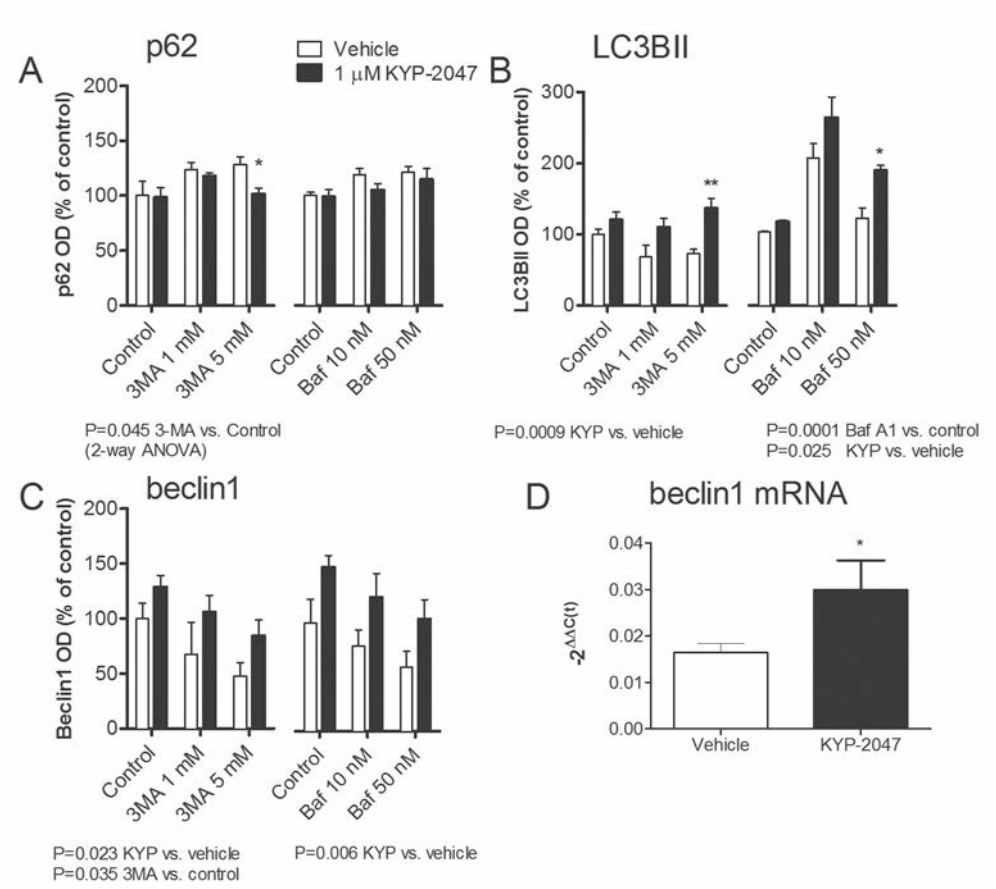

Figure 13: *The effects of autophagy inhibitors 3-methyladenine (3-MA) and bafilomycin A1 (Baf) combined with 1 μM KYP-2047 (a prolyl oligopeptidase inhibitor) or vehicle on autophagy in HEK-293 cell culture. 3-MA significantly increased accumulation marker, p62, levels and incubation with KYP-2047 significantly decreased the 5mM 3-MA-dependent increase in p62, whereas 24h incubation with Baf had no effect on p62 (A). 3-MA reduced the formation of autophagosomes but KYP-2047 overcame this by increasing the autophagosome marker, LC3BII, levels, Baf significantly increased autophagosomes and KYP-2047 further increased the LC3BII (B). Beclin 1 levels decreased by 3-MA and insignificantly by Baf, while KYP-2047 significantly increased beclin 1 in both cases (C). Beclin 1 mRNA level significantly increased after KYP-2047 treatment in qPCR analysis (D). n=3-6. * P<0.05; ** P<0.01 KYP-2047 vs. vehicle, Bonferroni post hoc test, 2-way ANOVA; in D * P<0.05, Student's t-test.*

Beclin 1 is a positive regulator of autophagy and both concentrations of 3-MA decreased the levels of beclin 1 ($F_{2,15}$ = 4.242; P = 0.035 3-MA effect, 2-way ANOVA; Fig. 13 C). Similar to 3-MA, both Baf concentrations insignificantly decreased the levels of beclin 1 dose-dependently. However, KYP-2047 significantly increased beclin 1 levels in all study groups (3-MA: $F_{1,5}$ = 6.42; P= 0.023 KYP-2047 effect; Baf: $F_{1,12}$ =11.00; P = 0.006 KYP-2047 effect, 2-way ANOVA) indicating a positive regulation of autophagy. To confirm the observations with beclin 1 levels in WB analysis, beclin 1 mRNA levels after KYP-2047 exposure were measured. 24h KYP-2047 exposure for HEK-293 cells significantly increased the beclin 1 mRNA levels (P = 0.025, Student's t-test; Fig. 13 D), indicating an activation of autophagy.

5.4 Lactacystin-induced ubiquitin-proteasome system deficiency as a mouse model of Parkinson's Disease and the effects of PREP inhibition in the model (IV)

UPS dysfunction is linked to aSyn pathology in PD. To characterize UPS inhibition as a PD mouse model, LC was administered above SNc using stereotactic microinjection. 10 days after the LC injection, young and aged mice were sacrificed, and IHC analysis of aSyn and markers

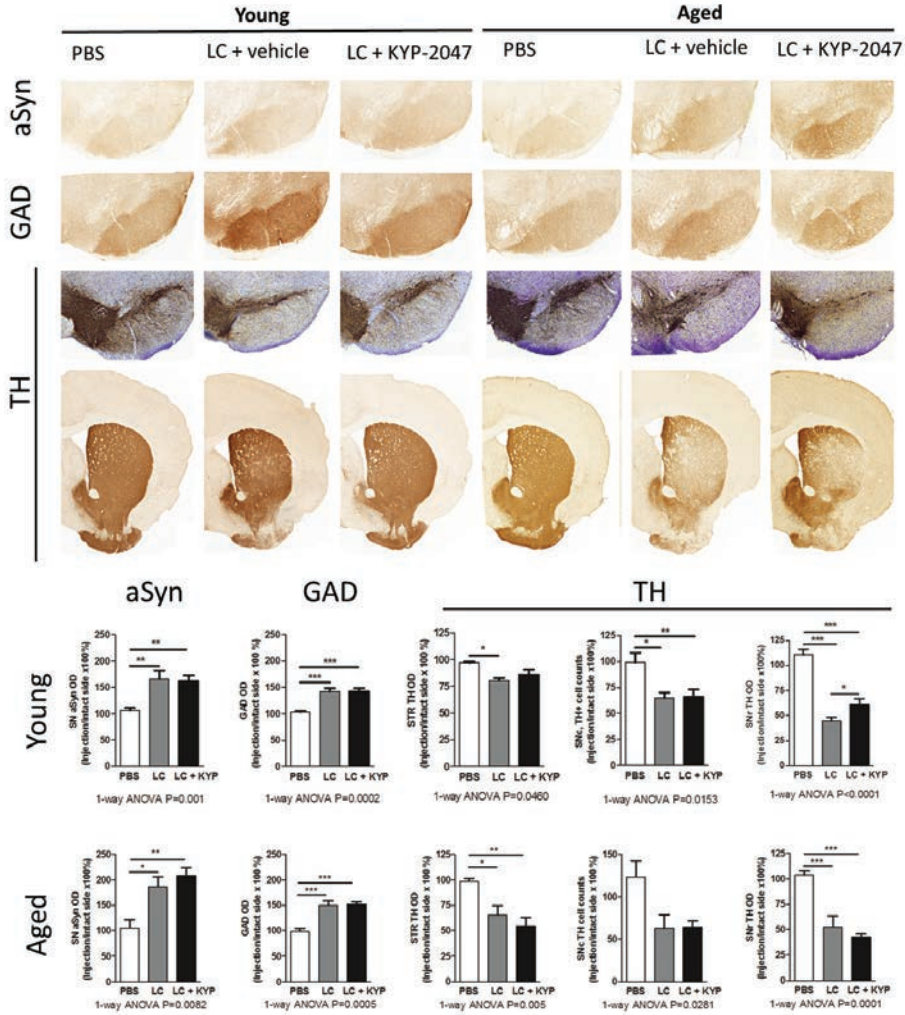

Figure 14: *Proteasome inhibitor lactacystin (LC) -induced α-synuclein (aSyn) accumulation and neurodegeneration in young and aged mice. Representative images of aSyn, glutamic acid decarboxylase (GAD) and tyrosine hydroxylase (TH) stained brain sections (A). Microinjection of LC above the substantia nigra (SN) pars compacta induces aSyn (B, G) and GAD (C, H) accumulation, TH+ neuron loss in SN (E-F, J-K) and loss of striatal (STR) TH+ terminals (D, I) of young and aged mice. LC-injected mice received a 5-day treatment of KYP-2047 (a prolyl oligopeptidase inhibitor) or vehicle immediately after LC microinjection. KYP-2047 reduced LC-induced TH OD loss. PBS microinjection was used as a sham control for LC. young n=4-9, aged n=3-4 (data for aged mice are supplemental results). * P<0.05; ** P<0.01; P<0.001 Newman-Keuls post hoc test, 1-way ANOVA.*

of DAergic, GABAergic and neuroinflammation were performed. IHC data for aged animals are supplemental to the manuscript. In IHC, significant accumulation of aSyn was observed in the lesioned side of the brain, particularly in the SN pars reticulata (SNr) (Fig. 14 B, G). Number of TH+ neurons in the SNc as well as density of TH+ fibres in the SNr were reduced (Fig. 14 E-F and J-K), while GABAergic marker GAD was significantly increased in the SNr (Fig. 14 C and H). In the STR, aSyn accumulation was not observed in IHC (data not shown), but small lesion was visible when TH OD was analysed in the STR (Fig. 14 D and I). In young mice, STR DA, DOPAC, HVA, 5-HT and 5-HIAA content were analysed, and LC induced significant depletion of DA and DOPAC (DA: $P < 0.0001$, $F_{1,23} = 30.82$, LC vs intact $P < 0.01$ in vehicle, Bonferroni post hoc test; DOPAC: $P = 0.0006$, $F_{1,22} = 16$, LC vs intact $P < 0.01$, Bonferroni post hoc test, 2-way ANOVA) whereas it did not have an effect of HVA (Fig. 15) or 5-HT and 5-HIAA (data not shown). In young mice, IHC staining for astroglial marker GFAP and microglial marker Iba1, revealed remarkable activation of glial cells throughout the lesioned hemisphere at the nigral level, and mild astroglial activation was also observed in the ipsilateral STR (Fig. 16).

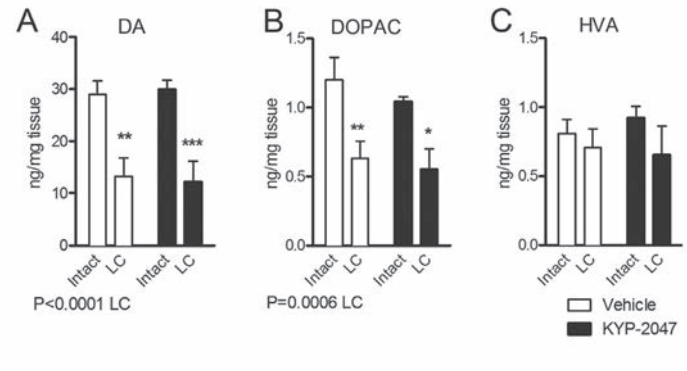

Figure 15: *Microinjection of lactacystin (LC) above substantia nigra pars compacta induced depletion of striatal dopamine DA (A) and 3,4 dihydroxyphenylacetic acid (DOPAC) (B) whereas homovanillic acid (HVA) (C) content was not significantly altered. Mice received a prolyl oligopeptidase inhibitor, KYP-2047 (10mg/kg/day i.p.), or vehicle for 5 days after LC-injection. Tissue samples were collected 10 days after LC. n=6-7. * P<0.05; ** P<0.01 LC vs. intact, Bonferroni post hoc test, 2-way ANOVA*

In motor behavioural tests, LC induced motor deficits, which were partially different between young and aged mice. Behavioral results for aged mice are supplemental data. LC reduced both horizontal and vertical activity of young mice, ($P = 0.0391$; $F_{2,27} = 3.664$; 1-way ANOVA; Fig. 17 A-B). Whereas, no significant differences were observed in aged mice (Fig. 17 C-D). In cylinder test, there was a statistically significant LC-effect ($P = 0.0380$; $F_{2,27} = 3.680$, 1-way ANOVA) when the landing paw preference was counted. LC mice used more contralateral paw compared to PBS (Fig. 17 E-F). In the group of aged mice, LC treated mice preferred to use ipsilateral paw for rearing significantly more than control group ($P = 0.0107$; $F_{2,7} = 9.294$, 1-way ANOVA; $P < 0.05$, PBS vs. LC, Newman-Keuls post hoc test). For the landing, aged LC mice used more ipsilateral paw but it did not significantly differ from PBS controls in post hoc test.

In order to study PREP inhibition in LC-based model, mice were treated with KYP-2047 for five days starting immediately after the LC microinjection. In young, KYP-2047 treated mice we did not see differences in IHC of aSyn in the SN or STR but smaller TH loss in the STR was observed after KYP-2047 treatment. Moreover, KYP-2047 treated mice had significantly higher amount of TH+ fibres left in the lesion side compared to vehicle treated mice. GAD remained

unchanged between the treatment groups, and KYP-2047 did not have an effect on DA content in the STR or activation of astroglia and microglia. In aged mice, neuroprotective effects with KYP-2047 were not observed (supplemental results).

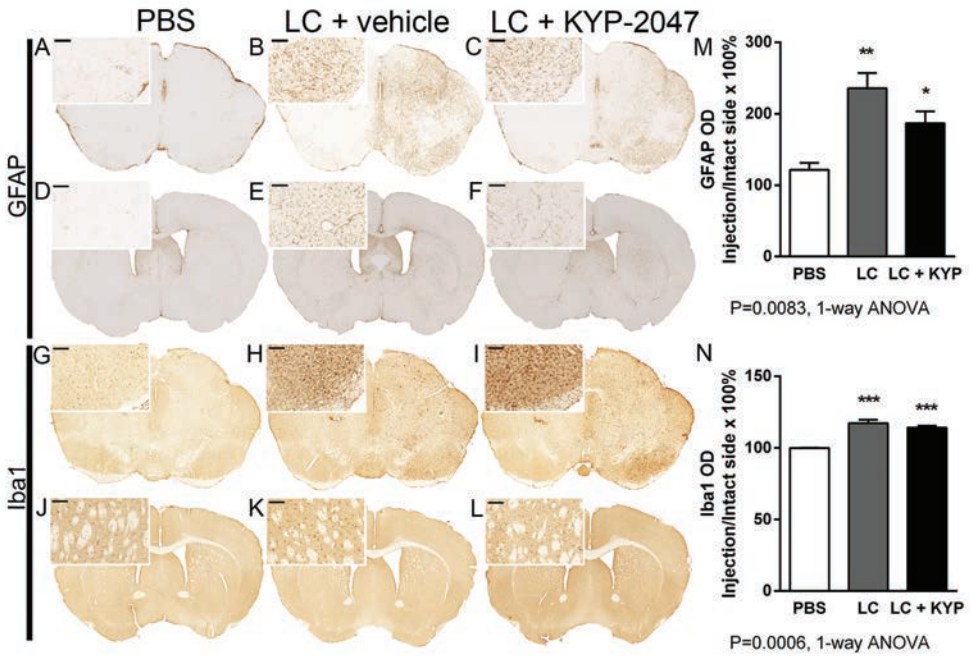

Figure 16: *Neuroinflammation around injected brain hemisphere after lactacystin (LC)-induced proteasome inhibition in the subsantia nigra pars compacta of mice (9 weeks old). Immunohistochemical staining and optical density (OD) analysis of astroglial (GFAP, glial fibrillary acidic protein, A-F, M) and microglial (Iba1, Ionized calcium binding adaptor molecule 1, G-L, N) cells. n=3. * P<0.05; ** P<0.01; *** P<0.001 vs. PBS control, Newman-Keuls post hoc test, 1-way ANOVA.*

In motor behavioural tests, LC-induced reduction of horizontal and vertical activity of young mice was not seen in the KYP-2047 treated group (vertical counts: $P = 0.0391$; $F_{2,27} = 3.664$; $P < 0.05$, vehicle vs. KYP-2047, Newman-Keuls post hoc test, 1-way ANOVA; Fig. 17 A-B). KYP-2047 did not have an effect on the activity of aged mice (Fig. 17 C-D). In cylinder test, no KYP-2047 or LC induced differences were observe in young mice upon rearing but the paw use for landing was at the same level between PBS and LC + KYP-2047 group, and LC + vehicle mice used more contralateral paw ($P = 0.0380$; $F_{2,27} = 3.680$, 1-way ANOVA) although this did not reach significance in post hoc tests (Fig. 17 E-F).

In the aged mice, LC-induced ipsilateral paw use was upended for the use of contralateral paw by KYP-2047; statistically significant difference between LC + vehicle and LC + KYP-2047 groups upon rearing ($P < 0.01$, Newman-Keuls post hoc test), and for the landing, ($P = 0.0053$; $F_{2,8} = 10.83$, 1-way ANOVA, $P < 0.05$ PBS vs. LC + KYP-2047, $P < 0.01$ LC + vehicle vs. LC + KYP-2047, Newman-Keuls post hoc test).

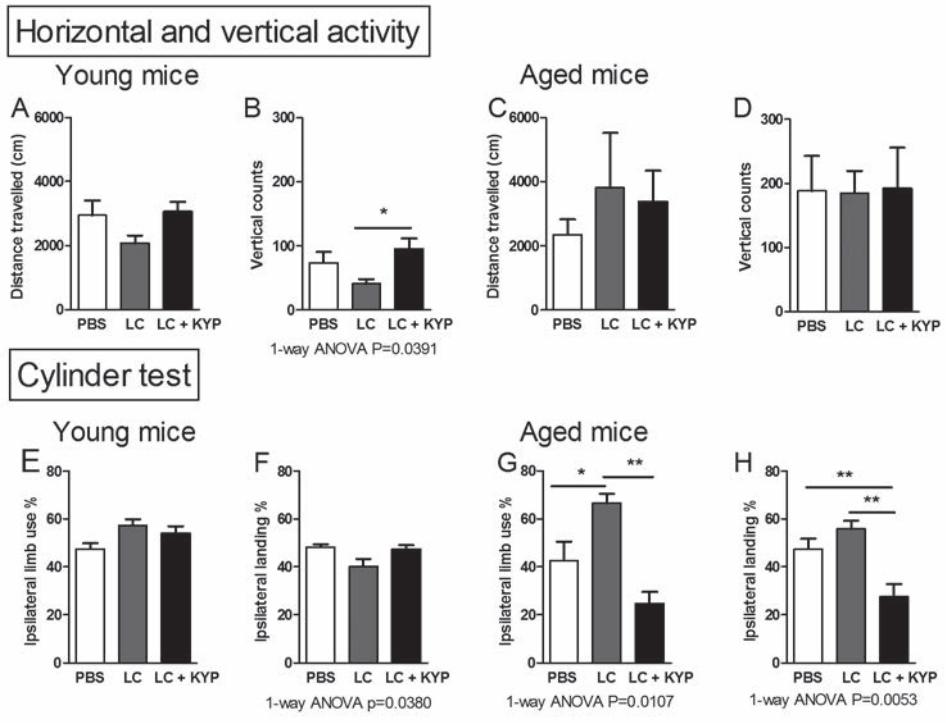

Figure 17: *The effect of KYP-2047 (a prolyl oligopeptidase inhibitor) on lactacystin (LC)-induced motor decline in mice. Characterization of motor behaviour of young and aged mice after microinjection of LC above substantia nigra pars compacta, PBS microinjection was used as a control. Mice were treated with KYP-2047 for 5 days after LC injection. Horizontal and vertical activities were measured for 2 hours and cylinder test was recorded for 5 min. Young n=4-9, aged n=3-4 (data for aged mice are supplemental results). * P<0.05; ** P<0.01 Newman-Keuls post hoc test, 1-way ANOVA.*

6 DISCUSSION

6.1 Enhanced dimerization of α-synuclein via direct protein-protein interaction with PREP is modulated by KYP-2047(I)

Earlier cell-free *in vitro* studies have shown that purified recombinant PREP enhances aSyn aggregation *in vitro*, whereas inactive mutant, PREP(S554A), did not have the same effect (Brandt *et al.*, 2008). Furthermore, inhibition of enzyme activity of PREP by small-molecule inhibitors abolished the aggregation-promoting effect of PREP. PREP inhibitors were also shown to reduce oxidative-stress-induced aSyn aggregation in cell culture models (Myöhänen *et al.*, 2012, Van der Veken *et al.*, 2012) and accumulation of aSyn in aSyn overexpressing TG mice (Myöhänen *et al.*, 2012). Furthermore, PREP had been shown to colocalize with aSyn in cell culture (Myöhänen *et al.*, 2012) and in brain of PD patients (Hannula *et al.*, 2013). These data suggests PREP inhibition as an interesting candidate for further investigation as an aSyn aggregation-modulating drug.

Dimerization is the first step of aSyn aggregation process (Wood, 1999, Uversky *et al.*, 2001a and 2007), and we showed that PREP and PREP(S554A) interact with aSyn in both MST and PCA, and that they promote dimerization of aSyn in PCA in living cells. This, together with the findings that PREP enhances aSyn aggregation in *in vitro* aggregation assay (Brandt *et al.*, 2008) suggest that PREP acts as a seeding point for aSyn nucleation as does the interaction of aSyn with some other proteins, such as Aβ (Masliah *et al.*, 2001), Tau (Giasson *et al.*, 2003), tubulin (Kim *et al.*, 2008) and FK506 binding proteins (Gerard *et al.*, 2010). Interestingly, we also observed that the interaction happened between catalytically inactive PREP and aSyn. PREP and PREP(S554A) could therefore both act as a seeding point for the aggregation.

PREP is an enzyme and its main physiological function is connected to degradation and maturation of small, less than 30 amino acids long, peptides (Toide *et al.*, 1995, Garcia-Horsman *et al.*, 2007). It does not cleave aSyn (Brandt *et al.*, 2008) and therefore it had been a question if PREP could have relevance in aSyn aggregation and what would be the mechanism of it. Interestingly, several studies provide evidence that PREP has other, in some cases enzyme activity-independent, neuronal functions in addition to its neuropeptide cleaving role, such as a role in cell-death via GAPDH regulated genotoxic stress (Matsuda *et al.*, 2013), a regulatory role in growth cone function via interaction with GAP-43 (Di Daniel *et al.*, 2009), a role in axonal transport and protein secretion (Schulz *et al.*, 2005), or regulation of insulin and glucagon secretion via hypothalamic regulatory pathway (Kim *et al.*, 2014). It was also shown in previously mentioned and other studies that PREP interacts with GAPDH and GAP-43 proteins (Di Daniel *et al.*, 2009, Szeltner *et al.*, 2010, Matsuda *et al.*, 2013), and now our studies show that PREP can interact with aSyn, thus regulating its dimerization and aggregation.

It was an intriguing finding that KYP-2047 only reduced PREP-induced aSyn dimerization and had no effect on PREP(S554A)-induced aSyn dimerization in the cell culture model. Other studies have shown that PREP adopts different conformational states, which can be modified by KYP-2047 or other inhibitors (Tarrago *et al.*, 2009, Szeltner *et al.*, 2010, Kichik *et al.*, 2011). This is supported by findings of this study indicating that KYP-2047 modifies the conformational

state of PREP but not PREP(S554A). Furthermore, when gating properties of PREP have been studied and modelled, it has been suggested to undergo conformational alterations upon inhibitor binding (Kaszuba *et al.*, 2012, Szeltner *et al.*, 2013, Kaushik *et al.*, 2014). These observations propose that the closed conformation of PREP, which can be induced by KYP-2047, binds to aSyn and reduces its dimerization, whereas other conformations promote aggregation. To study this further, the influence of different conformational states on aSyn interaction and aggregation could be examined. These methods could also be used to screen and characterize protein-protein interactions of PREP with other aggregate-prone proteins.

6.2 Characterization of brain α-synuclein pathology, dopaminergic system and neurotoxin sensitivity of $Snca^{tm(A30P)}$ mouse strain (II & III)

A30P mutated aSyn is associated with early-onset PD in humans (Krüger *et al.*, 1998). It is more prone to form fibrils than WT aSyn (Conway *et al.*, 2000b) and therefore appears to be more neurotoxic. The majority of TG mouse strains carry additional human aSyn transgene on top of endogenous Snca gene. The reason to use a mouse strain that had point mutation insertion in endogenous Snca gene and no aSyn TG addition, was to more closely mimic human genetic background in the disease model. In the earlier study, where $Snca^{tm(A30P)}$ mouse line was characterized, the main findings of Plaas et al. (2008) were age-dependent motor decline in beam walk and stride length tests, and reduced DA and DOPAC content in the STR. In the study II, horizontal and vertical activities, brain aSyn immunostaining, DA neurochemistry and 6-OHDA sensitivity were compared between Tm mice and WT littermates. We showed that Tm mice were more active during the first hours of activity measurement, they had accumulation of aSyn in the brain compared to WT mice, but there were no differences in the basal DA levels as the mice aged to 6, 13 or 16 months. Moreover, A30P mutation in Snca gene did not sensitize the 6 months old mice to toxicity of 6-OHDA. The main observations in this study were partially different than the results of Plaas et al. (2008)

Unexpectedly, we did not observe either age-dependent motor decline or DA depletion in the STR of Tm mice. Instead, we detected increased horizontal activity of aged and young mice in the beginning of the activity measurement and normal DA in the STR. The distinct observations between us and Plaas et al. might be explained by difference in the generation of the mice in the studies. aSyn regulates synaptic vesicular pool (Murphy *et al.*, 2000) and A30P mutation has been shown to reduce its vesicle binding activity (Jensen *et al.*, 1998). Therefore, altered presynaptic vesicle pool regulation affecting Tm mice could explain our observation of minor changes in motor behaviour. Moreover, A30P aSyn reduces DAT activity (Wersinger *et al.*, 2003) and inhibition of DAT is shown to cause hyperactive behaviour in monkeys (Andersen *et al.*, 2012). Increased motor activity has also been described in aSyn overexpressing mouse lines (Neumann *et al.*, 2002, Lam *et al.*, 2011, Farrell *et al.*, 2014). Furthermore, it is possible that TG mice develop compensatory mechanisms against pathological aSyn (Kreiner, 2015).

At 4 weeks post-lesion, 1.0 µg 6-OHDA reduced STR DA content in both genotypes by approximately 30 %, but it reached significance only in WT mice. The data is consistent with our behavioural observations where 6-OHDA did not induce significant rotational bias after

D-amphetamine challenge, although at 4 weeks post-lesion WT mice rotate to ipsilateral direction. A30P aSyn-induced alterations in DAT or VMAT2 activities could make Tm mice more vulnerable or resistant to 6-OHDA toxicity, because 6-OHDA is taken up into neurons via DAT and sequestration of it into vesicles via VMAT2 could reduce its toxicity (Cleren *et al.*, 2003, Schober, 2004). A30P aSyn is shown to be a negative regulator of DAT activity as compared to WT aSyn and they both protect cells from DA-mediated cellular stress and toxicity (Wersinger *et al.*, 2003). A30P aSyn could therefore reduce the 6-OHDA induced neurodegeneration. When toxin sensitivity was tested, no robust toxicity of 6-OHDA in general could be observed in either of the genotypes. Therefore it seems that A30P mutation in mouse Snca gene does not induce remarkable alterations in DAT or VMAT functions.

It is shown in mice that reduction of over 70 % of the SN TH+ neurons is required for motor deficit to occur (Grealish *et al.*, 2010), which supports the results of the current study where no great alterations in STR DA and in motor behaviour were detected. In literature, 6-OHDA is commonly used at higher doses than in our study: doses range from 4 ug (Akerud *et al.*, 2001, Alvarez-Fischer *et al.*, 2008), 8 ug (Morroni *et al.*, 2014), 10 ug (Hernandes *et al.*, 2013) and up to 20 ug (Silva *et al.*, 2005). It was therefore likely that the doses of 0.33 and 1.0 µg, as used in study II, were too small to induce striatal lesion.

In the earlier report by Plaas et al. (2008) of $Snca^{tm(A30P)}$ strain, brain aSyn was not characterized. We thus wanted to measure if mouse A30P aSyn accumulates in the brain more than WT aSyn. The mice of both genotypes had only one copy of Snca gene but the brain aSyn levels were increased in aged Tm mice in IHC and WB observations. aSyn accumulated in the brain also by age in both of the genotypes. In WB analysis, A30P aSyn appeared to form more oligomers than WT aSyn in aged mice. Oligomeric forms of aSyn tend to accumulate in neurons, which may explain the stronger IHC staining. These results are supported by earlier findings that human A30P aSyn causes early-onset PD in human, is more prone for aggregation than WT aSyn and disturbs its own cellular clearance (Krüger *et al.*, 1998, Conway *et al.*, 1998, Li *et al.*, 2001, Cuervo *et al.*, 2004). Mouse A30P aSyn may have differences in its aggregation and toxic properties, since it is normal to mouse to carry A53T mutation in aSyn whereas in human it is abnormal and associated with PD (Lavedan, 1998). Most of the studies that have examined aSyn toxicity and accumulation have been done using human aSyn, which is clearly justified. But the fundamental difference of the $Snca^{tm(A30P)}$ mouse not to have human aSyn expression makes it interesting for providing insight about differences between species. Indeed, A30P mutation appeared to cause aSyn accumulation and mild behavioural alterations, suggesting that it is more pathogenic than mouse WT aSyn.

For a good PD model and to study aSyn-modifying drugs, many features are expected from the model: LB-like aSyn accumulation and dopaminergic cell loss in the SNc, loss of DA in the STR and motor behaviour deficits are the most important (Beal, 2010). Even though, some degree of accumulation of A30P aSyn was observed we did not detect motor decline or loss of DA and from this point of view the $Snca^{tm(A30P)}$ mouse model did not meet the requirements for a PD model, at least until the age of 16 months, which was used as an endpoint. We observed accumulation of A30P aSyn and also some disturbances in the DAergic system and motor behaviour. This implicates that the model recapitulates some pathological alterations of PD or other synucleinopathies and more likely reflects the early changes occuring upon

aSyn accumulation. In this sense, it would be rational to use this model for studies of aSyn accumulation and its effects on brain function. In order to find a better mouse PD model with aSyn pathology, it would be interesting to combine Snca$^{tm(A30P)}$ mouse strain or some other mild aSyn pathology exhibiting TG mouse strain and pharmacological tools that induce aSyn aggregation or accumulation.

6.3 Beneficial effects of KYP-2047 treatment in Snca$^{tm(A30P)}$ mice and α-synuclein clearance associated with activation of macroautophagy (III)

Earlier studies had shown that PREP inhibition reduces the aggregation of aSyn in *in vitro* (Brandt *et al.*, 2008), cell culture (Myöhänen *et al.*, 2012, Van der Veken *et al.*, 2012) and in the brain of aSyn TG mice (Myöhänen *et al.*, 2012). Therefore, the purpose of the study III was to further assess the effects of KYP-2047 on aSyn conformations in Snca$^{tm(A30P)}$ mouse line. The main observations in study III were that KYP-2047 treatment reduced brain aSyn immunoreactivity in IHC, and in long-term treatment it also reduced HMW aSyn species in WB. Additionally, KYP-2047 modulated DA and metabolite levels in the STR, partly differentially. A30P aSyn oligomer accumulation was associated with reduced 20S proteasome activity, which returned to the control level after 28-day KYP-2047 treatment. Furthermore, short-term KYP-2047 treatment increased the brain LC3BII level, which is a marker of autophagosomes, suggesting enhanced autophagy. When PREP inhibition and autophagy were studied more closely in cell culture, KYP-2047 was shown to enhance beclin 1-mediated autophagy.

It is shown that oligomeric forms are the neurotoxic species of aSyn (Feng *et al.*, 2010, Winner *et al.*, 2011, Colla *et al.*, 2012b) and their reduction is suggested as a feasible PD-modifying therapy option (Outeiro and Kazantsev, 2008, Lashuel *et al.*, 2013). Because we did not observe robust PD-like pathology in Snca$^{tm(A30P)}$ mice, we did not expect a lot of changes, for example in behavioural assays, in association with drug treatments. The lack of strong aSyn pathology is also a drawback of this model because it limits the possibilities to fully evaluate the effects of drug treatment. Nonetheless, reduced load of HMW aSyn oligomers was observed in Tm mice after 28-day KYP-2047 administration. Interestingly, we also measured altered DA and metabolite levels in the STR following the KYP-2047 treatment. Short-term KYP-2047 administration appeared to increase DA metabolite levels in both mouse strains but 28-day treatment robustly increased DA and HVA levels only in Tm mice. We therefore suggest that the elevated DA and HVA levels after longer treatment are associated with reduced HMW aSyn amount and follow the changes in aSyn-mediated modulation of DA turnover. These alterations could occur via altered aSyn effects on DA production or degradation, since aSyn overexpression and accumulation have been associated with Nurr1 downregulation in cell culture (Baptista *et al.*, 2003) and in PD patients (Jankovic *et al.*, 2005), Nurr1 reduction can lead to reduction of expression of DAT, TH, VMAT2 and AADC (Baptista *et al.*, 2003, Jankovic *et al.*, 2005). aSyn has been shown to inhibit TH activity (Perez *et al.*, 2002, Peng *et al.*, 2005) and aSyn aggregation into LB-like inclusions has also been linked to reduced inhibitory capacity over TH activity (Alerte *et al.*, 2008, Wu *et al.*, 2012). Because no changes were observed in TH immunorectivity between genotypes or treatments it is likely that reduced aSyn amount in KYP-2047 treated Tm mice could contribute to increased activity of TH and subsequently increased DA content in the brain.

Interestingly, we also noticed reduced DAT immunoreactivity in the STR after 28-day KYP-2047 treatment in both of the genotypes. aSyn overexpression is associated with augmented DAT expression in mice (Bellucci *et al.*, 2011), KYP-2047-mediated aSyn reduction could have thus induced DAT down regulation.

The observations of KYP-2047-induced reduction of HMW aSyn were done in the aged Tm mice, which had A30P aSyn accumulation in the brain. Since KYP-2047 had an effect on already accumulated aSyn load, it raised the question if PREP could have an effect on aSyn cellular clearance. Therefore, the relevant pathways for aSyn clearance were studied more closely. UPS is important for aSyn degradation, but it can be compromised by A30P aSyn or HMW aSyn (Tanaka *et al.*, 2001, Snyder *et al.*, 2003, Alvarez-Castelao *et al.*, 2014). As expected, we observed mild reduction of 20S proteasome activity in aged Tm mice. Proteasome dysfunction has been associated with aSyn overexpression also in other studies (Chen *et al.*, 2006). KYP-2047 itself does not have an effect on proteasome activity in cell culture (unpublished data, Myöhänen TT) and because PREP inhibition did not have the same effect on both genotypes it is likely that the recovery of proteasomal activity after KYP-2047 treatment in Tm mice is a result of reduced aSyn oligomer burden. Thus, we ruled out the possibility of PREP inhibition as a proteasomal function modifying agent.

Macroautophagy is an interesting target for drug research due to its inducible nature. It is also thought to participate in the degradation of HMW protein complexes, including aSyn. Elevated levels of LC3BII in Tm mice after KYP-2047 treatment could reflect either enhanced autophagy or accumulation of autophagosomes as a result of their blocked lysosomal degradation (Klionsky *et al.*, 2008). We therefore tested the effect of KYP-2047 together with autophagy inhibitors in cell culture. KYP-2047 reversed the 3-MA-inhibited formation of autophagosomes and reduced the level of accumulation marker, p62. Moreover, when the fusion of the autophagosome and the lysosome was blocked with Baf, KYP-2047 treatment further elevated the LC3BII levels. This data points to a KYP-2047-mediated increase in the formation of autophagosomes, which was further supported by the findings that KYP-2047 elevated the levels of beclin 1 in autophagy inhibitor assay in WB and increased amount of beclin 1 mRNA. Beclin 1 is a positive regulator of autophagy, which is controlled by a complex network of many positive and negative regulators (Spencer *et al.*, 2009, Kang *et al.*, 2011, Fu *et al.*, 2013). Beclin 1 is also an anti-apoptotic protein (Kang *et al.*, 2011, Decuypere *et al.*, 2012). Our results suggest that PREP could be one of the direct modulators which interact with beclin 1, or it could have an effect on some downstream factor along the cascade. Some studies have suggested that PREP is an indirect negative regulator of inositol 1,4,5- triphosphate, because PREP inhibitors and loss of PREP coding gene have been shown to transiently elevate inositol 1,4,5- triphosphate levels (Williams *et al.*, 1999, Harwood, 2011). Inositol 1,4,5 –triphosphate receptor-mediated signaling may positively or negatively regulate autophagy depending on the cellular conditions (Parys *et al.*, 2012). Based on the findings of this and other studies showing a positive role of PREP inhibition on aSyn clearance and cell survival (Lambeir, 2011, Myöhänen *et al.*, 2012, Dokleja *et al.*, 2014), the inositol 1,4,5-triphosphatecould be a target for the observed actions of PREP inhibitors. However, as multiple pathways play a role in autophagy the mechanism for the observed beclin 1-mediated autophagy enhancement and resulting aSyn clearance remains to be further clarified in the future.

Autophagy enhancement has proved to facilitate protection against aSyn toxicity; in cell culture, curcumin-directed autophagy enhancement protects cells from A53T aSyn toxicity (Jiang *et al.*, 2013) and lentivirus-mediated beclin 1 overexpression effectively reduced aSyn accumulation (Spencer *et al.*, 2009). It is intriguing that PREP inhibition has been shown to modulate Aβ formation and secretion in cell culture and to prevent the formation of amyloid-like inclusions in a mouse model (Shinoda *et al.*, 1997, Kato *et al.*, 1997), but it was also shown that PREP is not directly involved in Aβ formation and degradation (Petit *et al.*, 2000). In light of the findings of Study III, it is an interesting question whether the beneficial effects of PREP inhibition seen in the mouse study that were not related to direct effect of PREP on Aβ, could have been associated with autophagy inductory function of PREP inhibition. At least in cell culture, autophagy-induction has been proven to be neuroprotective against Aβ (Hung *et al.*, 2009).

6.4 Lactacystin-induced proteasome inhibition as a mouse model of Parkinson's disease and effects of KYP-2047 (IV)

Impaired UPS function in the SN is connected to PD pathophysiology (McNaught and Jenner, 2001, McNaught *et al.*, 2003). It is not only aSyn, which accumulate in LB-like inclusions, but over 70 components have been indentified in the LBs, for example aSyn- or synphilin-binding proteins, proteins associated with proteasome or autophagy, lipids and many more (Wakabayashi *et al.*, 2007). UPS pathway is in part responsible for cellular clearance of aSyn (Bennett *et al.*, 1999, Webb *et al.*, 2003, Ebrahimi-Fakhari *et al.*, 2011). However, aSyn inhibits the function of proteasomes (Bence *et al.*, 2001, Tanaka *et al.*, 2001, Snyder *et al.*, 2003, Lindersson *et al.*, 2004), other factors such as genetic mutations and oxidative stress may also impair UPS (Betarbet *et al.*, 2005). UPS dysfunction may be responsible for increased aSyn accumulation, making the proteasome a cofactor in PD pathophysiology. Moreover, aSyn genetic overexpression is only a minor cause for PD and in many TG mouse models, very robust PD-like phenotype is not seen in spite of high expression of aSyn. To that end it was reasonable to study the features of proteasome-inhibition as a PD mouse model, which was the first aim of study IV. Autophagy inductors have already been studied in some LC models: in cell culture, natural substances with an autophagy enhancing effect have been shown to improve cell viability (Bae *et al.*, 2011 and 2014), and autophagy enhancement by rapamycin has been beneficial in a mouse study, where LC was injected into MFB (Pan *et al.*, 2008). We hypothesized that autophagy induction by KYP-2047 might have beneficial neuroprotective effects against toxicity of proteasome inhibition. Therefore, the second aim of study IV was to evaluate the ability of KYP-2047 to protect neurons against toxicity of LC.

The main findings after unilateral LC administration above the SN were increased amount of aSyn and GAD-immunoreactivity in the lesioned side of the SN, associated with TH+ neuron and fibre loss in the SNc and TH+ terminal loss and reduction of DA content in the STR. Similar to PD, astroglial and microglial activation was observed throughout the injected hemisphere. LC also induced motor behaviour alterations in cylinder test and horizontal and vertical acitivy measurement.

In earlier studies, LC injection has been introduced in the MFB or STR (Fornai *et al.*, 2003, Vernon *et al.*, 2011, Shen *et al.*, 2013, Konieczny *et al.*, 2014), and a recent paper described a mouse model based on intranigral LC injection, where Bentea et al. (2015) showed similar results to us: reduced amount of TH+ neurons, increased amount of aSyn and behavioural deficits. In study IV, the end-point for the experiment was 10 days, which seems to be sufficient for the manifestation of a PD-like phenotype. In Bentea et al. (2015) LC-induced lesion was shown to be non-progressive when lesion severity was compared at 1 and 3 weeks post-injection. LC induced rapid-onset neurodegeneration, which has been observed also in other studies (Vernon *et al.*, 2011, Bentea *et al.*, 2015). LC is an irreversible inhibitor of the proteasome (Fenteany and Schreiber, 1998), but it is possible that some spontaneous recovery occurs at later time points if the effect of LC is lost as new proteasomes are synthetized in the cells. Therefore, the LC model can be useful for an assessment of neuroprotective drugs but whether it is suitable for an evaluation of long-term treatments, remains to be elucidated.

LC reduced both the number of TH+ neurons and fibres in the SN, which was consistent with the observed striatal DA depletion. Interestingly, we did not see as great a loss of DAergic TH+ terminals in the STR as would have been expected from the DA content. In young mice, KYP-2047 appeared to partially protect TH+ fibres in the SN and dopaminergic terminals in the STR, but could neither rescue cell bodies in the SNc nor restore DA in the STR. Additionally, in the behavioural assays KYP-2047 treatment opposed some of the LC-induced changes. This data suggests a neuroprotective effect of PREP inhibition over dopaminercig system.

LC did not have an effect on 5-HT and 5-HIAA levels in the STR. In Bentea et al (2015), parvalbumin IHC, a marker of GABAergic neurons was assessed in the SN and no changes in the number of neurons were observed. Therefore, the UPS inhibition seems to be specifically toxic to DAergic neurons in the SNc. In our hands the expression of GABAergic marker GAD was significantly increased in the SNr. These results suggest that the observed GAD increase occurs due to reduced DAergic inhibition. Earlier studies with PD toxin models support this finding as increased GABAergic activity (Wang *et al.*, 2010) and GAD mRNA expression (Salin *et al.*, 2002, Wang *et al.*, 2010) in the 6-OHDA lesion side of PD rat model were reported.

Increased aSyn amount and pS129 aSyn after UPS inhibition have been shown (Bentea *et al.*, 2015). Also in our study, increased aSyn accumulation in the SN was measured in the LC-lesioned side. In standard aSyn IHC, we did not detect differences in aSyn amount in the brain after KYP-2047. We tried to use PK-treatment, described in (Angot *et al.*, 2012) and aSyn IHC to study the insoluble aSyn in the brain sections, but the assay did not work in our hands. Therefore, it remains a challenge to set up a functional assay for aSyn conformational analysis.

Previous studies have reported microglial and astroglial activation in the SN after LC injection into MFB (Zhu *et al.*, 2007, Li *et al.*, 2010). aSyn has been shown to activate inflammatory responses of astroglial cells, (Lee *et al.*, 2010a, Fellner *et al.*, 2013). In this study, aSyn immunoreactivity was mainly increased in the SN, whereas marked astrogliosis and microgliosis were evident throughout the whole hemisphere at the nigral level. The widespread activation cannot be explained solely by direct influence of LC, because it has a local effect in the SN. This points to a more widespread activation of an inflammation cascade due to UPS inhibition and imbalance in protein homeostasis. Glial activation is linked to PD pathogenesis; microglia and

astroglia normally have neuronal and brain tissue homeostasis supporting functions and they are activated upon stress, inflammation and neurodegeneration. It has been proposed that they may promote neurodegeneration by pro-neuroinflammatory signals or they might be neuroprotective by participating in the degradation of pathological aSyn and release neuroprotective factors (Brück *et al.*, 2015). Regulation of glial responses has been suggested as an option to target neurodegenerative diseases (Hirsch and Hunot, 2009). Based on the findings of study IV, LC-based model could be utilized in the study of neuroinflammation in PD.

Neurodegeneration is a complex process and if it has proceeded enough, neuroprotective treatments might not be effective. Now KYP-2047 was administered for 5 days, immediately after LC injection. In other neuroprotection studies, the treatments have been generally started 7 days before (Zhu *et al.*, 2007, Li *et al.*, 2010) or after (Zhu *et al.*, 2007, Pan *et al.*, 2008) the LC injection and continued 4 weeks post-injection, at which time point significant neuroprotective effects were observed. In study IV, the endpoint was 10 days, and it is likely that the observed changes in the markers of DAergic system after KYP-2047 administration reflect early recovery after LC microinjection.

Taken together, UPS inhibition induces fast-onset PD-like phenotype in mice recapitulating the cardinal features of PD pathology: aSyn accumulation, DAergic neuron and DA loss, motor impairment and neuroinflammation. Moreover, KYP-2047-mediated partial neuroprotection was seen in young mice. This suggests that PREP inhibition can, at least in part, overcome the cellular deficits caused by UPS impairment.

7 CONCLUSIONS

The aim of this work has been to study the effects of PREP inhibition in relation to aSyn aggregation *in vitro* and *in vivo*. In the study, multiple approaches were used in order to induce and examine aSyn aggregation and accumulation *in vivo*. Our findings support the earlier studies that PREP inhibitors reduce aSyn aggregation, and provide evidence about mechanisms underlying this phenomena. Furthermore, PREP inhibition could be a beneficial aSyn-modifying treatment strategy in PD and other synucleinopathies. The main findings of the cell culture and *in vitro* models in addition to studies with TG mice and toxin administrations to mice, are:

I PREP and aSyn interact via direct protein-protein interaction. The interaction enhances aSyn dimerization independently of PREP enzyme activity, and aSyn dimerization is reduced when PREP is inhibited. This might be explained by PREP conformation shift into a compact form by the inhibitor.

II A30P point mutation in mouse Snca gene ($Snca^{tm(A30P)}$ strain) slightly induces aSyn aggregation but does not produce PD-like phenotype since it lacks motor deficit and TH-positive cell loss.

III In $Snca^{tm(A30P)}$ mice, PREP-inhibition reduces the amount of HMW forms of aSyn, which are considered to be the neurotoxic aSyn species. In the mouse model and in cell culture, KYP-2047 induces macroautophagic protein clearance, which may explain the reduced aSyn burden.

IV Nigral administration of a proteasome inhibitor, lactacystin, produces fast-onset PD-like phenotype in mice, which is characterized by aSyn accumulation, neuroinflammation, loss of TH-positive neurons in the sustantia nigra and striatum together with motor behavioural deficits. KYP-2047 partially protected substantia nigra TH-positive fibres against toxicity of lactacystin and had beneficial effect on motor behaviour.

8 ACKNOWLEDGEMENTS

This work was carried out at the Division of Pharmacology and Pharmacotherapy, Faculty of Pharmacy, University of Helsinki during the years 2011 and 2015.

The financial support from the following funders is gratefully acknowledged: FinPharma Doctoral Program Pharmacy section, The Emil Aaltonen Foundation, The Finnish Parkinson Foundation and The Finnish Pharmaceutical Society.

I wish to express my deepest gratitude to my supervisors Docent Timo Myöhänen and Professor (emeritus) Pekka Männistö. Timo is warmly thanked for giving me the opportunity to work in his group, for guidance and support on my way of becoming a scientist, and for introducing me to the world of α-synuclein and prolyl oligopeptidase. Thank you for reminding me during the times of despair that "it will go well / hyvin se menee". Pekka, thank you for sharing your expertise in pharmacology and neuroscience. I appreciate guidance with scientific writing and encouragement that you have given.

Professor Raimo Tuominen is thanked for agreeing to act as a custos in the public defense of this thesis and for giving advice during the years.

Reviewers of this thesis, Professors Anne-Marie Lambeir and Markus Forsberg, are thanked for the constructive comments and suggestions, which substantially improved the thesis manuscript.

I would like to thank Professor Heikki Tanila for agreeing to act as my opponent in the public defense of this thesis.

I wish to express my gratitude to all my co-authors for their contribution, which has made this work possible. Especially I would like to thank Dr. Marjo Piltonen for sharing her knowledge in the beginning of my PhD project, Dr. Brandon Harvey and Dr. Christopher Richie, for sharing their expertise and giving me the great opportunity to learn molecular biology methods in NIDA, Baltimore, and M.Sc. Xu Yan and M.Sc.Katrina Albert for great collaboration. Dr. Mikko Airavaara, for generous assistance and advice with my experiments and Docent Henri Huttunen for sharing his expertise.

The current and former colleagues of Division of Pharmacology and Pharmacotherapy are warmly thanked for their help during all these years. Particularly, Johanna, Iida, Susanne, Virpi and Jaakko, I appreciate our scientific discussions over the years. I would like to express my gratitude to laboratory technicians Marjo Vaha and Liisa Lappalainen for outstanding technical assistance with my experiments. I would especially like to thank Kati Rautio, without her, I would most likely still be doing sectioning and stainings.

I am deeply thankful to my dear colleagues in Myöhänen research group. Mirva for friendship since the first day of our master's studies, for sharing so many great moments and for the support in the difficult times. Reinis, Ulrika and Susanna, I greatly appreciate your friendship and the positive environment in the office that you have created.

I would also like to thank all my friends outside the world of science for continuous encouragement and most importantly all the discussions and free time activities from dinners and late-nights, to travels and networking activities. Especially Laura, Eve M., Liisa, Eve R., Merja and Piia, I am so lucky to have such a great friends around me.

Finally, I express my deepest gratitude to my dearly loved family. I want to thank my mother Tuula, my brother Sakari, and my sister Johanna and her family, my father Kalle and his family, for endless love and support. You mean the world to me.

Helsinki, September 2015

Mari

9 REFERENCES

Abeliovich, A. (2000). Mice lacking alpha-synuclein display functional deficits in the nigrostriatal dopamine system. Neuron 25: 239-52.

Abeywardana, T., Pratt, M. R. (2015). Extent of inhibition of alpha-synuclein aggregation in vitro by SUMOylation is conjugation site- and SUMO isoform-selective. Biochemistry 54: 959-61.

Abou-Sleiman, P.M., Muqit, M. M. & Wood, N. W. (2006). Expanding insights of mitochondrial dysfunction in Parkinson's disease. Nat.Rev.Neurosci. 7: 207-19.

Ahn, K.J., Paik, S. R., Chung, K. C. & Kim, J. (2006). Amino acid sequence motifs and mechanistic features of the membrane translocation of alpha-synuclein. J.Neurochem. 97: 265-79.

Airavaara, M., Mijatovic, J., Vihavainen, T., Piepponen, T. P., Saarma, M. & Ahtee, L. (2006). In heterozygous GDNF knockout mice the response of striatal dopaminergic system to acute morphine is altered. Synapse 59: 321-9.

Akerud, P., Canals, J. M., Snyder, E. Y. & Arenas, E. (2001). Neuroprotection through delivery of glial cell line-derived neurotrophic factor by neural stem cells in a mouse model of Parkinson's disease. J.Neurosci. 21: 8108-18.

Alerte, T.N., Akinfolarin, A. A., Friedrich, E. E., Mader, S. A., Hong, C. S. & Perez, R. G. (2008). Alpha-synuclein aggregation alters tyrosine hydroxylase phosphorylation and immunoreactivity: lessons from viral transduction of knockout mice. Neurosci.Lett. 435: 24-9.

Alvarez-Castelao, B., Goethals, M., Vandekerckhove, J. & Castano, J. G. (2014). Mechanism of cleavage of alpha-synuclein by the 20S proteasome and modulation of its degradation by the RedOx state of the N-terminal methionines. Biochim.Biophys.Acta 1843: 352-65.

Alvarez-Erviti, L., Seow, Y., Schapira, A. H., Gardiner, C., Sargent, I. L., Wood, M. J., *et al.* (2011). Lysosomal dysfunction increases exosome-mediated alpha-synuclein release and transmission. Neurobiol.Dis. 42: 360-7.

Alvarez-Fischer, D., Henze, C., Strenzke, C., Westrich, J., Ferger, B., Hoglinger, G. U., *et al.* (2008). Characterization of the striatal 6-OHDA model of Parkinson's disease in wild type and alpha-synuclein-deleted mice. Exp.Neurol. 210: 182-93.

Ancolio, K., Alves da Costa, C., Ueda, K. & Checler, F. (2000). Alpha-synuclein and the Parkinson's disease-related mutant Ala53Thr-alpha-synuclein do not undergo proteasomal degradation in HEK293 and neuronal cells. Neurosci.Lett. 285: 79-82.

Andersen, M.L., Sawyer, E. K., Carroll, F. I. & Howell, L. L. (2012). Influence of chronic dopamine transporter inhibition by RTI-336 on motor behavior, sleep, and hormone levels in rhesus monkeys. Exp.Clin.Psychopharmacol. 20: 77-83.

Anderson, J.P., Walker, D. E., Goldstein, J. M., de Laat, R., Banducci, K., Caccavello, R. J., *et al.* (2006). Phosphorylation of Ser-129 is the dominant pathological modification of alpha-synuclein in familial and sporadic Lewy body disease. J.Biol.Chem. 281: 29739-52.

Angot, E., Steiner, J. A., Lema Tome, C. M., Ekstrom, P., Mattsson, B., Björklund, A., *et al.* (2012). Alpha-synuclein cell-to-cell transfer and seeding in grafted dopaminergic neurons in vivo. PLoS One 7: e39465.

Arima, K. (1998). Immunoelectronmicroscopic demonstration of NACP/alpha-synuclein-epitopes on the filamentous component of Lewy bodies in Parkinson's disease and in dementia with Lewy bodies. Brain Res. 808: 93-100.

Auluck, P.K., Chan, H. Y., Trojanowski, J. Q., Lee, V. M. & Bonini, N. M. (2002). Chaperone suppression of alpha-synuclein toxicity in a Drosophila model for Parkinson's disease. Science 295: 865-8.

Baba, M., Nakajo, S., Tu, P. H., Tomita, T., Nakaya, K., Lee, V. M., *et al.* (1998). Aggregation of alpha-synuclein in Lewy bodies of sporadic Parkinson's disease and dementia with Lewy bodies. Am.J.Pathol. 152: 879-84.

Bae, E.J., Lee, H. J., Rockenstein, E., Ho, D. H., Park, E. B., Yang, N. Y., *et al.* (2012). Antibody-aided clearance of extracellular alpha-synuclein prevents cell-to-cell aggregate transmission. J.Neurosci. 32: 13454-69.

Bae, N., Ahn, T., Chung, S., Oh, M. S., Ko, H., Oh, H., *et al.* (2011). The neuroprotective effect of modified Yeoldahanso-tang via autophagy enhancement in models of Parkinson's disease. J.Ethnopharmacol. 134: 313-22.

Bae, N., Chung, S., Kim, H. J., Cha, J. W., Oh, H., Gu, M. Y., *et al.* (2014). Neuroprotective effect of modified Chungsimyeolda-tang, a traditional Korean herbal formula, via autophagy induction in models of Parkinsons disease. J.Ethnopharmacol. 159C: 93-101.

Baptista, M.J., O'Farrell, C., Daya, S., Ahmad, R., Miller, D. W., Hardy, J., *et al.* (2003). Co-ordinate transcriptional regulation of dopamine synthesis genes by alpha-synuclein in human neuroblastoma cell lines. J.Neurochem. 85: 957-68.

Bayer, T.A. (1999). Alpha-synuclein accumulates in Lewy bodies in Parkinson's disease and dementia with Lewy bodies but not in Alzheimer's disease beta]-amyloid plaque cores. Neurosci.Lett. 266: 213-6.

Beal, M.F. (2010). Parkinson's disease: a model dilemma. Nature 466: S8-10.

Bellucci, A., Navarria, L., Falarti, E., Zaltieri, M., Bono, F., Collo, G., *et al.* (2011). Redistribution of DAT/alpha-synuclein complexes visualized by "in situ" proximity ligation assay in transgenic mice modelling early Parkinson's disease. PLoS One 6: e27959.

Bence, N.F., Sampat, R. M. & Kopito, R. R. (2001). Impairment of the ubiquitin-proteasome system by protein aggregation. Science 292: 1552-5.

Bennett, M.C., Bishop, J. F., Leng, Y., Chock, P. B., Chase, T. N. & Mouradian, M. M. (1999). Degradation of alpha-synuclein by proteasome. J.Biol.Chem. 274: 33855-8.

Bentea, E., Van der Perren, A., Van Liefferinge, J., El Arfani, A., Albertini, G., Demuyser, T., *et al.* (2015). Nigral proteasome inhibition in mice leads to motor and non-motor deficits and increased expression of Ser129 phosphorylated alpha-synuclein. Front.Behav.Neurosci. 9: 68.

Betarbet, R., Sherer, T. B. & Greenamyre, J. T. (2005). Ubiquitin-proteasome system and Parkinson's diseases. Exp.Neurol. 191 Suppl 1: S17-27.

Betemps, D., Verchere, J., Brot, S., Morignat, E., Bousset, L., Gaillard, D., *et al.* (2014). Alpha-synuclein spreading in M83 mice brain revealed by detection of pathological alpha-synuclein by enhanced ELISA. Acta Neuropathol.Commun. 2: 29,5960-2-29.

Biasini, E., Fioriti, L., Ceglia, I., Invernizzi, R., Bertoli, A., Chiesa, R., *et al.* (2004). Proteasome inhibition and aggregation in Parkinson's disease: a comparative study in untransfected and transfected cells. J.Neurochem. 88: 545-53.

Bisaglia, M., Mammi, S. & Bubacco, L. (2009). Structural insights on physiological functions and pathological effects of alpha-synuclein. FASEB J. 23: 329-40.

Braak, H., Del Tredici, K., Rub, U., de Vos, R. A., Jansen Steur, E. N. & Braak, E. (2003). Staging of brain pathology related to sporadic Parkinson's disease. Neurobiol.Aging 24: 197-211.

Braak, H., Ghebremedhin, E., Rub, U., Bratzke, H. & Del Tredici, K. (2004). Stages in the development of Parkinson's disease-related pathology. Cell Tissue Res. 318: 121-34.

Brandt, I., Gerard, M., Sergeant, K., Devreese, B., Baekelandt, V., Augustyns, K., *et al.* (2008). Prolyl oligopeptidase stimulates the aggregation of alpha-synuclein. Peptides 29: 1472-8.

Brück, D., Wenning, G. K., Stefanova, N. & Fellner, L. (2015). Glia and alpha-synuclein in neurodegeneration: A complex interaction. Neurobiol.Dis. (in press).

Burré, J., Sharma, M., Tsetsenis, T., Buchman, V., Etherton, M. R. & Südhof, T. C. (2010). Alpha-synuclein promotes SNARE-complex assembly in vivo and in vitro. Science 329: 1663-7.

Büttner, S., Delay, C., Franssens, V., Bammens, T., Ruli, D., Zaunschirm, S., *et al.* (2010). Synphilin-1 enhances alpha-synuclein aggregation in yeast and contributes to cellular stress and cell death in a Sir2-dependent manner. PLoS One 5: e13700.

Cao, S., Theodore, S. & Standaert, D. G. (2010). Fcgamma receptors are required for NF-kappaB signaling, microglial activation and dopaminergic neurodegeneration in an AAV-synuclein mouse model of Parkinson's disease. Mol.Neurodegener 5: 42,1326-5-42.

Chadchankar, H., Ihalainen, J., Tanila, H. & Yavich, L. (2011). Decreased reuptake of dopamine in the dorsal striatum in the absence of alpha-synuclein. Brain Res. 1382: 37-44.

Chan, T., Chow, A. M., Cheng, X. R., Tang, D. W., Brown, I. R. & Kerman, K. (2012). Oxidative Stress Effect of Dopamine on alpha-Synuclein: Electroanalysis of Solvent Interactions. ACS Chem. Neurosci. 3: 569-74.

Chandra, S., Gallardo, G., Fernandez-Chacon, R., Schluter, O. M. & Südhof, T. C. (2005). Alpha-synuclein cooperates with CSPalpha in preventing neurodegeneration. Cell 123: 383-96.

Chartier-Harlin, M.C., Kachergus, J., Roumier, C., Mouroux, V., Douay, X., Lincoln, S., *et al.* (2004). Alpha-synuclein locus duplication as a cause of familial Parkinson's disease. Lancet 364: 1167-9.

Chen, L., Jin, J., Davis, J., Zhou, Y., Wang, Y., Liu, J., *et al.* (2007). Oligomeric alpha-synuclein inhibits tubulin polymerization. Biochem.Biophys.Res.Commun. 356: 548-53.

Chen, L., Thiruchelvam, M. J., Madura, K. & Richfield, E. K. (2006). Proteasome dysfunction in aged human alpha-synuclein transgenic mice. Neurobiol.Dis. 23: 120-6.

Chen, L., Xie, Z., Turkson, S. & Zhuang, X. (2015). A53T human alpha-synuclein overexpression in transgenic mice induces pervasive mitochondria macroautophagy defects preceding dopamine neuron degeneration. J.Neurosci. 35: 890-905.

Chesselet, M.F., Richter, F. (2011). Modelling of Parkinson's disease in mice. Lancet Neurol. 10: 1108-18.

Chesselet, M.F., Richter, F., Zhu, C., Magen, I., Watson, M. B. & Subramaniam, S. R. (2012). A progressive mouse model of Parkinson's disease: the Thy1-aSyn ("Line 61") mice. Neurotherapeutics 9: 297-314.

Choi, W., Zibaee, S., Jakes, R., Serpell, L. C., Davletov, B., Crowther, R. A., *et al.* (2004). Mutation E46K increases phospholipid binding and assembly into filaments of human alpha-synuclein. FEBS Lett. 576: 363-8.

Chu, Y., Kordower, J. H. (2010). Lewy body pathology in fetal grafts. Ann.N.Y.Acad.Sci. 1184: 55-67.

Clark, J., Clore, E. L., Zheng, K., Adame, A., Masliah, E. & Simon, D. K. (2010). Oral N-acetyl-cysteine attenuates loss of dopaminergic terminals in alpha-synuclein overexpressing mice. PLoS One 5: e12333.

Cleren, C., Naudin, B. & Costentin, J. (2003). Apparent opposite effects of tetrabenazine and reserpine on the toxic effects of 1-methyl-4-phenylpyridinium or 6-hydroxydopamine on nigro-striatal dopaminergic neurons. Brain Res. 989: 187-95.

Colla, E., Coune, P., Liu, Y., Pletnikova, O., Troncoso, J. C., Iwatsubo, T., *et al.* (2012a). Endoplasmic reticulum stress is important for the manifestations of alpha-synucleinopathy in vivo. J.Neurosci. 32: 3306-20.

Colla, E., Jensen, P. H., Pletnikova, O., Troncoso, J. C., Glabe, C. & Lee, M. K. (2012b). Accumulation of toxic alpha-synuclein oligomer within endoplasmic reticulum occurs in alpha-synucleinopathy in vivo. J.Neurosci. 32: 3301-5.

Colley, W.C., Sung, T. C., Roll, R., Jenco, J., Hammond, S. M., Altshuller, Y., *et al.* (1997). Phospholipase D2, a distinct phospholipase D isoform with novel regulatory properties that provokes cytoskeletal reorganization. Curr.Biol. 7: 191-201.

Conway, K.A., Harper, J. D. & Lansbury, P. T. (2000a). Fibrils formed in vitro from alpha-synuclein and two mutant forms linked to Parkinson's disease are typical amyloid. Biochemistry 39: 2552-63.

Conway, K.A., Harper, J. D. & Lansbury, P. T. (1998). Accelerated in vitro fibril formation by a mutant alpha-synuclein linked to early-onset Parkinson disease. Nat.Med. 4: 1318-20.

Conway, K.A., Lee, S. J., Rochet, J. C., Ding, T. T., Williamson, R. E. & Lansbury, P. T.,Jr (2000b). Acceleration of oligomerization, not fibrillization, is a shared property of both alpha-synuclein mutations linked to early-onset Parkinson's disease: implications for pathogenesis and therapy. Proc. Natl.Acad.Sci.U.S.A. 97: 571-6.

Conway, K.A., Rochet, J. C., Bieganski, R. M. & Lansbury, P. T.,Jr (2001). Kinetic stabilization of the alpha-synuclein protofibril by a dopamine-alpha-synuclein adduct. Science 294: 1346-9.

Crews, L., Spencer, B., Desplats, P., Patrick, C., Paulino, A., Rockenstein, E., *et al.* (2010). Selective molecular alterations in the autophagy pathway in patients with Lewy body disease and in models of alpha-synucleinopathy. PLoS One 5: e9313.

Crowther, R.A., Jakes, R., Spillantini, M. G. & Goedert, M. (1998). Synthetic filaments assembled from C-terminally truncated alpha-synuclein. FEBS Lett. 436: 309-12.

Cuervo, A.M., Stefanis, L., Fredenburg, R., Lansbury, P. T. & Sulzer, D. (2004). Impaired degradation of mutant alpha-synuclein by chaperone-mediated autophagy. Science 305: 1292-5.

Cuervo, A.M., Wong, E. (2014). Chaperone-mediated autophagy: roles in disease and aging. Cell Res. 24: 92-104.

Culvenor, J.G., McLean, C. A., Cutt, S., Campbell, B. C., Maher, F., Jäkälä, P., *et al.* (1999). Non-Abeta component of Alzheimer's disease amyloid (NAC) revisited. NAC and alpha-synuclein are not associated with Abeta amyloid. Am.J.Pathol. 155: 1173-81.

Cunningham, D.F., O'Connor, B. (1997). Proline specific peptidases. Biochim.Biophys.Acta 1343: 160-86.

Danzer, K.M., Kranich, L. R., Ruf, W. P., Cagsal-Getkin, O., Winslow, A. R., Zhu, L., *et al.* (2012). Exosomal cell-to-cell transmission of alpha synuclein oligomers. Mol.Neurodegener 7: 42,1326-7-42.

Davidson, W.S., Jonas, A., Clayton, D. F. & George, J. M. (1998). Stabilization of alpha-synuclein secondary structure upon binding to synthetic membranes. J.Biol.Chem. 273: 9443-9.

Decressac, M., Mattsson, B. & Björklund, A. (2012a). Comparison of the behavioural and histological characteristics of the 6-OHDA and alpha-synuclein rat models of Parkinson's disease. Exp.Neurol.

Decressac, M., Mattsson, B., Lundblad, M., Weikop, P. & Björklund, A. (2012b). Progressive neurodegenerative and behavioural changes induced by AAV-mediated overexpression of alpha-synuclein in midbrain dopamine neurons. Neurobiol.Dis. 45: 939-53.

Decuypere, J.P., Parys, J. B. & Bultynck, G. (2012). Regulation of the autophagic bcl-2/beclin 1 interaction. Cells 1: 284-312.

Del Tredici, K., Rub, U., De Vos, R. A., Bohl, J. R. & Braak, H. (2002). Where does parkinson disease pathology begin in the brain? J.Neuropathol.Exp.Neurol. 61: 413-26.

Desplats, P., Lee, H. J., Bae, E. J., Patrick, C., Rockenstein, E., Crews, L., *et al.* (2009). Inclusion formation and neuronal cell death through neuron-to-neuron transmission of alpha-synuclein. Proc. Natl.Acad.Sci.U.S.A. 106: 13010-5.

Di Daniel, E., Glover, C. P., Grot, E., Chan, M. K., Sanderson, T. H., White, J. H., *et al.* (2009). Prolyl oligopeptidase binds to GAP-43 and functions without its peptidase activity. Mol.Cell.Neurosci. 41: 373-82.

Dice, J.F. (2007). Chaperone-mediated autophagy. Autophagy 3: 295-9.

Dijkstra, A.A., Voorn, P., Berendse, H. W., Groenewegen, H. J., Netherlands Brain Bank, Rozemuller, A. J., *et al.* (2014). Stage-dependent nigral neuronal loss in incidental Lewy body and Parkinson's disease. Mov.Disord. 29: 1244-51.

Ding, T.T., Lee, S. J., Rochet, J. C. & Lansbury, P. T.,Jr (2002). Annular alpha-synuclein protofibrils are produced when spherical protofibrils are incubated in solution or bound to brain-derived membranes. Biochemistry 41: 10209-17.

Dokleja, L., Hannula, M. J. & Myöhänen, T. T. (2014). Inhibition of prolyl oligopeptidase increases the survival of alpha-synuclein overexpressing cells after rotenone exposure by reducing alpha-synuclein oligomers. Neurosci.Lett. 583: 37-42.

Dong, Z., Ferger, B., Feldon, J. & Bueler, H. (2002). Overexpression of Parkinson's disease-associated alpha-synucleinA53T by recombinant adeno-associated virus in mice does not increase the vulnerability of dopaminergic neurons to MPTP. J.Neurobiol. 53: 1-10.

Doty, R.L. (2012). Olfactory dysfunction in Parkinson disease. Nat.Rev.Neurol. 8: 329-39.

Doyle, K.M., Kennedy, D., Gorman, A. M., Gupta, S., Healy, S. J. & Samali, A. (2011). Unfolded proteins and endoplasmic reticulum stress in neurodegenerative disorders. J.Cell.Mol.Med. 15: 2025-39.

Duda, J.E., Giasson, B. I., Chen, Q., Gur, T. L., Hurtig, H. I., Stern, M. B., *et al.* (2000). Widespread nitration of pathological inclusions in neurodegenerative synucleinopathies. Am.J.Pathol. 157: 1439-45.

Ebrahimi-Fakhari, D., Cantuti-Castelvetri, I., Fan, Z., Rockenstein, E., Masliah, E., Hyman, B. T., *et al.* (2011). Distinct roles in vivo for the ubiquitin-proteasome system and the autophagy-lysosomal pathway in the degradation of alpha-synuclein. J.Neurosci. 31: 14508-20.

El-Agnaf, O., Jakes, R., Curran, M. D. & Wallace, A. (1998a). Effects of the mutations Ala30 to Pro and Ala53 to Thr on the physical and morphological properties of alpha-synuclein protein implicated in Parkinson's disease. FEBS Lett. 440: 67-70.

El-Agnaf, O.M., Bodles, A. M., Guthrie, D. J., Harriott, P. & Irvine, G. B. (1998b). The N-terminal region of non-A beta component of Alzheimer's disease amyloid is responsible for its tendency to assume beta-sheet and aggregate to form fibrils. Eur.J.Biochem. 258: 157-63.

Engelender, S. (1999). Synphilin-1 associates with alpha-synuclein and promotes the formation of cytosolic inclusions. Nature Genet. 22: 110-4.

Escobar, V.D., Kuo, Y. M., Orrison, B. M., Giasson, B. I. & Nussbaum, R. L. (2014). Transgenic mice expressing S129 phosphorylation mutations in alpha-synuclein. Neurosci.Lett. 563: 96-100.

Fahn, S. (2003). Description of Parkinson's disease as a clinical syndrome. Ann.N.Y.Acad.Sci. 991: 1-14.

Farrell, K.F., Krishnamachari, S., Villanueva, E., Lou, H., Alerte, T. N., Peet, E., *et al.* (2014). Non-motor parkinsonian pathology in aging A53T alpha-synuclein mice is associated with progressive synucleinopathy and altered enzymatic function. J.Neurochem. 128: 536-46.

Fearnley, J.M., Lees, A. J. (1991). Ageing and Parkinson's disease: substantia nigra regional selectivity. Brain 114 (Pt 5): 2283-301.

Feder, M.E., Hofmann, G. E. (1999). Heat-shock proteins, molecular chaperones, and the stress response: evolutionary and ecological physiology. Annu.Rev.Physiol. 61: 243-82.

Fellner, L., Irschick, R., Schanda, K., Reindl, M., Klimaschewski, L., Poewe, W., *et al.* (2013). Toll-like receptor 4 is required for alpha-synuclein dependent activation of microglia and astroglia. Glia 61: 349-60.

Feng, L.R., Federoff, H. J., Vicini, S. & Maguire-Zeiss, K. A. (2010). Alpha-synuclein mediates alterations in membrane conductance: a potential role for alpha-synuclein oligomers in cell vulnerability. Eur.J.Neurosci. 32: 10-7.

Fenteany, G., Schreiber, S. L. (1998). Lactacystin, proteasome function, and cell fate. J.Biol.Chem. 273: 8545-8.

Fernagut, P.O., Hutson, C. B., Fleming, S. M., Tetreaut, N. A., Salcedo, J., Masliah, E., *et al.* (2007). Behavioral and histopathological consequences of paraquat intoxication in mice: Effects of alpha-synuclein over-expression. Synapse 61: 991-1001.

Fleming, S.M., Chesselet, M. F. (2006). Behavioral phenotypes and pharmacology in genetic mouse models of Parkinsonism. Behav.Pharmacol. 17: 383-91.

Fleming, S.M., Salcedo, J., Fernagut, P. O., Rockenstein, E., Masliah, E., Levine, M. S., *et al.* (2004). Early and progressive sensorimotor anomalies in mice overexpressing wild-type human alpha-synuclein. J.Neurosci. 24: 9434-40.

Fleming, S.M., Tetreault, N. A., Mulligan, C. K., Hutson, C. B., Masliah, E. & Chesselet, M. (2008). Olfactory deficits in mice overexpressing human wildtype alpha-synuclein. Eur.J.Neurosci. 28: 247-56.

Fornai, F., Lenzi, P., Gesi, M., Ferrucci, M., Lazzeri, G., Busceti, C. L., *et al.* (2003). Fine structure and biochemical mechanisms underlying nigrostriatal inclusions and cell death after proteasome inhibition. J.Neurosci. 23: 8955-66.

Franco, R., Li, S., Rodriguez-Rocha, H., Burns, M. & Panayiotidis, M. I. (2010). Molecular mechanisms of pesticide-induced neurotoxicity: Relevance to Parkinson's disease. Chem.Biol.Interact. 188: 289-300.

Freichel, C., Neumann, M., Ballard, T., Muller, V., Woolley, M., Ozmen, L., *et al.* (2007). Age-dependent cognitive decline and amygdala pathology in alpha-synuclein transgenic mice. Neurobiol. Aging 28: 1421-35.

Fu, L.L., Cheng, Y. & Liu, B. (2013). Beclin-1: autophagic regulator and therapeutic target in cancer. Int.J.Biochem.Cell Biol. 45: 921-4.

Fujiwara, H., Hasegawa, M., Dohmae, N., Kawashima, A., Masliah, E., Goldberg, M. S., *et al.* (2002). Alpha-Synuclein is phosphorylated in synucleinopathy lesions. Nat.Cell Biol. 4: 160-4.

Fülop, V., Bocskei, Z. & Polgar, L. (1998). Prolyl oligopeptidase: an unusual beta-propeller domain regulates proteolysis. Cell 94: 161-70.

Gallegos, S., Pacheco, C., Peters, C., Opazo, C. M. & Aguayo, L. G. (2015). Features of alpha-synuclein that could explain the progression and irreversibility of Parkinson's disease. Front.Neurosci. 9: 59.

Galvin, J.E., Lee, V. M. & Trojanowski, J. Q. (2001). Synucleinopathies: clinical and pathological implications. Arch.Neurol. 58: 186-90.

Garcia-Horsman, J.A., Männistö, P. T. & Venäläinen, J. I. (2007). On the role of prolyl oligopeptidase in health and disease. Neuropeptides 41: 1-24.

Gass, J., Khosla, C. (2007). Prolyl endopeptidases. Cell Mol.Life Sci. 64: 345-55.

George, J.M., Jin, H., Woods, W. S. & Clayton, D. F. (1995). Characterization of a novel protein regulated during the critical period for song learning in the zebra finch. Neuron 15: 361-72.

Gerard, M., Deleersnijder, A., Daniels, V., Schreurs, S., Munck, S., Reumers, V., *et al.* (2010). Inhibition of FK506 binding proteins reduces alpha-synuclein aggregation and Parkinson's disease-like pathology. J.Neurosci. 30: 2454-63.

Giasson, B.I. (2000). Oxidative damage linked to neurodegeneration by selective alpha-synuclein nitration in synucleinopathy lesions. Science 290: 985-9.

Giasson, B.I., Duda, J. E., Quinn, S. M., Zhang, B., Trojanowski, J. Q. & Lee, V. M. (2002). Neuronal alpha-synucleinopathy with severe movement disorder in mice expressing A53T human alpha-synuclein. Neuron 34: 521-33.

Giasson, B.I., Lee, V. M. & Trojanowski, J. Q. (2003). Interactions of amyloidogenic proteins. Neuromolecular Med. 4: 49-58.

Giasson, B.I., Murray, I. V., Trojanowski, J. Q. & Lee, V. M. (2001). A hydrophobic stretch of 12 amino acid residues in the middle of alpha-synuclein is essential for filament assembly. J.Biol.Chem. 276: 2380-6.

Giasson, B.I., Uryu, K., Trojanowski, J. Q. & Lee, V. M. -. (1999). Mutant and wild-type human alpha-synuclein assemble into elongated filaments with distinct morphologies in vitro. J.Biol.Chem. 274: 7619-22.

Gispert, S., Del Turco, D., Garrett, L., Chen, A., Bernard, D. J., Hamm-Clement, J., *et al.* (2003). Transgenic mice expressing mutant A53T human alpha-synuclein show neuronal dysfunction in the absence of aggregate formation. Mol.Cell.Neurosci. 24: 419-29.

Goldman, J.E., Yen, S. H., Chiu, F. C. & Peress, N. S. (1983). Lewy bodies of Parkinson's disease contain neurofilament antigens. Science 221: 1082-4.

Gosavi, N., Lee, H. J., Lee, J. S., Patel, S. & Lee, S. J. (2002). Golgi fragmentation occurs in the cells with prefibrillar alpha-synuclein aggregates and precedes the formation of fibrillar inclusion. J.Biol. Chem. 277: 48984-92.

Grealish, S., Mattsson, B., Draxler, P. & Björklund, A. (2010). Characterisation of behavioural and neurodegenerative changes induced by intranigral 6-hydroxydopamine lesions in a mouse model of Parkinson's disease. Eur.J.Neurosci. 31: 2266-78.

Guo, J.T., Chen, A. Q., Kong, Q., Zhu, H., Ma, C. M. & Qin, C. (2008). Inhibition of vesicular monoamine transporter-2 activity in alpha-synuclein stably transfected SH-SY5Y cells. Cell.Mol. Neurobiol. 28: 35-47.

Haas, A.L., Siepmann, T. J. (1997). Pathways of ubiquitin conjugation. FASEB J. 11: 1257-68.

Hannula, M.J., Myöhänen, T. T., Tenorio-Laranga, J., Männistö, P. T. & Garcia-Horsman, J. A. (2013). Prolyl oligopeptidase colocalizes with alpha-synuclein, beta-amyloid, tau protein and astroglia in the post-mortem brain samples with Parkinson's and Alzheimer's diseases. Neuroscience 242: 140-50.

Hansen, C., Angot, E., Bergstrom, A. L., Steiner, J. A., Pieri, L., Paul, G., *et al.* (2011). Alpha-Synuclein propagates from mouse brain to grafted dopaminergic neurons and seeds aggregation in cultured human cells. J.Clin.Invest. 121: 715-25.

Harwood, A.J. (2011). Prolyl oligopeptidase, inositol phosphate signalling and lithium sensitivity. CNS Neurol.Disord.Drug Targets 10: 333-9.

Hasegawa, M., Fujiwara, H., Nonaka, T., Wakabayashi, K., Takahashi, H., Lee, V. M., *et al.* (2002). Phosphorylated alpha-synuclein is ubiquitinated in alpha-synucleinopathy lesions. J.Biol.Chem. 277: 49071-6.

Hashimoto, M., Hsu, L. J., Sisk, A., Xia, Y., Takeda, A., Sundsmo, M., *et al.* (1998). Human recombinant NACP/alpha-synuclein is aggregated and fibrillated in vitro: relevance for Lewy body disease. Brain Res. 799: 301-6.

Hashimoto, M., Hsu, L. J., Xia, Y., Takeda, A., Sisk, A., Sundsmo, M., *et al.* (1999a). Oxidative stress induces amyloid-like aggregate formation of NACP/alpha-synuclein in vitro. Neuroreport 10: 717-21.

Hashimoto, M., Rockenstein, E., Mante, M., Mallory, M. & Masliah, E. (2001). beta-Synuclein inhibits alpha-synuclein aggregation: a possible role as an anti-parkinsonian factor. Neuron 32: 213-23.

Hashimoto, M., Takeda, A., Hsu, L. J., Takenouchi, T. & Masliah, E. (1999b). Role of cytochrome c as a stimulator of alpha-synuclein aggregation in Lewy body disease. J.Biol.Chem. 274: 28849-52.

Hauser, R.A., Freeman, T. B., Snow, B. J., Nauert, M., Gauger, L., Kordower, J. H., *et al.* (1999). Long-term evaluation of bilateral fetal nigral transplantation in Parkinson disease. Arch.Neurol. 56: 179-87.

Hernandes, M.S., Santos, G. D., Cafe-Mendes, C. C., Lima, L. S., Scavone, C., Munhoz, C. D., *et al.* (2013). Microglial cells are involved in the susceptibility of NADPH oxidase knockout mice to 6-hydroxy-dopamine-induced neurodegeneration. PLoS One 8: e75532.

Hirsch, E.C., Hunot, S. (2009). Neuroinflammation in Parkinson's disease: a target for neuroprotection? Lancet Neurol. 8: 382-97.

Hokenson, M.J., Uversky, V. N., Goers, J., Yamin, G., Munishkina, L. A. & Fink, A. L. (2004). Role of individual methionines in the fibrillation of methionine-oxidized alpha-synuclein. Biochemistry 43: 4621-33.

Hung, S.Y., Huang, W. P., Liou, H. C. & Fu, W. M. (2009). Autophagy protects neuron from Abeta-induced cytotoxicity. Autophagy 5: 502-10.

Ikeda, M., Kawarabayashi, T., Harigaya, Y., Sasaki, A., Yamada, S., Matsubara, E., *et al.* (2009). Motor impairment and aberrant production of neurochemicals in human alpha-synuclein A30P+A53T transgenic mice with alpha-synuclein pathology. Brain Res. 1250: 232-41.

Inden, M., Kitamura, Y., Abe, M., Tamaki, A., Takata, K. & Taniguchi, T. (2011). Parkinsonian rotenone mouse model: reevaluation of long-term administration of rotenone in C57BL/6 mice. Biol. Pharm.Bull. 34: 92-6.

Ischiropoulos, H. (2009). Protein tyrosine nitration--an update. Arch.Biochem.Biophys. 484: 117-21.

Iwai, A., Masliah, E., Yoshimoto, M., Ge, N., Flanagan, L., de Silva, H. A., *et al.* (1995). The precursor protein of non-A beta component of Alzheimer's disease amyloid is a presynaptic protein of the central nervous system. Neuron 14: 467-75.

Iwata, A., Maruyama, M., Akagi, T., Hashikawa, T., Kanazawa, I., Tsuji, S., *et al.* (2003). Alpha-synuclein degradation by serine protease neurosin: implication for pathogenesis of synucleinopathies. Hum.Mol.Genet. 12: 2625-35.

Jäkälä, P., Puoliväli, J., Kerokoski, P. & van Groen, T. (2002). Intracellular alpha-synuclein accumulation in transgenic mice expressing A30P alpha-synuclein mutation. Neurobiology of aging23, S252.

Jakes, R., Spillantini, M. G. & Goedert, M. (1994). Identification of two distinct synucleins from human brain. FEBS Lett. 345: 27-32.

Jalkanen, A.J., Hakkarainen, J. J., Lehtonen, M., Venäläinen, T., Kaariainen, T. M., Jarho, E., *et al.* (2011a). Brain Pharmacokinetics of Two Prolyl Oligopeptidase Inhibitors, JTP-4819 and KYP-2047, in the Rat. Basic Clin.Pharmacol.Toxicol.

Jalkanen, A.J., Puttonen, K. A., Venäläinen, J. I., Sinerva, V., Mannila, A., Ruotsalainen, S., *et al.* (2007). Beneficial effect of prolyl oligopeptidase inhibition on spatial memory in young but not in

old scopolamine-treated rats. Basic Clin.Pharmacol.Toxicol. 100: 132-8.

Jalkanen, A.J., Savolainen, K. & Forsberg, M. M. (2011b). Inhibition of prolyl oligopeptidase by KYP-2047 fails to increase the extracellular neurotensin and substance P levels in rat striatum. Neurosci.Lett. 502: 107-11.

Jankovic, J., Chen, S. & Le, W. D. (2005). The role of Nurr1 in the development of dopaminergic neurons and Parkinson's disease. Prog.Neurobiol. 77: 128-38.

Jarho, E.M., Venäläinen, J. I., Huuskonen, J., Christiaans, J. A., Garcia-Horsman, J. A., Forsberg, M. M., *et al.* (2004). A cyclopent-2-enecarbonyl group mimics proline at the P2 position of prolyl oligopeptidase inhibitors. J.Med.Chem. 47: 5605-7.

Jariel-Encontre, I., Bossis, G. & Piechaczyk, M. (2008). Ubiquitin-independent degradation of proteins by the proteasome. Biochim.Biophys.Acta 1786: 153-77.

Jellinger, K.A. (2004). Lewy body-related alpha-synucleinopathy in the aged human brain. J.Neural Transm. 111: 1219-35.

Jenco, J.M., Rawlingson, A., Daniels, B. & Morris, A. J. (1998). Regulation of phospholipase D2: selective inhibition of mammalian phospholipase D isoenzymes by alpha- and beta-synucleins. Biochemistry 37: 4901-9.

Jenner, P. (2003). Oxidative stress in Parkinson's disease. Ann.Neurol. 53 Suppl 3: S26,36; discussion S36-8.

Jensen, P.H., Hojrup, P., Hager, H., Nielsen, M. S., Jacobsen, L., Olesen, O. F., *et al.* (1997). Binding of Abeta to alpha- and beta-synucleins: identification of segments in alpha-synuclein/NAC precursor that bind Abeta and NAC. Biochem.J. 323 (Pt 2): 539-46.

Jensen, P.H., Nielsen, M. H., Jakes, R., Dotti, C. G. & Goedert, M. (1998). Binding of alpha-synuclein to rat brain vesicles is abolished by familial Parkinson's disease mutation. J.Biol.Chem. 273: 26292-4.

Jiang, T.F., Zhang, Y. J., Zhou, H. Y., Wang, H. M., Tian, L. P., Liu, J., *et al.* (2013). Curcumin ameliorates the neurodegenerative pathology in A53T alpha-synuclein cell model of Parkinson's disease through the downregulation of mTOR/p70S6K signaling and the recovery of macroautophagy. J.Neuroimmune Pharmacol. 8: 356-69.

Jin, H., Clayton, D. F. (1997). Synelfin regulation during the critical period for song learning in normal and isolated juvenile zebra finches. Neurobiol.Learn.Mem. 68: 271-84.

Jo, E., McLaurin, J., Yip, C. M., St George-Hyslop, P. & Fraser, P. E. (2000). Alpha-Synuclein membrane interactions and lipid specificity. J.Biol.Chem. 275: 34328-34.

Junn, E., Ronchetti, R. D., Quezado, M. M., Kim, S. Y. & Mouradian, M. M. (2003). Tissue transglutaminase-induced aggregation of alpha-synuclein: Implications for Lewy body formation in Parkinson's disease and dementia with Lewy bodies. Proc.Natl.Acad.Sci.U.S.A. 100: 2047-52.

Kahle, P.J. (2000). Subcellular localization of wild-type and Parkinson's disease-associated mutant alpha-synuclein in human and transgenic mouse brain. J.Neurosci. 20: 6365-73.

Kahle, P.J., Neumann, M., Ozmen, L., Muller, V., Odoy, S., Okamoto, N., *et al.* (2001). Selective insolubility of alpha-synuclein in human Lewy body diseases is recapitulated in a transgenic mouse model. Am.J.Pathol. 159: 2215-25.

Kang, R., Zeh, H. J., Lotze, M. T. & Tang, D. (2011). The Beclin 1 network regulates autophagy and apoptosis. Cell Death Differ. 18: 571-80.

Kaszuba, K., Rog, T., Danne, R., Canning, P., Fülop, V., Juhasz, T., *et al.* (2012). Molecular dynamics, crystallography and mutagenesis studies on the substrate gating mechanism of prolyl oligopeptidase. Biochimie 94: 1398-411.

Kato, A., Fukunari, A., Sakai, Y. & Nakajima, T. (1997). Prevention of amyloid-like deposition by a selective prolyl endopeptidase inhibitor, Y-29794, in senescence-accelerated mouse. J.Pharmacol. Exp.Ther. 283: 328-35.

Kaushik, S., Etchebest, C. & Sowdhamini, R. (2014). Decoding the structural events in substrate-gating mechanism of eukaryotic prolyl oligopeptidase using normal mode analysis and molecular dynamics simulations. Proteins 82: 1428-43.

Khodr, C.E., Becerra, A., Han, Y. & Bohn, M. C. (2014). Targeting alpha-synuclein with a microRNA-embedded silencing vector in the rat substantia nigra: positive and negative effects. Brain Res. 1550: 47-60.

Khodr, C.E., Sapru, M. K., Pedapati, J., Han, Y., West, N. C., Kells, A. P., *et al.* (2011). An alpha-synuclein AAV gene silencing vector ameliorates a behavioral deficit in a rat model of Parkinson's disease, but displays toxicity in dopamine neurons. Brain Res. 1395: 94-107.

Kichik, N., Tarrago, T., Claasen, B., Gairi, M., Millet, O. & Giralt, E. (2011). 15N relaxation NMR studies of prolyl oligopeptidase, an 80 kDa enzyme, reveal a pre-existing equilibrium between different conformational states. Chembiochem 12: 2737-9.

Kim, H.Y., Cho, M. K., Kumar, A., Maier, E., Siebenhaar, C., Becker, S., *et al.* (2009). Structural properties of pore-forming oligomers of alpha-synuclein. J.Am.Chem.Soc. 131: 17482-9.

Kim, J.D., Toda, C., D'Agostino, G., Zeiss, C. J., DiLeone, R. J., Elsworth, J. D., *et al.* (2014). Hypothalamic prolyl endopeptidase (PREP) regulates pancreatic insulin and glucagon secretion in mice. Proc.Natl.Acad.Sci.U.S.A.

Kim, M., Jung, W., Lee, I. H., Bhak, G., Paik, S. R. & Hahn, J. S. (2008). Impairment of microtubule system increases alpha-synuclein aggregation and toxicity. Biochem.Biophys.Res.Commun. 365: 628-35.

Kisos, H., Pukass, K., Ben-Hur, T., Richter-Landsberg, C. & Sharon, R. (2012). Increased neuronal alpha-synuclein pathology associates with its accumulation in oligodendrocytes in mice modeling alpha-synucleinopathies. PLoS One 7: e46817.

Klionsky, D.J., Abeliovich, H., Agostinis, P., Agrawal, D. K., Aliev, G., Askew, D. S., *et al.* (2008). Guidelines for the use and interpretation of assays for monitoring autophagy in higher eukaryotes. Autophagy 4: 151-75.

Klucken, J., Shin, Y., Masliah, E., Hyman, B. T. & McLean, P. J. (2004). Hsp70 Reduces alpha-Synuclein Aggregation and Toxicity. J.Biol.Chem. 279: 25497-502.

Komatsu, M., Waguri, S., Ueno, T., Iwata, J., Murata, S., Tanida, I., *et al.* (2005). Impairment of starvation-induced and constitutive autophagy in Atg7-deficient mice. J.Cell Biol. 169: 425-34.

Konieczny, J., Jantas, D., Lenda, T., Domin, H., Czarnecka, A., Kuter, K., *et al.* (2014). Lack of neuroprotective effect of celastrol under conditions of proteasome inhibition by lactacystin in in vitro and in vivo studies: implications for Parkinson's disease. Neurotox Res. 26: 255-73.

Kordower, J.H., Chu, Y., Hauser, R. A., Freeman, T. B. & Olanow, C. W. (2008a). Lewy body-like pathology in long-term embryonic nigral transplants in Parkinson's disease. Nat.Med. 14: 504-6.

Kordower, J.H., Chu, Y., Hauser, R. A., Olanow, C. W. & Freeman, T. B. (2008b). Transplanted dopaminergic neurons develop PD pathologic changes: a second case report. Mov.Disord. 23: 2303-6.

Kordower, J.H., Freeman, T. B., Snow, B. J., Vingerhoets, F. J., Mufson, E. J., Sanberg, P. R., *et al.* (1995). Neuropathological evidence of graft survival and striatal reinnervation after the transplantation of fetal mesencephalic tissue in a patient with Parkinson's disease. N.Engl.J.Med. 332: 1118-24.

Kreiner, G. (2015). Compensatory mechanisms in genetic models of neurodegeneration: are the mice better than humans? Front.Cell.Neurosci. 9: 56.

Kroemer, G., Reed, J. C. (2000). Mitochondrial control of cell death. Nat.Med. 6: 513-9.

Krüger, R., Kuhn, W., Muller, T., Woitalla, D., Graeber, M., Kosel, S., *et al.* (1998). Ala30Pro mutation in the gene encoding alpha-synuclein in Parkinson's disease. Nat.Genet. 18: 106-8.

Krumova, P., Meulmeester, E., Garrido, M., Tirard, M., Hsiao, H. H., Bossis, G., *et al.* (2011). Sumoylation inhibits alpha-synuclein aggregation and toxicity. J.Cell Biol. 194: 49-60.

Kudo, T., Loh, D. H., Truong, D., Wu, Y. & Colwell, C. S. (2011). Circadian dysfunction in a mouse model of Parkinson's disease. Exp.Neurol. 232: 66-75.

Kurz, A., Double, K. L., Lastres-Becker, I., Tozzi, A., Tantucci, M., Bockhart, V., *et al.* (2010). A53T-alpha-synuclein overexpression impairs dopamine signaling and striatal synaptic plasticity in old mice. PLoS One 5: e11464.

Kuzuhara, S., Mori, H., Izumiyama, N., Yoshimura, M. & Ihara, Y. (1988). Lewy bodies are ubiquitinated. A light and electron microscopic immunocytochemical study. Acta Neuropathol. 75: 345-53.

Lam, H.A., Wu, N., Cely, I., Kelly, R. L., Hean, S., Richter, F., *et al.* (2011). Elevated tonic extracellular dopamine concentration and altered dopamine modulation of synaptic activity precede dopamine loss in the striatum of mice overexpressing human alpha-synuclein. J.Neurosci.Res. 89: 1091-102.

Lambeir, A.M. (2011). Interaction of prolyl oligopeptidase with alpha-synuclein. CNS Neurol.Disord. Drug Targets 10: 349-54.

Laplante, M., Sabatini, D. M. (2009). mTOR signaling at a glance. J.Cell.Sci. 122: 3589-94.

Lashuel, H.A., Petre, B. M., Wall, J., Simon, M., Nowak, R. J., Walz, T., *et al.* (2002). Alpha-synuclein, especially the Parkinson's disease-associated mutants, forms pore-like annular and tubular protofibrils. J.Mol.Biol. 322: 1089-102.

Lashuel, H.A., Overk, C. R., Oueslati, A. & Masliah, E. (2013). The many faces of alpha-synuclein: from structure and toxicity to therapeutic target. Nature reviews.Neuroscience 14: 38-48.

Lauwers, E., Debyser, Z., Van Dorpe, J., De Strooper, B., Nuttin, B. & Baekelandt, V. (2003). Neuropathology and neurodegeneration in rodent brain induced by lentiviral vector-mediated overexpression of alpha-synuclein. Brain Pathol. 13: 364-72.

Lavedan, C. (1998). The synuclein family. Genome Res. 2: 871-80.

Lee, E.N., Lee, S. Y., Lee, D., Kim, J. & Paik, S. R. (2003). Lipid interaction of alpha-synuclein during the metal-catalyzed oxidation in the presence of Cu2+ and H2O2. J.Neurochem. 84: 1128-42.

Lee, H.J., Khoshaghideh, F., Patel, S. & Lee, S. J. (2004). Clearance of alpha-synuclein oligomeric intermediates via the lysosomal degradation pathway. J.Neurosci. 24: 1888-96.

Lee, H.J., Suk, J. E., Bae, E. J. & Lee, S. J. (2008). Clearance and deposition of extracellular alpha-synuclein aggregates in microglia. Biochem.Biophys.Res.Commun. 372: 423-8.

Lee, H.J., Suk, J. E., Patrick, C., Bae, E. J., Cho, J. H., Rho, S., *et al.* (2010a). Direct transfer of alpha-synuclein from neuron to astroglia causes inflammatory responses in synucleinopathies. J.Biol. Chem. 285: 9262-72.

Lee, M.K., Stirling, W., Xu, Y., Xu, X., Qui, D., Mandir, A. S., *et al.* (2002). Human alpha-synuclein-harboring familial Parkinson's disease-linked Ala-53 --> Thr mutation causes neurodegenerative disease with alpha-synuclein aggregation in transgenic mice. Proc.Natl.Acad.Sci.U.S.A. 99: 8968-73.

Lee, S.J., Desplats, P., Lee, H. J., Spencer, B. & Masliah, E. (2012). Cell-to-cell transmission of alpha-synuclein aggregates. Methods Mol.Biol. 849: 347-59.

Lee, S.J., Desplats, P., Sigurdson, C., Tsigelny, I. & Masliah, E. (2010b). Cell-to-cell transmission of non-prion protein aggregates. Nat.Rev.Neurol. 6: 702-6.

Lesage, S., Anheim, M., Letournel, F., Bousset, L., Honore, A., Rozas, N., *et al.* (2013). G51D alpha-synuclein mutation causes a novel parkinsonian-pyramidal syndrome. Ann.Neurol. 73: 459-71.

Li, C., Guo, Y., Xie, W., Li, X., Janokovic, J. & Le, W. (2010). Neuroprotection of pramipexole in UPS impairment induced animal model of Parkinson's disease. Neurochem.Res. 35: 1546-56.

Li, J., Uversky, V. N. & Fink, A. L. (2001). Effect of familial Parkinson's disease point mutations A30P and A53T on the structural properties, aggregation, and fibrillation of human alpha-synuclein. Biochemistry 40: 11604-13.

Li, J.Y., Englund, E., Holton, J. L., Soulet, D., Hagell, P., Lees, A. J., *et al.* (2008). Lewy bodies in grafted neurons in subjects with Parkinson's disease suggest host-to-graft disease propagation. Nat. Med. 14: 501-3.

Li, W., West, N., Colla, E., Pletnikova, O., Troncoso, J. C., Marsh, L., *et al.* (2005). Aggregation promoting C-terminal truncation of alpha-synuclein is a normal cellular process and is enhanced by the familial Parkinson's disease-linked mutations. Proc.Natl.Acad.Sci.U.S.A. 102: 2162-7.

Lim, Y., Kehm, V. M., Lee, E. B., Soper, J. H., Li, C., Trojanowski, J. Q., *et al.* (2011). Alpha-Syn suppression reverses synaptic and memory defects in a mouse model of dementia with Lewy bodies. J.Neurosci. 31: 10076-87.

Lim, Y., Kehm, V. M., Li, C., Trojanowski, J. Q. & Lee, V. M. (2010). Forebrain overexpression of alpha-synuclein leads to early postnatal hippocampal neuron loss and synaptic disruption. Exp. Neurol. 221: 86-97.

Lin, X., Parisiadou, L., Sgobio, C., Liu, G., Yu, J., Sun, L., *et al.* (2012). Conditional expression of Parkinson's disease-related mutant alpha-synuclein in the midbrain dopaminergic neurons causes progressive neurodegeneration and degradation of transcription factor nuclear receptor related 1. J.Neurosci. 32: 9248-64.

Lindersson, E., Beedholm, R., Højrup, P., Moos, T., Gai, W., Hendil, K. B., *et al.* (2004). Proteasomal Inhibition by α-Synuclein Filaments and Oligomers. Journal of Biological Chemistry 279: 12924-34.

Lo Bianco, C., Shorter, J., Regulier, E., Lashuel, H., Iwatsubo, T., Lindquist, S., *et al.* (2008). Hsp104 antagonizes alpha-synuclein aggregation and reduces dopaminergic degeneration in a rat model of Parkinson disease. J.Clin.Invest. 118: 3087-97.

Lu, Y., Prudent, M., Fauvet, B., Lashuel, H. A. & Girault, H. H. (2011). Phosphorylation of alpha-Synuclein at Y125 and S129 alters its metal binding properties: implications for understanding the role of alpha-Synuclein in the pathogenesis of Parkinson's Disease and related disorders. ACS Chem. Neurosci. 2: 667-75.

Luk, K.C., Kehm, V., Carroll, J., Zhang, B., O'Brien, P., Trojanowski, J. Q., *et al.* (2012a). Pathological alpha-synuclein transmission initiates Parkinson-like neurodegeneration in nontransgenic mice. Science 338: 949-53.

Luk, K.C., Kehm, V. M., Zhang, B., O'Brien, P., Trojanowski, J. Q. & Lee, V. M. (2012b). Intracerebral inoculation of pathological alpha-synuclein initiates a rapidly progressive neurodegenerative alpha-synucleinopathy in mice. J.Exp.Med. 209: 975-86.

Luk, K.C., Song, C., O'Brien, P., Stieber, A., Branch, J. R., Brunden, K. R., *et al.* (2009). Exogenous alpha-synuclein fibrils seed the formation of Lewy body-like intracellular inclusions in cultured cells. Proc.Natl.Acad.Sci.U.S.A. 106: 20051-6.

Lynch-Day, M.A., Mao, K., Wang, K., Zhao, M. & Klionsky, D. J. (2012). The role of autophagy in Parkinson's disease. Cold Spring Harb Perspect.Med. 2: a009357.

Machiya, Y., Hara, S., Arawaka, S., Fukushima, S., Sato, H., Sakamoto, M., *et al.* (2010). Phosphorylated alpha-synuclein at Ser-129 is targeted to the proteasome pathway in a ubiquitin-independent manner. J.Biol.Chem. 285: 40732-44.

Mak, S.K., McCormack, A. L., Manning-Bog, A. B., Cuervo, A. M. & Di Monte, D. A. (2010). Lysosomal degradation of alpha-synuclein in vivo. J.Biol.Chem. 285: 13621-9.

Mandler, M., Valera, E., Rockenstein, E., Mante, M., Weninger, H., Patrick, C., *et al.* (2015). Active immunization against alpha-synuclein ameliorates the degenerative pathology and prevents demyelination in a model of multiple system atrophy. Mol.Neurodegener 10: 10.

Mandler, M., Valera, E., Rockenstein, E., Weninger, H., Patrick, C., Adame, A., *et al.* (2014). Next-generation active immunization approach for synucleinopathies: implications for Parkinson's disease clinical trials. Acta Neuropathol. 127: 861-79.

Manning-Bog, A.B., McCormack, A. L., Li, J., Uversky, V. N., Fink, A. L. & Di Monte, D. A. (2002). The herbicide paraquat causes up-regulation and aggregation of alpha-synuclein in mice: paraquat and alpha-synuclein. J.Biol.Chem. 277: 1641-4.

Manning-Bog, A.B., McCormack, A. L., Purisai, M. G., Bolin, L. M. & Di Monte, D. A. (2003). Alpha-synuclein overexpression protects against paraquat-induced neurodegeneration. J.Neurosci. 23: 3095-9.

Mantle, D., Falkous, G., Ishiura, S., Blanchard, P. J. & Perry, E. K. (1996). Comparison of proline endopeptidase activity in brain tissue from normal cases and cases with Alzheimer's disease, Lewy body dementia, Parkinson's disease and Huntington's disease. Clin.Chim.Acta 249: 129-39.

Maroteaux, L., Campanelli, J. T. & Scheller, R. H. (1988). Synuclein: a neuron-specific protein localized to the nucleus and presynaptic nerve terminal. J.Neurosci. 8: 2804-15.

Martin, L.J., Pan, Y., Price, A. C., Sterling, W., Copeland, N. G., Jenkins, N. A., *et al.* (2006). Parkinson's disease alpha-synuclein transgenic mice develop neuronal mitochondrial degeneration and cell death. J.Neurosci. 26: 41-50.

Martinez-Vicente, M., Talloczy, Z., Kaushik, S., Massey, A. C., Mazzulli, J., Mosharov, E. V., *et al.* (2008). Dopamine-modified alpha-synuclein blocks chaperone-mediated autophagy. J.Clin.Invest. 118: 777-88.

Masliah, E. (2000). Dopaminergic loss and inclusion body formation in alpha-synuclein mice: implications for neurodegenerative disorders. Science 287: 1265-9.

Masliah, E., Rockenstein, E., Adame, A., Alford, M., Crews, L., Hashimoto, M., *et al.* (2005). Effects of alpha-synuclein immunization in a mouse model of Parkinson's disease. Neuron 46: 857-68.

Masliah, E., Rockenstein, E., Mante, M., Crews, L., Spencer, B., Adame, A., *et al.* (2011). Passive immunization reduces behavioral and neuropathological deficits in an alpha-synuclein transgenic model of Lewy body disease. PLoS One 6: e19338.

Masliah, E., Rockenstein, E., Veinbergs, I., Sagara, Y., Mallory, M., Hashimoto, M., *et al.* (2001). beta-amyloid peptides enhance alpha-synuclein accumulation and neuronal deficits in a transgenic mouse model linking Alzheimer's disease and Parkinson's disease. Proc.Natl.Acad.Sci.U.S.A. 98: 12245-50.

Masuda-Suzukake, M., Nonaka, T., Hosokawa, M., Oikawa, T., Arai, T., Akiyama, H., *et al.* (2013). Prion-like spreading of pathological alpha-synuclein in brain. Brain 136: 1128-38.

Matsuda, T., Sakaguchi, M., Tanaka, S., Yoshimoto, T. & Takaoka, M. (2013). Prolyl oligopeptidase is a glyceraldehyde-3-phosphate dehydrogenase-binding protein that regulates genotoxic stress-induced cell death. Int.J.Biochem.Cell Biol. 45: 850-7.

McCormack, A.L., Mak, S. K., Henderson, J. M., Bumcrot, D., Farrer, M. J. & Di Monte, D. A. (2010). Alpha-synuclein suppression by targeted small interfering RNA in the primate substantia nigra. PLoS One 5: e12122.

McFarland, N.R., Dimant, H., Kibuuka, L., Ebrahimi-Fakhari, D., Desjardins, C. A., Danzer, K. M., *et al.* (2014). Chronic treatment with novel small molecule Hsp90 inhibitors rescues striatal dopamine levels but not alpha-synuclein-induced neuronal cell loss. PLoS One 9: e86048.

McNaught, K.S., Belizaire, R., Isacson, O., Jenner, P. & Olanow, C. W. (2003). Altered proteasomal function in sporadic Parkinson's disease. Exp.Neurol. 179: 38-46.

McNaught, K.S., Björklund, L. M., Belizaire, R., Isacson, O., Jenner, P. & Olanow, C. W. (2002). Proteasome inhibition causes nigral degeneration with inclusion bodies in rats. Neuroreport 13: 1437-41.

McNaught, K.S., Jenner, P. (2001). Proteasomal function is impaired in substantia nigra in Parkinson's disease. Neurosci.Lett. 297: 191-4.

Metcalf, D.J., Garcia-Arencibia, M., Hochfeld, W. E. & Rubinsztein, D. C. (2012). Autophagy and misfolded proteins in neurodegeneration. Exp.Neurol. 238: 22-8.

Miracco, C., Cosci, E., Oliveri, G., Luzi, P., Pacenti, L., Monciatti, I., *et al.* (2007). Protein and mRNA expression of autophagy gene Beclin 1 in human brain tumours. Int.J.Oncol. 30: 429-36.

Miyazaki, A., Toide, K., Sasaki, Y., Ichitani, Y. & Iwasaki, T. (1998). Effect of a prolyl endopeptidase inhibitor, JTP-4819, on radial maze performance in hippocampal-lesioned rats. Pharmacol.Biochem.Behav. 59: 361-8.

Morain, P., Lestage, P., De Nanteuil, G., Jochemsen, R., Robin, J. L., Guez, D., *et al.* (2002). S 17092: a prolyl endopeptidase inhibitor as a potential therapeutic drug for memory impairment. Preclinical and clinical studies. CNS Drug Rev. 8: 31-52.

Morroni, F., Sita, G., Tarozzi, A., Cantelli-Forti, G. & Hrelia, P. (2014). Neuroprotection by 6-(methylsulfinyl)hexyl isothiocyanate in a 6-hydroxydopamine mouse model of Parkinsons disease. Brain Res. 1589: 93-104.

Murphy, D.D., Rueter, S. M., Trojanowski, J. Q. & Lee, V. M. (2000). Synucleins are developmentally expressed, and alpha-synuclein regulates the size of the presynaptic vesicular pool in primary hippocampal neurons. J.Neurosci. 20: 3214-20.

Myöhänen, T.T., Garcia-Horsman, J. A., Tenorio-Laranga, J. & Männistö, P. T. (2009). Issues about the physiological functions of prolyl oligopeptidase based on its discordant spatial association with substrates and inconsistencies among mRNA, protein levels, and enzymatic activity. J.Histochem. Cytochem. 57: 831-48.

Myöhänen, T.T., Hannula, M. J., Van Elzen, R., Gerard, M., Van Der Veken, P., Garcia-Horsman, J. A., *et al.* (2012). A prolyl oligopeptidase inhibitor, KYP-2047, reduces alpha-synuclein protein levels and aggregates in cellular and animal models of Parkinson's disease. Br.J.Pharmacol.

Myöhänen, T.T., Venäläinen, J. I., Garcia-Horsman, J. A. & Männistö, P. T. (2008). Spatial association of prolyl oligopeptidase, inositol 1,4,5-triphosphate type 1 receptor, substance P and its neurokinin-1 receptor in the rat brain: an immunohistochemical colocalization study. Neuroscience 153: 1177-89.

Myöhänen, T.T., Venäläinen, J. I., Tupala, E., Garcia-Horsman, J. A., Miettinen, R. & Männistö, P. T. (2007). Distribution of immunoreactive prolyl oligopeptidase in human and rat brain. Neurochem. Res. 32: 1365-74.

Nemani, V.M., Lu, W., Berge, V., Nakamura, K., Onoa, B., Lee, M. K., *et al.* (2010). Increased expression of alpha-synuclein reduces neurotransmitter release by inhibiting synaptic vesicle reclustering after endocytosis. Neuron 65: 66-79.

Nestler, EJ, Hyman, S & Malenka, R (2009). *Molecular neuropharmacology: a foundation for clinical neuroscience.* New York: McGraw-Hill Medical.

Neumann, M., Kahle, P. J., Giasson, B. I., Ozmen, L., Borroni, E., Spooren, W., *et al.* (2002). Misfolded proteinase K-resistant hyperphosphorylated alpha-synuclein in aged transgenic mice with locomotor deterioration and in human alpha-synucleinopathies. J.Clin.Invest. 110: 1429-39.

Nuber, S., Petrasch-Parwez, E., Winner, B., Winkler, J., von Horsten, S., Schmidt, T., *et al.* (2008). Neurodegeneration and motor dysfunction in a conditional model of Parkinson's disease. J.Neurosci. 28: 2471-84.

Nuber, S., Tadros, D., Fields, J., Overk, C. R., Ettle, B., Kosberg, K., *et al.* (2014). Environmental neurotoxic challenge of conditional alpha-synuclein transgenic mice predicts a dopaminergic olfactory-striatal interplay in early PD. Acta Neuropathol. 127: 477-94.

Nykänen, N.P., Kysenius, K., Sakha, P., Tammela, P. & Huttunen, H. J. (2012). gamma-Aminobutyric acid type A (GABAA) receptor activation modulates tau phosphorylation. J.Biol.Chem. 287: 6743-52.

Okochi, M. (2000). Constitutive phosphorylation of the Parkinson's disease-associated alpha-synuclein. J.Biol.Chem. 275: 390-7.

Oliveras-Salva, M., Van der Perren, A., Casadei, N., Stroobants, S., Nuber, S., D'Hooge, R., *et al.* (2013). rAAV2/7 vector-mediated overexpression of alpha-synuclein in mouse substantia nigra induces protein aggregation and progressive dose-dependent neurodegeneration. Mol.Neurodegener 8: 44,1326-8-44.

Ono, K., Ikemoto, M., Kawarabayashi, T., Ikeda, M., Nishinakagawa, T., Hosokawa, M., *et al.* (2009). A chemical chaperone, sodium 4-phenylbutyric acid, attenuates the pathogenic potency in human alpha-synuclein A30P + A53T transgenic mice. Parkinsonism Relat.Disord. 15: 649-54.

Osterberg, V.R., Spinelli, K. J., Weston, L. J., Luk, K. C., Woltjer, R. L. & Unni, V. K. (2015). Progressive aggregation of alpha-synuclein and selective degeneration of lewy inclusion-bearing neurons in a mouse model of parkinsonism. Cell.Rep. 10: 1252-60.

Ott, M., Robertson, J. D., Gogvadze, V., Zhivotovsky, B. & Orrenius, S. (2002). Cytochrome c release from mitochondria proceeds by a two-step process. Proc.Natl.Acad.Sci.U.S.A. 99: 1259-63.

Outeiro, T.F., Kazantsev, A. (2008). Drug Targeting of alpha-Synuclein Oligomerization in Synucleinopathies. Perspect.Medicin Chem. 2: 41-9.

Outeiro, T.F., Klucken, J., Bercury, K., Tetzlaff, J., Putcha, P., Oliveira, L. M., *et al.* (2009). Dopamine-induced conformational changes in alpha-synuclein. PLoS One 4: e6906.

Paik, S.R., Lee, J. H., Kim, D. H., Chang, C. S. & Kim, Y. S. (1998). Self-oligomerization of NACP, the precursor protein of the non-amyloid beta/A4 protein (A beta) component of Alzheimer's disease amyloid, observed in the presence of a C-terminal A beta fragment (residues 25-35). FEBS Lett. 421: 73-6.

Paik, S.R., Shin, H. J., Lee, J. H., Chang, C. S. & Kim, J. (1999). Copper(II)-induced self-oligomerization of alpha-synuclein. Biochem.J. 340 (Pt 3): 821-8.

Pan, T., Kondo, S., Zhu, W., Xie, W., Jankovic, J. & Le, W. (2008). Neuroprotection of rapamycin in lactacystin-induced neurodegeneration via autophagy enhancement. Neurobiol.Dis. 32: 16-25.

Pan-Montojo, F., Anichtchik, O., Dening, Y., Knels, L., Pursche, S., Jung, R., *et al.* (2010). Progression of Parkinson's disease pathology is reproduced by intragastric administration of rotenone in mice. PLoS One 5: e8762.

Parihar, M.S., Parihar, A., Fujita, M., Hashimoto, M. & Ghafourifar, P. (2009). Alpha-synuclein overexpression and aggregation exacerbates impairment of mitochondrial functions by augmenting oxidative stress in human neuroblastoma cells. Int.J.Biochem.Cell Biol. 41: 2015-24.

Parihar, M.S., Parihar, A., Fujita, M., Hashimoto, M. & Ghafourifar, P. (2008). Mitochondrial association of alpha-synuclein causes oxidative stress. Cell Mol.Life Sci. 65: 1272-84.

Parkinson, J. (1817). An essay on the shaking palsy. Sherwood, Neely and Jones, London

Parys, J.B., Decuypere, J. P. & Bultynck, G. (2012). Role of the inositol 1,4,5-trisphosphate receptor/Ca2+-release channel in autophagy. Cell.Commun.Signal. 10: 17,811X-10-17.

Paxinou, E., Chen, Q., Weisse, M., Giasson, B. I., Norris, E. H., Rueter, S. M., *et al.* (2001). Induction of alpha-synuclein aggregation by intracellular nitrative insult. J.Neurosci. 21: 8053-61.

Peltonen, I., Myöhänen, T. T. & Männistö, P. T. (2011). Association of prolyl oligopeptidase with conventional neurotransmitters in the brain. CNS Neurol.Disord.Drug Targets 10: 311-8.

Peng, X., Tehranian, R., Dietrich, P., Stefanis, L. & Perez, R. G. (2005). Alpha-synuclein activation of protein phosphatase 2A reduces tyrosine hydroxylase phosphorylation in dopaminergic cells. J.Cell.Sci. 118: 3523-30.

Perez, R.G., Waymire, J. C., Lin, E., Liu, J. J., Guo, F. & Zigmond, M. J. (2002). A role for alpha-synuclein in the regulation of dopamine biosynthesis. J.Neurosci. 22: 3090-9.

Perrin, R.J., Woods, W. S., Clayton, D. F. & George, J. M. (2000). Interaction of human alpha-synuclein and Parkinson's disease variants with phospholipids. J.Biol.Chem. 275: 34393-8.

Petit, A., Barelli, H., Morain, P. & Checler, F. (2000). Novel proline endopeptidase inhibitors do not modify Abeta40/42 formation and degradation by human cells expressing wild-type and swedish mutated beta-amyloid precursor protein. Br.J.Pharmacol. 130: 1613-7.

Pham, C.L., Leong, S. L., Ali, F. E., Kenche, V. B., Hill, A. F., Gras, S. L., *et al.* (2009). Dopamine and the dopamine oxidation product 5,6-dihydroxylindole promote distinct on-pathway and off-pathway aggregation of alpha-synuclein in a pH-dependent manner. J.Mol.Biol. 387: 771-85.

Pickart, C.M. (2000). Ubiquitin in chains. Trends Biochem.Sci. 25: 544-8.

Plaas, M., Karis, A., Innos, J., Rebane, E., Baekelandt, V., Vaarmann, A., *et al.* (2008). Alpha-synuclein A30P point-mutation generates age-dependent nigrostriatal deficiency in mice. J.Physiol. Pharmacol. 59: 205-16.

Polymeropoulos, M.H., Lavedan, C., Leroy, E., Ide, S. E., Dehejia, A., Dutra, A., *et al.* (1997). Mutation in the alpha-synuclein gene identified in families with Parkinson's disease. Science 276: 2045-7.

Proukakis, C., Dudzik, C. G., Brier, T., MacKay, D. S., Cooper, J. M., Millhauser, G. L., *et al.* (2013). A novel alpha-synuclein missense mutation in Parkinson disease. Neurology 80: 1062-4.

Rapti, K., Louis-Jeune, V., Kohlbrenner, E., Ishikawa, K., Ladage, D., Zolotukhin, S., *et al.* (2012). Neutralizing antibodies against AAV serotypes 1, 2, 6, and 9 in sera of commonly used animal models. Mol.Ther. 20: 73-83.

Rasia, R.M., Bertoncini, C. W., Marsh, D., Hoyer, W., Cherny, D., Zweckstetter, M., *et al.* (2005). Structural characterization of copper(II) binding to alpha-synuclein: Insights into the bioinorganic chemistry of Parkinson's disease. Proc.Natl.Acad.Sci.U.S.A. 102: 4294-9.

Recasens, A., Dehay, B., Bove, J., Carballo-Carbajal, I., Dovero, S., Perez-Villalba, A., *et al.* (2014). Lewy body extracts from Parkinson disease brains trigger alpha-synuclein pathology and neurodegeneration in mice and monkeys. Ann.Neurol. 75: 351-62.

Reith, M.E., Xu, C. & Chen, N. H. (1997). Pharmacology and regulation of the neuronal dopamine transporter. Eur.J.Pharmacol. 324: 1-10.

Reyes, J.F., Rey, N. L., Bousset, L., Melki, R., Brundin, P. & Angot, E. (2014). Alpha-synuclein transfers from neurons to oligodendrocytes. Glia 62: 387-98.

Richter, F., Hamann, M. & Richter, A. (2007). Chronic rotenone treatment induces behavioral effects but no pathological signs of parkinsonism in mice. J.Neurosci.Res. 85: 681-91.

Rideout, H.J., Larsen, K. E., Sulzer, D. & Stefanis, L. (2001). Proteasomal inhibition leads to formation of ubiquitin/alpha-synuclein-immunoreactive inclusions in PC12 cells. J.Neurochem. 78: 899-908.

Rockenstein, E., Mallory, M., Hashimoto, M., Song, D., Shults, C. W., Lang, I., *et al.* (2002). Differential neuropathological alterations in transgenic mice expressing alpha-synuclein from the platelet-derived growth factor and Thy-1 promoters. J.Neurosci.Res. 68: 568-78.

Rockenstein, E., Nuber, S., Overk, C. R., Ubhi, K., Mante, M., Patrick, C., *et al.* (2014). Accumulation of oligomer-prone alpha-synuclein exacerbates synaptic and neuronal degeneration in vivo. Brain 137: 1496-513.

Rockenstein, E., Schwach, G., Ingolic, E., Adame, A., Crews, L., Mante, M., *et al.* (2005). Lysosomal pathology associated with alpha-synuclein accumulation in transgenic models using an eGFP fusion protein. J.Neurosci.Res. 80: 247-59.

Rutherford, N.J., Moore, B. D., Golde, T. E. & Giasson, B. I. (2014). Divergent effects of the H50Q and G51D SNCA mutations on the aggregation of alpha-synuclein. J.Neurochem. 131: 859-67.

Salin, P., Manrique, C., Forni, C. & Kerkerian-Le Goff, L. (2002). High-frequency stimulation of the subthalamic nucleus selectively reverses dopamine denervation-induced cellular defects in the output structures of the basal ganglia in the rat. J.Neurosci. 22: 5137-48.

Sampathu, D.M., Giasson, B. I., Pawlyk, A. C., Trojanowski, J. Q. & Lee, V. M. (2003). Ubiquitination of alpha-synuclein is not required for formation of pathological inclusions in alpha-synucleinopathies. Am.J.Pathol. 163: 91-100.

Savolainen, M.H., Richie, C. T., Harvey, B. K., Männistö, P. T., Maguire-Zeiss, K. A. & Myöhänen, T. T. (2014). The beneficial effect of a prolyl oligopeptidase inhibitor, KYP-2047, on alpha-synuclein clearance and autophagy in A30P transgenic mouse. Neurobiol.Dis. 68: 1-15.

Schapira, A.H. (2015). Glucocerebrosidase and Parkinson disease: Recent advances. Mol.Cell.Neurosci. 66: 37-42.

Schmidt, F., Levin, J., Kamp, F., Kretzschmar, H., Giese, A. & Botzel, K. (2012). Single-channel electrophysiology reveals a distinct and uniform pore complex formed by alpha-synuclein oligomers in lipid membranes. PLoS One 7: e42545.

Schneeberger, A., Mandler, M., Mattner, F. & Schmidt, W. (2012). Vaccination for Parkinson's disease. Parkinsonism Relat.Disord. 18 Suppl 1: S11-3.

Schober, A. (2004). Classic toxin-induced animal models of Parkinson's disease: 6-OHDA and MPTP. Cell Tissue Res. 318: 215-24.

Schulz, I., Zeitschel, U., Rudolph, T., Ruiz-Carrillo, D., Rahfeld, J. U., Gerhartz, B., *et al.* (2005). Subcellular localization suggests novel functions for prolyl endopeptidase in protein secretion. J.Neurochem. 94: 970-9.

Serpell, L.C., Berriman, J., Jakes, R., Goedert, M. & Crowther, R. A. (2000). Fiber diffraction of synthetic alpha-synuclein filaments shows amyloid-like cross-beta] conformation. Proc.Natl.Acad. Sci.USA 97: 4897-902.

Shen, Y.F., Tang, Y., Zhang, X. J., Huang, K. X. & Le, W. D. (2013). Adaptive changes in autophagy after UPS impairment in Parkinson's disease. Acta Pharmacol.Sin. 34: 667-73.

Shimshek, D.R., Mueller, M., Wiessner, C., Schweizer, T. & van der Putten, P. H. (2010). The HSP70 molecular chaperone is not beneficial in a mouse model of alpha-synucleinopathy. PLoS One 5: e10014.

Shimura, H., Schlossmacher, M. G., Hattori, N., Frosch, M. P., Trockenbacher, A., Schneider, R., *et al.* (2001). Ubiquitination of a new form of alpha-synuclein by parkin from human brain: implications for Parkinson's disease. Science 293: 263-9.

Shinoda, M., Toide, K., Ohsawa, I. & Kohsaka, S. (1997). Specific inhibitor for prolyl endopeptidase suppresses the generation of amyloid beta protein in NG108-15 cells. Biochem.Biophys.Res.Commun. 235: 641-5.

Shishido, Y., Furushiro, M., Tanabe, S., Taniguchi, A., Hashimoto, S., Yokokura, T., *et al.* (1998). Effect of ZTTA, a prolyl endopeptidase inhibitor, on memory impairment in a passive avoidance test of rats with basal forebrain lesions. Pharm.Res. 15: 1907-10.

Silva, R.M., Ries, V., Oo, T. F., Yarygina, O., Jackson-Lewis, V., Ryu, E. J., *et al.* (2005). CHOP/GADD153 is a mediator of apoptotic death in substantia nigra dopamine neurons in an in vivo neurotoxin model of parkinsonism. J.Neurochem. 95: 974-86.

Simuni, T., Sethi, K. (2008). Nonmotor manifestations of Parkinson's disease. Ann.Neurol. 64 Suppl 2: S65-80.

Singleton, A.B., Farrer, M., Johnson, J., Singleton, A., Hague, S., Kachergus, J., *et al.* (2003). Alpha-Synuclein locus triplication causes Parkinson's disease. Science 302: 841.

Smith, W.W., Jiang, H., Pei, Z., Tanaka, Y., Morita, H., Sawa, A., *et al.* (2005). Endoplasmic reticulum stress and mitochondrial cell death pathways mediate A53T mutant alpha-synuclein-induced toxicity. Hum.Mol.Genet. 14: 3801-11.

Snyder, H., Mensah, K., Theisler, C., Lee, J., Matouschek, A. & Wolozin, B. (2003). Aggregated and monomeric alpha-synuclein bind to the S6' proteasomal protein and inhibit proteasomal function. J.Biol.Chem. 278: 11753-9.

Spencer, B., Potkar, R., Trejo, M., Rockenstein, E., Patrick, C., Gindi, R., *et al.* (2009). Beclin 1 gene transfer activates autophagy and ameliorates the neurodegenerative pathology in alpha-synuclein models of Parkinson's and Lewy body diseases. J.Neurosci. 29: 13578-88.

Spillantini, M.G. (1997). Alpha-synuclein in Lewy bodies. Nature 388: 839-40.

Spillantini, M.G., Crowther, R. A., Jakes, R., Hasegawa, M. & Goedert, M. (1998). Alpha-Synuclein in filamentous inclusions of Lewy bodies from Parkinson's disease and dementia with lewy bodies. Proc.Natl.Acad.Sci.U.S.A. 95: 6469-73.

Spillantini, M.G., Goedert, M. (2000). The alpha-synucleinopathies: Parkinson's disease, dementia with Lewy bodies, and multiple system atrophy. Ann.N.Y.Acad.Sci. 920: 16-27.

St Martin, J.L., Klucken, J., Outeiro, T. F., Nguyen, P., Keller-McGandy, C., Cantuti-Castelvetri, I., *et al.* (2007). Dopaminergic neuron loss and up-regulation of chaperone protein mRNA induced by targeted over-expression of alpha-synuclein in mouse substantia nigra. J.Neurochem. 100: 1449-57.

Südhof, T.C. (1995). The synaptic vesicle cycle: a cascade of protein-protein interactions. Nature 375: 645-53.

Sung, J.Y., Park, S. M., Lee, C. H., Um, J. W., Lee, H. J., Kim, J., *et al.* (2005). Proteolytic cleavage of extracellular secreted alpha-synuclein via matrix metalloproteinases. J.Biol.Chem. 280: 25216-24.

Surguchov, A. (2008). Molecular and cellular biology of synucleins. Int.Rev.Cell.Mol.Biol. 270: 225-317.

Swant, J., Goodwin, J. S., North, A., Ali, A. A., Gamble-George, J., Chirwa, S., *et al.* (2011). Alpha-Synuclein stimulates a dopamine transporter-dependent chloride current and modulates the activity of the transporter. J.Biol.Chem. 286: 43933-43.

Szeltner, Z., Juhasz, T., Szamosi, I., Rea, D., Fülop, V., Modos, K., *et al.* (2013). The loops facing the active site of prolyl oligopeptidase are crucial components in substrate gating and specificity. Biochim.Biophys.Acta 1834: 98-111.

Szeltner, Z., Morawski, M., Juhasz, T., Szamosi, I., Liliom, K., Csizmok, V., *et al.* (2010). GAP43 shows partial co-localisation but no strong physical interaction with prolyl oligopeptidase. Biochim.Biophys.Acta 1804: 2162-76.

Takeda, A., Mallory, M., Sundsmo, M., Honer, W., Hansen, L. & Masliah, E. (1998). Abnormal accumulation of NACP/alpha-synuclein in neurodegenerative disorders. Am.J.Pathol. 152: 367-72.

Takeuchi, H., Yanagida, T., Inden, M., Takata, K., Kitamura, Y., Yamakawa, K., *et al.* (2009). Nicotinic receptor stimulation protects nigral dopaminergic neurons in rotenone-induced Parkinson's disease models. J.Neurosci.Res. 87: 576-85.

Tanaka, Y., Engelender, S., Igarashi, S., Rao, R. K., Wanner, T., Tanzi, R. E., *et al.* (2001). Inducible expression of mutant α-synuclein decreases proteasome activity and increases sensitivity to mitochondria-dependent apoptosis. Human Molecular Genetics 10: 919-26.

Tanik, S.A., Schultheiss, C. E., Volpicelli-Daley, L. A., Brunden, K. R. & Lee, V. M. (2013). Lewy body-like alpha-synuclein aggregates resist degradation and impair macroautophagy. J.Biol.Chem. 288: 15194-210.

Tarrago, T., Martin-Benito, J., Sabido, E., Claasen, B., Madurga, S., Gairi, M., *et al.* (2009). A new side opening on prolyl oligopeptidase revealed by electron microscopy. FEBS Lett. 583: 3344-8.

Tehranian, R., Montoya, S. E., Van Laar, A. D., Hastings, T. G. & Perez, R. G. (2006). Alpha-synuclein inhibits aromatic amino acid decarboxylase activity in dopaminergic cells. J.Neurochem. 99: 1188-96.

Tenreiro, S., Reimao-Pinto, M. M., Antas, P., Rino, J., Wawrzycka, D., Macedo, D., *et al.* (2014). Phosphorylation modulates clearance of alpha-synuclein inclusions in a yeast model of Parkinson's disease. PLoS Genet. 10: e1004302.

Theodore, S., Cao, S., McLean, P. J. & Standaert, D. G. (2008). Targeted overexpression of human alpha-synuclein triggers microglial activation and an adaptive immune response in a mouse model of Parkinson disease. J.Neuropathol.Exp.Neurol. 67: 1149-58.

Tofaris, G.K., Garcia Reitbock, P., Humby, T., Lambourne, S. L., O'Connell, M., Ghetti, B., *et al.* (2006). Pathological changes in dopaminergic nerve cells of the substantia nigra and olfactory bulb in mice transgenic for truncated human alpha-synuclein(1-120): implications for Lewy body disorders. J.Neurosci. 26: 3942-50.

Tofaris, G.K., Layfield, R. & Spillantini, M. G. (2001). Alpha-Synuclein Metabolism and Aggregation is Linked to Ubiquitin-Independent Degradation by the Proteasome. FEBS Lett. 509: 22-6.

Tofaris, G.K., Razzaq, A., Ghetti, B., Lilley, K. S. & Spillantini, M. G. (2003). Ubiquitination of alpha-synuclein in Lewy bodies is a pathological event not associated with impairment of proteasome function. J.Biol.Chem. 278: 44405-11.

Toide, K., Iwamoto, Y., Fujiwara, T. & Abe, H. (1995). JTP-4819: a novel prolyl endopeptidase inhibitor with potential as a cognitive enhancer. J.Pharmacol.Exp.Ther. 274: 1370-8.

Toide, K., Shinoda, M., Fujiwara, T. & Iwamoto, Y. (1997). Effect of a novel prolyl endopeptidase inhibitor, JTP-4819, on spatial memory and central cholinergic neurons in aged rats. Pharmacol. Biochem.Behav. 56: 427-34.

Tsigelny, I.F., Bar-On, P., Sharikov, Y., Crews, L., Hashimoto, M., Miller, M. A., *et al.* (2007). Dynamics of alpha-synuclein aggregation and inhibition of pore-like oligomer development by beta-synuclein. FEBS J. 274: 1862-77.

Tsigelny, I.F., Sharikov, Y., Wrasidlo, W., Gonzalez, T., Desplats, P. A., Crews, L., *et al.* (2012). Role of alpha-synuclein penetration into the membrane in the mechanisms of oligomer pore formation. FEBS J. 279: 1000-13.

Tu, P.-. (1998). Glial cytoplasmic inclusions in white matter oligodendrocytes of multiple system atrophy brains contain insoluble alpha-synuclein. Ann.Neurol. 44: 415-22.

Ueda, K. (1993). Molecular cloning of cDNA encoding an unrecognized component of amyloid in Alzheimer disease. Proc.Natl.Acad.Sci.USA 90: 11282-6.

Uversky, V.N. (2007). Neuropathology, biochemistry, and biophysics of alpha-synuclein aggregation. J.Neurochem. 103: 17-37.

Uversky, V.N. (2004). Neurotoxicant-induced animal models of Parkinson's disease: understanding the role of rotenone, maneb and paraquat in neurodegeneration. Cell Tissue Res. 318: 225-41.

Uversky, V.N., Li, J. & Fink, A. K. (2001a). Evidence for a partially folded intermediate in alpha-synuclein fibril formation. J.Biol.Chem. 276: 10737-44.

Uversky, V.N., Li, J. & Fink, A. L. (2001b). Pesticides directly accelerate the rate of alpha-synuclein fibril formation: a possible factor in Parkinson's disease. FEBS Lett. 500: 105-8.

Uversky, V.N., Yamin, G., Munishkina, L. A., Karymov, M. A., Millett, I. S., Doniach, S., *et al.* (2005). Effects of nitration on the structure and aggregation of alpha-synuclein. Brain Res.Mol. Brain Res. 134: 84-102.

Uversky, V.N., Yamin, G., Souillac, P. O., Goers, J., Glaser, C. B. & Fink, A. L. (2002). Methionine oxidation inhibits fibrillation of human alpha-synuclein in vitro. FEBS Lett. 517: 239-44.

Valera, E., Masliah, E. (2013). Immunotherapy for neurodegenerative diseases: focus on alpha-synucleinopathies. Pharmacol.Ther. 138: 311-22.

van de Berg, W.D., Hepp, D. H., Dijkstra, A. A., Rozemuller, J. A., Berendse, H. W. & Foncke, E. (2012). Patterns of alpha-synuclein pathology in incidental cases and clinical subtypes of Parkinson's disease. Parkinsonism Relat.Disord. 18 Suppl 1: S28-30.

van der Putten, H., Wiederhold, K. H., Probst, A., Barbieri, S., Mistl, C., Danner, S., *et al.* (2000). Neuropathology in mice expressing human alpha-synuclein. J.Neurosci. 20: 6021-9.

Van der Veken, P., Fülop, V., Rea, D., Gerard, M., Van Elzen, R., Joossens, J., *et al.* (2012). P2-substituted N-acylprolylpyrrolidine inhibitors of prolyl oligopeptidase: biochemical evaluation, binding mode determination, and assessment in a cellular model of synucleinopathy. J.Med.Chem. 55: 9856-67.

Vernon, A.C., Crum, W. R., Johansson, S. M. & Modo, M. (2011). Evolution of extra-nigral damage predicts behavioural deficits in a rat proteasome inhibitor model of Parkinson's disease. PLoS One 6: e17269.

Vilchez, D., Saez, I. & Dillin, A. (2014). The role of protein clearance mechanisms in organismal ageing and age-related diseases. Nat.Commun. 5: 5659.

Vogiatzi, T., Xilouri, M., Vekrellis, K. & Stefanis, L. (2008). Wild type alpha-synuclein is degraded by chaperone-mediated autophagy and macroautophagy in neuronal cells. J.Biol.Chem. 283: 23542-56.

Volpicelli-Daley, L.A., Luk, K. C., Patel, T. P., Tanik, S. A., Riddle, D. M., Stieber, A., *et al.* (2011). Exogenous alpha-synuclein fibrils induce Lewy body pathology leading to synaptic dysfunction and neuron death. Neuron 72: 57-71.

Wakabayashi, K., Tanji, K., Mori, F. & Takahashi, H. (2007). The Lewy body in Parkinson's disease: molecules implicated in the formation and degradation of alpha-synuclein aggregates. Neuropathology 27: 494-506.

Wakamatsu, M., Ishii, A., Iwata, S., Sakagami, J., Ukai, Y., Ono, M., *et al.* (2008). Selective loss of nigral dopamine neurons induced by overexpression of truncated human alpha-synuclein in mice. Neurobiol.Aging 29: 574-85.

Wang, J., Martin, E., Gonzales, V., Borchelt, D. R. & Lee, M. K. (2008). Differential regulation of small heat shock proteins in transgenic mouse models of neurodegenerative diseases. Neurobiol. Aging 29: 586-97.

Wang, Y., Zhang, Q. J., Liu, J., Ali, U., Gui, Z. H., Hui, Y. P., *et al.* (2010). Changes in firing rate and pattern of GABAergic neurons in subregions of the substantia nigra pars reticulata in rat models of Parkinson's disease. Brain Res. 1324: 54-63.

Watanabe, Y., Tatebe, H., Taguchi, K., Endo, Y., Tokuda, T., Mizuno, T., *et al.* (2012). p62/SQSTM1-dependent autophagy of Lewy body-like alpha-synuclein inclusions. PLoS One 7: e52868.

Webb, J.L., Ravikumar, B., Atkins, J., Skepper, J. N. & Rubinsztein, D. C. (2003). Alpha-Synuclein is degraded by both autophagy and the proteasome. J.Biol.Chem. 278: 25009-13.

Weinreb, P.H., Zhen, W., Poon, A. W., Conway, K. A. & Lansbury, P. T.,Jr (1996). NACP, a protein implicated in Alzheimer's disease and learning, is natively unfolded. Biochemistry 35: 13709-15.

Wersinger, C., Prou, D., Vernier, P., Niznik, H. B. & Sidhu, A. (2003). Mutations in the lipid-binding domain of alpha-synuclein confer overlapping, yet distinct, functional properties in the regulation of dopamine transporter activity. Mol.Cell.Neurosci. 24: 91-105.

Wersinger, C., Sidhu, A. (2005). Disruption of the interaction of alpha-synuclein with microtubules enhances cell surface recruitment of the dopamine transporter. Biochemistry 44: 13612-24.

Williams, R.S., Eames, M., Ryves, W. J., Viggars, J. & Harwood, A. J. (1999). Loss of a prolyl oligopeptidase confers resistance to lithium by elevation of inositol (1,4,5) trisphosphate. EMBO J. 18: 2734-45.

Wills, J., Credle, J., Oaks, A. W., Duka, V., Lee, J. H., Jones, J., *et al.* (2012). Paraquat, but not maneb, induces synucleinopathy and tauopathy in striata of mice through inhibition of proteasomal and autophagic pathways. PLoS One 7: e30745.

Winner, B., Jappelli, R., Maji, S. K., Desplats, P. A., Boyer, L., Aigner, S., *et al.* (2011). In vivo demonstration that alpha-synuclein oligomers are toxic. Proc.Natl.Acad.Sci.U.S.A. 108: 4194-9.

Winslow, A.R., Chen, C. W., Corrochano, S., Acevedo-Arozena, A., Gordon, D. E., Peden, A. A., *et al.* (2010). Alpha-Synuclein impairs macroautophagy: implications for Parkinson's disease. J.Cell Biol. 190: 1023-37.

Wirdefeldt, K., Adami, H. O., Cole, P., Trichopoulos, D. & Mandel, J. (2011). Epidemiology and etiology of Parkinson's disease: a review of the evidence. Eur.J.Epidemiol. 26 Suppl 1: S1-58.

Wood, S.J. (1999). Alpha-synuclein fibrillogenesis is nucleation-dependent. J.Biol.Chem. 274: 19509-12.

Wu, J., Lou, H., Alerte, T. N., Stachowski, E. K., Chen, J., Singleton, A. B., *et al.* (2012). Lewy-like aggregation of alpha-synuclein reduces protein phosphatase 2A activity in vitro and in vivo. Neuroscience 207: 288-97.

Wu, N., Joshi, P. R., Cepeda, C., Masliah, E. & Levine, M. S. (2010). Alpha-synuclein overexpression in mice alters synaptic communication in the corticostriatal pathway. J.Neurosci.Res. 88: 1764-76.

Xilouri, M., Brekk, O. R., Kirik, D. & Stefanis, L. (2013). LAMP2A as a therapeutic target in Parkinson disease. Autophagy 9: 2166-8.

Xilouri, M., Vogiatzi, T., Vekrellis, K., Park, D. & Stefanis, L. (2009). Abberant alpha-synuclein confers toxicity to neurons in part through inhibition of chaperone-mediated autophagy. PLoS One 4: e5515.

Yavich, L., Oksman, M., Tanila, H., Kerokoski, P., Hiltunen, M., van Groen, T., *et al.* (2005). Locomotor activity and evoked dopamine release are reduced in mice overexpressing A30P-mutated human alpha-synuclein. Neurobiol.Dis. 20: 303-13.

Yavich, L., Tanila, H., Vepsalainen, S. & Jäkälä, P. (2004). Role of alpha-synuclein in presynaptic dopamine recruitment. J.Neurosci. 24: 11165-70.

Yorimitsu, T., Klionsky, D. J. (2005). Autophagy: molecular machinery for self-eating. Cell Death Differ. 12 Suppl 2: 1542-52.

Zarranz, J.J., Alegre, J., Gomez-Esteban, J. C., Lezcano, E., Ros, R., Ampuero, I., *et al.* (2004). The new mutation, E46K, of alpha-synuclein causes Parkinson and Lewy body dementia. Ann.Neurol. 55: 164-73.

Zhang, X., Xie, W., Qu, S., Pan, T., Wang, X. & Le, W. (2005). Neuroprotection by iron chelator against proteasome inhibitor-induced nigral degeneration. Biochem.Biophys.Res.Commun. 333: 544-9.

Zhou, R.M., Huang, Y. X., Li, X. L., Chen, C., Shi, Q., Wang, G. R., *et al.* (2010). Molecular interaction of alpha-synuclein with tubulin influences on the polymerization of microtubule in vitro and structure of microtubule in cells. Mol.Biol.Rep. 37: 3183-92.

Zhu, W., Xie, W., Pan, T., Xu, P., Fridkin, M., Zheng, H., *et al.* (2007). Prevention and restoration of lactacystin-induced nigrostriatal dopamine neuron degeneration by novel brain-permeable iron chelators. FASEB J. 21: 3835-44.

Recent Publications in this Series

60/2015 Chakravarthi Kanduri
Genomics Approaches to Study Music Perception and Performance
61/2015 Jussi Kupari
Studies on Peripheral Nervous System Development and Function in Mice Deficient for the Neurturin Receptor GFRα2
62/2015 Anton Tokariev
Studying Connectivity in the Neonatal EEG
63/2015 Eva María del Amo Páez
Computational Prediction and Pharmacokinetic Simulations for Drug Discovery and Development
64/2015 Reija Silvennoinen
Physiological Modulation of the Reverse Cholesterol Transport Pathway *in vivo*
65/2015 Heli Venhoranta
Inherited Developmental Diseases Related to Reproductive Failures in Cattle
66/2015 Juhana Rautiola
Angiogenesis Inhibitors in Metastatic Renal Cancer with Emphasis on Prognostic Clinical and Molecular Factors
67/2015 Terhi Peuralinna
Genetics of Neurodegeneration: Alzheimer, Lewy Body and Motor Neuron Diseases in the Finnish Population
68/2015 Manuela Tumiati
Rad51c is a Tumor Suppressor in Mammary and Sebaceous Glands
69/2015 Mikko Helenius
Role of Purinergic Signaling in Pathological Pulmonary Vascular Remodeling
70/2015 Kaisa Rajakylä
The Nuclear Import Mechanism of SRF Co-Activator MKL1
71/2015 Johanna Lotsari-Salomaa
Epigenetic Characteristics of Lynch Syndrome-Associated and Sporadic Tumorigenesis
72/2015 Tea Pemovska
Individualized Chemical Systems Medicine of Acute and Chronic Myeloid Leukemia
73/2015 Simona Bramante
Oncolytic Adenovirus Coding for GM-CSF in Treatment of Cancer
74/2015 Alhadi Almangush
Histopathological Predictors of Early Stage Oral Tongue Cancer
75/2015 Otto Manninen
Imaging Studies in the Mouse Model of Progressive Myoclonus Epilepsy of Unverricht-Lundborg Type, EPM1
76/2015 Mordekhay Medvedovsky
Methodological and Clinical Aspects of Ictal and Interictal MEG
77/2015 Marika Melamies
Studies on Canine Lower Respiratory Tract with Special Reference to Inhaled Corticosteroids
78/2015 Elina Välimäki
Activation of Inflammasome and Protein Secretion by Endogenous Danger and Microbe-Derived Signals in Human Macrophages
79/2015 Terhi Keltanen
Postmortem Biochemistry - Analysis of Metabolic Imbalance

Helsinki 2015 ISSN 2342-3161 ISBN 978-951-51-1542-3